

Mr S. H. Tower
35310

ELECTRICAL COMMUNICATION

ITT

VOLUME 37 • NUMBER 3 • 1962

ELECTRICAL COMMUNICATION

Technical Journal Published Quarterly by

INTERNATIONAL TELEPHONE and TELEGRAPH CORPORATION

320 Park Avenue, New York 22, New York

President: H. S. Geneen

Secretary: J. J. Navin

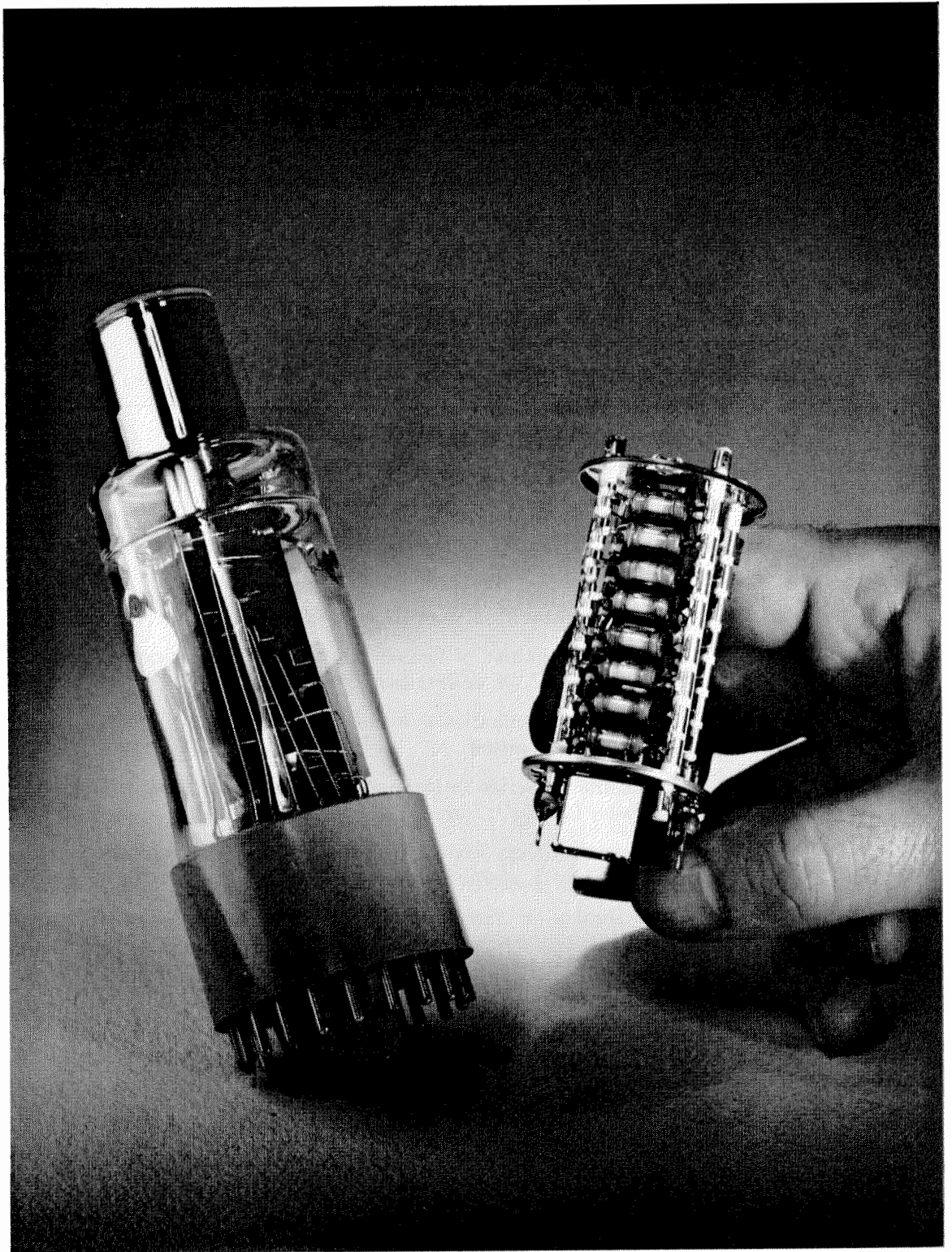
CONTENTS

Volume 37	1962	Number 3
This Issue in Brief		171
Recent Engineering Developments		174
Eglin Gulf Test Range <i>by Harry Altman</i>		181
Flight Simulator for Mirage III <i>by S. M. Poole</i>		196
Potential Application of Recent Advances in Communication Technology <i>by L. A. deRosa and E. W. Keller</i>		202
Dewdrop Communication System Performance <i>by W. G. Donaldson and J. P. Barbera</i>		222
Parametric Converter Performance on a Beyond-the-Horizon Microwave Link <i>by J. Harvey</i>		230
Experimental Data Transmission System for Switched Telephone Lines <i>by H. Marko and H. Aulhorn</i>		238
New Display for Frequency-Modulated Continuous-Wave Radars <i>by H. T. Naidich</i>		252
World's Telephones—1961		262
United States Patents Issued to International Telephone and Telegraph System ; February–April 1961		268
In Memoriam—Paul Hartmann		271
Note		
Book: Understanding Digital Computers <i>by Paul Siegel</i>		221
Contributors to This Issue		272

Copyright © 1962 by INTERNATIONAL TELEPHONE and TELEGRAPH CORPORATION

EDITOR, H. P. Westman

Subscription: \$2.00 per year; 50¢ per copy



Shown with a conventional design is a multiplier phototube without an enclosing envelope. Designed for use in an evacuated environment, the absence of a glass envelope avoids reflection, absorption, and spectral filtering of the impinging radiation.

Eglin Gulf Test Range—This missile test range in the Gulf of Mexico runs for 450 miles (725 kilometers) along the western coast of Florida from Eglin Air Force Base to Key West. It is capable of simultaneously supporting the launching of three missiles against three drones.

The instrumentation provides for tracking and acquiring high-precision data from all the airborne vehicles and, in addition, remotely controlling the missiles or drones in flight. All the radars on the range are synchronized through the communication system to prevent interference between radars or with the airborne beacons. The range includes multiple radars, telemetering, and optical facilities as the primary sources of data utilized for missile performance evaluation.

A vast network of communications, including microwave line-of-sight and forward-scatter systems, exists along the range to transmit the digital data and to provide operational integration of the range facilities. By the use of signaling and control techniques, the best data existing during a mission is made available to operational personnel to perform control or destruction functions, and, in addition, is recorded on master recorders to be used for evaluation.

A variety of display equipment including special-purpose units, consoles, plotting boards, height chart recorders, et cetera, are provided to permit continuous monitoring and control of missile and drone performance.

Time correlation for all data and display devices is established by a master time generator and synchronized slave generators at each site.

A frequency-monitoring and interference-control system performs the functions of detecting, monitoring, recording, and locating signals that could adversely affect a mission.

A range-wide count-down system, which supplies accurate visual time displays, and several voice communication systems play important roles in coordinating the operation of this integrated range facility.

Flight Simulator for Mirage III—Flight simulators, which offer an economical and safe means of training aircraft personnel, originally characterized the general performance of a class of aircraft. In contrast, modern simulators portray the performance of a particular aircraft in great detail.

The Mirage III is a single-seater single-engine fighter-interceptor. A training simulator designed for it starts with an exact replica of its cockpit. In performance, it provides for the starting of the engine on the ground, all flight conditions including radio aids, detection by radar, and interception by guided missiles or gunfire, to final engine shutdown after landing. The effects of altitude, attitude, wind, rain, and other weather conditions, as well as over a hundred faults that can be introduced by the instructor, are provided for.

A synthetic sound system reproduces the acoustic outputs of engines, generators, converters, hydraulic pumps, undercarriage, flaps, and dive-brake operation as modified by the conditions of flight.

The effects of these many variables are synthesized and integrated through the use of a computer. The 6 basic transistor-operated computer elements are amplifiers, switching amplifiers, modulators, demodulators, differentiators, and noise generators. Servomechanisms used for converting electric signals to shaft positions or for integrating must have large dynamic range and fast response to represent the high-performance characteristics of the aircraft.

The entire simulator, including the cockpit; instructor's console, fault, and recording equipment; computer; power supplies; and air-conditioning apparatus is mounted in a semi-trailer and operates from any 3-phase alternating-current mains through its own voltage regulator.

Potential Applications of Recent Advancements in Communication Technology—It is assumed that communication needs will double in the next five years and the large volume of data that must be handled accurately at high speed will further complicate the problems beyond the limitations of present techniques.

The noise temperature of each element in a communication system can be referred to a single point in that system as an addition to its effective temperature for over-all signal-to-noise calculations. It is safer to use this concept of effective noise temperature than that of noise factor because small errors in noise factor result in large errors in temperature.

Noise or temperature radiation from outer-space bodies and from the earth through undesired minor lobes in the antenna pattern are estimated as are losses in the atmosphere, ionosphere, and transmission lines for paths between the earth and the moon, Venus, and artificial satellites.

For a potentially useful spectrum window above 10^5 gigacycles per second, consideration is given to black-body radiators and to coherent X, gamma, and ultraviolet rays.

Codes of the parity-check type are limited in application to high-priority systems. Attention should be given to transmission waveforms differing sufficiently from prevailing noise waveforms to reduce their correlation functions to zero.

High-speed switching of circuits handling huge quantities of data with various destinations is required if both terminal equipment and transmission paths are to be utilized fully.

Dewdrop Communication System Performance—Dewdrop, a section of the Dewline system, is a 691-mile (1112-kilometer) link between Thule, Greenland, and Cape Dyer, Canada. It employs single-sideband suppressed-carrier modulation and quadruple-diversity tropospheric-scatter transmission.

Military operational requirements have placed more-stringent transmission objectives on the system than originally contemplated. Even with increased transmitter power, it is not as reliable as other sections of the Dewline. It would probably be unsatisfactory for high-speed data transmission.

Vertical polarization has given consistently better performance than horizontal polarization. Frequency-selective fading has been more severe than was anticipated. During some periods of anomalous propagation, recordings showed that 50 percent of the small fades occurred approximately simultaneously at the four receivers and 90 percent of the complete fades occurred on all four receivers.

In a population of 1500 vacuum tubes and 100 000 electrical components, an average of 300 were replaced during a period of six months. The duality of the diversity system prevented each such replacement from being an outage. In contrast, propagation conditions were responsible in one month for 90 percent of the outage time.

The narrow bandwidth of single-sideband signals and the absence of a definite threshold above intrinsic receiver noise are advantages but a serious disadvantage is the low operating efficiency of the linear power amplifiers in the transmitters.

Parametric Converter Performance on a Beyond-the-Horizon Microwave Link—Experimental parametric converters were installed on a quadruple-diversity link of the White Alice system. Two parametric receivers with noise figures of 1.5 decibels were operated simultaneously with two normal receivers of 8.8-decibel noise figures. Comparative measurements showed improvements of 7 decibels in telephone-channel noise and 10-fold in teletype error rates.

Experimental Data Transmission System for Switched Telephone Lines—Existing switched telephone lines offer a convenient path for data transmission capable of much higher speeds than conventional telegraph channels. Reasons are given for selecting a duplex system with serial transmission of elements over the full bandwidth, rather than dividing the frequency band into the conventional several parallel telegraph channels. Frequency modulation is favored for simplicity of equipment and adjustments.

Adequate accuracy cannot be obtained with a simple system so an error-detecting code using row, column, and diagonal check elements that must be satisfied simultaneously for a 63-element block was selected for an experimental system. The 63-element block of 42 information and 21 check elements was chosen as a compromise with regard to the cost of storage facilities. With a cyclic code, a larger block of 105 information elements and 22 check elements can produce greater protection against undetected block errors.

The experimental system was tested extensively on the Stuttgart public telephone network and confirmed the design considerations and met the estimated requirements for commercial service.

New Display for Frequency-Modulated Continuous-Wave Radars—The large majority of contemporary radars are of the pulse type, although in the early days of the radar art much of the work involved continuous-wave transmission. An important advantage of pulsed radars is the ease with which targets can be displayed. As the echo time of a pulsed transmission is proportional to the range of a target, many types of cathode-ray-tube displays have been devel-

oped to present the data in a manner most suitable for the particular application. In effect, these displays are scaled-down maps of the radar area and are generated by deflecting the electron beam of a cathode-ray tube in synchronism with the radiated transmission. At the time the echo is received, the beam is intensified, forming a blip on the face of the cathode-ray tube. The scale of the presentation can easily be adjusted by varying the speed of deflection of the electron beam across the face of the tube.

Continuous-wave radars have many advantages but their use has been limited to specialized cases, principally in situations where only one target is of interest, such as in a radio altimeter.

This paper describes a continuous-wave system capable of resolving a large number of targets and of displaying these multiple targets on a cathode-ray tube. The coordinates of these targets on this display are proportional to the range and velocity of the individual targets.

To obtain range information from a continuous-wave transmission, it is necessary to frequency modulate the wave. In this case, three modes of transmission are used to resolve the ambiguities that would result when echoes are received from multiple targets, each with different range and velocity.

Various aspects of such a system are discussed, and the concept of a frequency-modulated continuous-wave "plane" is extended to enable a better understanding of the operation of the components of such a system. The means of displaying this plane on a simple cathode-ray tube are presented; three versions are indicated, a full display, a sector display, and an expanded tracking display. Photographs of the displays with test patterns and under actual multiple-target flight tests are shown, indicating the results achieved on this project.

Recent Engineering Developments

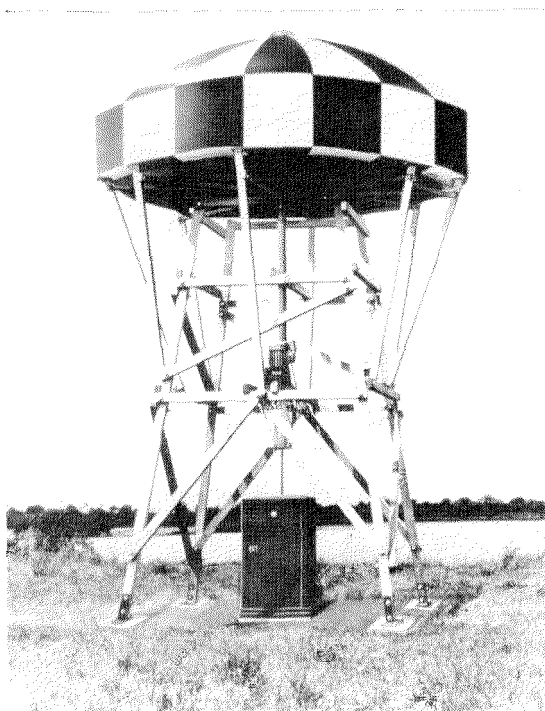
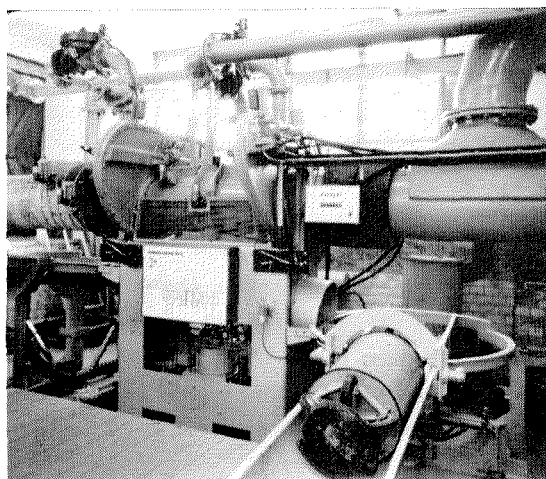


Figure 1—The glass-fiber radome, 22 feet (6.7 meters) high and 14 feet (4.3 meters) in diameter, encloses two dipoles rotating on a 12-foot (3.7-meter) crossarm. The receiving equipment is in the weather-proof cabinet on the ground. The bearing indicator and its driving unit are remotely located, usually in the airport control tower.



Tubeless Tube—Any apparently transparent enclosure of a multiplier phototube will filter out some wavelengths of the impinging radiation. To avoid this spectral loss in sensitivity, a vacuum-type multiplier phototube has been developed that omits the glass envelope. It is designed to operate in any vacuum environment, such as outer space. The tube was, therefore, constructed to withstand firing by rocket. A conventional tube and the unenclosed type are shown in the frontispiece.

One design has an electron multiplier gain of 100 000 at 2000 volts. The key to the new tube was the development of cathode materials that would withstand exposure to the atmosphere without becoming poisoned before reaching the evacuated environment in which the tube is to operate.

ITT Industrial Laboratories Division

Direction Finder Using True Doppler Technique

—A true Doppler effect is obtained in the direction finder shown in Figure 1 by rotating two vertical receiving dipoles horizontally about a central point. The principles of this ground-based very-high-frequency automatic direction finder produce not only highly accurate indications of the direction of arrival of signals but eliminate the need for much of the electrical complexity associated with other wide-base systems. This results in low initial cost and improved dependability of operations under unfavorable conditions.

The practical effectiveness of rotating even large antenna structures has been well established in other fields and the electrical simplicity gained from such a design reduces not only cost but, in particular, maintenance to a highly significant extent permitting installation

Figure 2—Pneumatic-tube station installed for Deutsche Bundespost for transporting mail. The wheeled carrier holding about 1000 letters is in the lower right ready to enter the tube.

in secondary airports having technically limited personnel.

Standard Telephones and Cables

Pneumatic Tubes for Transporting Mail—The slow progress of trucks in heavy traffic, measured in some places to average between 6 and 10 kilometers (3.7 and 6.2 miles) per hour makes attractive the use of underground pneumatic tubes for transporting mail from one post office to another.

As part of its investigation of this problem, the Deutsche Bundespost had an experimental pneumatic tube system installed in Berlin. The cement-asbestos tube is 400 meters (1312 feet) long and 450 millimeters (17.8 inches) in diameter.

The cylindrical carriers, shown in Figure 2, run on small radially mounted wheels and accommodate a standard post-office tray that holds about 1000 normal-size letters. Trays are loaded and unloaded automatically. Bumpers are provided at both ends of each carrier.

The blower system operates at 4000 millimeters (13 feet) water head and is capable of propelling 30 carriers at a time along a tube 10 kilometers (6.2 miles) long. The experimental carriers operate at a speed of 36 kilometers (22.4 miles) per hour. The capacity of 150 carriers per hour provides transportation for 150 000 letters per hour.

Standard Elektrik Lorenz

Submarine Cable Test Equipment—Test equipment for use in maintaining submarine cable telephone systems covers a range from 10 to 1500 kilocycles per second. Frequency accuracy and harmonic content permit measurements to be made at selected frequencies while the system is carrying traffic and on individual channels that are not then in use.

The oscillator in the transmit trolley, shown in Figure 3, has an over-all accuracy of frequency setting to within 25 cycles per second and can

be set to within 3 cycles per second at specific 5-kilocycle-per-second intervals within its frequency range. Accuracy of level measurement is assured by inclusion of a milliwatt test set and direct-current calibration equipment.

The receive trolley uses a double-superheterodyne receiver with narrow-band filters as a selective detector. An attenuator and a signal level measuring unit are included. Very small amplitudes of received signals can be measured in the presence of an interfering signal that is 60 decibels higher in level and only 2 kilocycles per second removed in frequency.

Standard Telephones and Cables

Data Processing Center—Recently, the services of a major data processing center have been made available on a rental basis or for complete

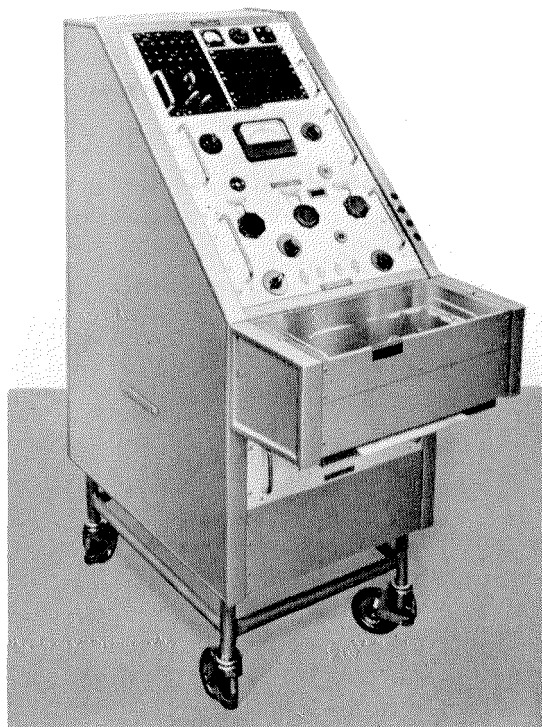


Figure 3—Transmit trolley for testing submarine telephone cable systems.

Recent Engineering Developments

projects including initiation of a program, processing on a computer, and program checking.

The installation includes a completely transistor-operated 7090 computer, a 1401 data-processing system, and a variety of peripheral equipment. The services of a staff of 250 computer programmers and program analysts are also available. See Figure 4.

International Electric Corporation

Ceramic Triode for Radio-Frequency Heating—

The use of ceramic insulation permits the power triode shown in Figure 5 to operate at its rated anode voltage of 6000 to produce 24 kilowatts output at 100 megacycles per second. An equivalent glass-insulated unit would be limited to half this frequency for full output.

Designed for radio-frequency heating service, its short coaxial stem is convenient for cavity mounting and its improved cathode has a large reserve of emission. Models are available for forced-air, vapor, and water cooling.

Standard Telephones and Cables

Tape-Controlled Machine Tool—Automatic control permits economical manufacture of



Figure 4—These yards of paper are but a minute's work for the printer of the 1401 data processing system. Associated equipment includes a 7090 computer.

small quantities of machined items. It is cheaper also to store a control record for replacement parts that may be needed later than to manufacture an estimated number of parts themselves when the initial production is in process and store them for future possible need.

The control system shown in Figure 6 uses punched paper tape to store the required instructions. The cabinet at the right contains the tape, code converter, register, and facilities for supervising the operation of the milling machine.

Standard Elektrik Lorenz

Airborne Radio Communication and Navigation System—

A transistor-operated very-high-frequency transmitter-receiver measuring 5¾ by 3¾ by 8 inches (14.6 by 9.5 by 20.3 centimeters) has been developed for light aircraft or for emergency use in larger aircraft. It is shown in Figure 7.



Figure 5—Ceramic-insulated triode for radio-frequency heating produces full output of 24 kilowatts at 100 megacycles per second.

It provides 400 switched channels at 50-kilo-cycle-per-second spacing in the 116-to-136-megacycle-per-second band. The power output of 200 milliwatts may be increased by adding a 6- or a 25-watt amplifier.

Three matching units are available to provide for instrument landing, very-high-frequency omnidirectional range, and marker receivers and instrument drives.

Standard Telephones and Cables

Silicon Rectifiers—The diffusion technique permits the manufacture of silicon rectifiers having high uniformity of the thickness of the semiconductor layer and of the penetration of the doping material. This permits performance characteristics to be held within close limits. The forward-current resistance may be made so small that rectifiers may be operated in parallel without series resistors to apportion the load.

Characteristic sizes of the SiG series of silicon rectifiers may be seen in Figure 8. Current ratings run from 0.5 to 10 amperes and peak reverse voltages are from 200 to 800 volts.

Hermetically sealed in metal, the axial-lead units may be soldered directly in place without heat sinks. Those with screw mounts are intended to be fitted into heat sinks and rectifiers can be supplied with either the anode or the cathode connected to the body.

Standard Elektrik Lorenz

Germanium Photoelectric Cells—Two new germanium-junction photoelectric cells have been announced. The *PG40B* is only 0.08 inch (2 millimeters) in diameter, which permits close packing for reading punched tape or punched cards. It is shown in Figure 9.

Its average sensitivity is 30 milliamperes per lumen. The spectral response peaks at 1.7 microns and cuts off at 2 microns. Minimum and maximum bias voltages are 1 and 50 volts

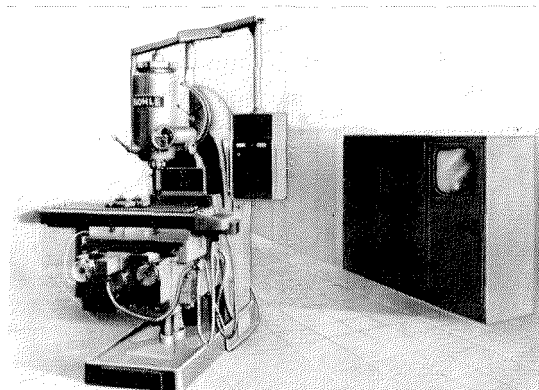


Figure 6—Tape-controlled machine tool.

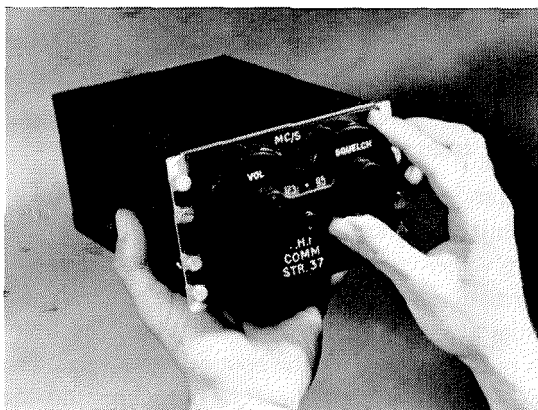


Figure 7—Transistor-operated very-high-frequency transmitter-receiver for light aircraft.

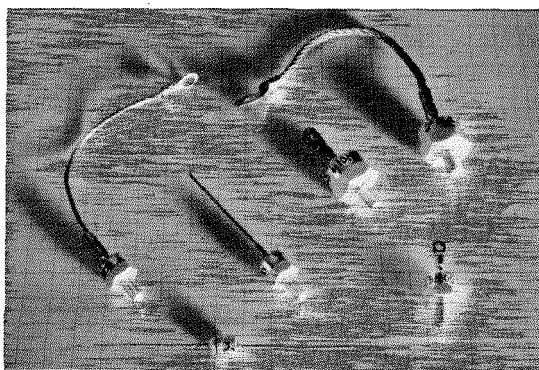


Figure 8—Variety of SiG silicon rectifiers with ratings from 0.5 to 10 amperes and peak reverse voltages of 200 to 800 volts.

Recent Engineering Developments

and maximum dark current is 200 microamperes. Dissipation is 15 milliwatts. Response extends to 50 kilocycles per second. Minimum dynamic resistance at 25 volts is 0.5 megohm.

The larger cell, type *PG50A*, is $\frac{7}{32}$ inch (5.6 millimeters) in diameter. It has similar characteristics but will withstand a maximum bias of 100 volts and will dissipate 50 milliwatts.

Standard Telephones and Cables

Large-Screen Precision Oscilloscope—A rectangular-screen cathode-ray oscilloscope developed for measurement use may be seen in Figure 10. Calibration of the 14-inch (36-centimeter) screen applies over an area of 6 by 8 inches (15 by 20 centimeters). The 0.5-millimeter spot is magnetically deflected over a frequency range from zero to 5 megacycles per second.

A random sampling technique is used. The circuit periodically determines the two deflecting values simultaneously and stores this information. When the magnetic deflection circuits are stabilized for these values, the beam is pulsed to produce the spot on the screen. The persistence of both the *P31* phosphor and the eye create an impression of continuity of trace.

Preamplifiers for the vertical and horizontal deflecting systems are interchangeable and may be designed for dual-trace or other special characteristics. Extensive use is made of transistors.

ITT Industrial Products Division

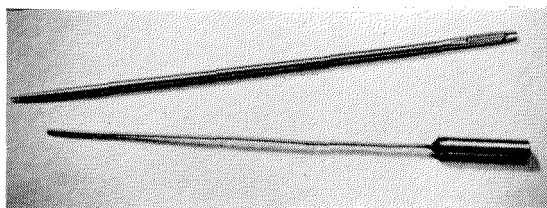


Figure 9—The *PG40B* germanium-junction photoelectric cell having a diameter of 0.08 inch (2 millimeters) compared with a needle.

Electronic Remote Control of Railway Substations—A fully electronic remote control system has been developed for the French national railways. It controls 9 electric substations on the 110-kilometer (68.4-mile) electrified rail line between Tarascon and Marseilles. From Marseilles, 313 equipments, such as sectionalizing switches and circuit breakers, are remotely controlled.

The state of each controlled item in a substation is constantly checked by electronic means. This information is encoded and several code message exchanges between the control center and substations assures the accuracy of transmission. Synchronization between the communicating stations is not required. At the control center, a high-capacity electronic scanner converts the received information into an instantaneous display of the system conditions.

The use of semiconductor devices that are in either the on or off condition provides high reliability and requires very little maintenance. The high speed at which the electronic equipment operates and with which information is transmitted between the control center and substations permits the control center to operate with but one set of equipment for selecting individually the items being controlled and eliminates the necessity for both selection and transmission apparatus in the substations as would be required with the former systems based on relays.

Part of the system is already in service and the remainder will be cut over in mid 1962.

Compagnie Générale de Constructions Téléphoniques

Data Transmission Demonstrations—A number of demonstrations of data transmission techniques were given recently by ITT Europe companies to delegates attending meetings of the Comité Consultatif International Télégraphique et Téléphonique Special Study Group A on Data Transmission in Geneva in October and of the Air Transport Association

and International Air Transport Association Working Group on Data Communication in Amsterdam in November.

At both meetings, Standard Radio & Telefon (Sweden) exhibited modem equipment for medium-speed transmission on telephone lines and maintenance apparatus for the measurement and analysis of error rates and error distribution. Standard Elektrik Lorenz (Germany) exhibited an experimental system for medium-speed transmission of data over telephone lines incorporating error correction by automatic retransmission of blocks of data.

At the Geneva meeting, Standard Telecommunication Laboratories (England) demonstrated very-low-speed transmission using parallel tones. At Amsterdam, Standard Telephones and Cables (England) demonstrated the remote interrogation of a Stantec Zebra computer at Harlow, England, over an international circuit at speeds of 1000 to 1500 bauds. This demonstration was repeated from London in August and from the company display at the Computer Exhibition in London in October. A similar demonstration was given from Paris by Le Matériel Téléphonique in September.

United Kingdom–France Microwave Link—More than 30 years ago, in 1931, communication across the English Channel at 1.7 gigacycles per second was demonstrated for the first time. This two-way telephone and teleprinter link was a joint venture of Standard Telephones and Cables in England and Le Matériel Téléphonique in France. The transmitters produced less than a watt of output and paraboloidal reflectors provided 3-degree directivity for both transmission and reception.

A second generation of this link was recently completed by the same two companies for telephone and television service. The cross-channel hop is from Tolsford Hill, near Folkestone in England, to Fiennes, near Calais in France, and thence via a repeater at Cassel to Loos, near Lille, a 150-kilometer (93-mile) system.

The separate telephone and television equipments use the same antennas for transmission and reception. Operation in the 4-gigacycle-per-second band with frequency modulation is in accordance with the recommendations of the International Consulting Committee on Radio. Traveling-wave amplifiers produce outputs of 5 watts. The paraboloidal reflectors are coupled by waveguides to the equipments.

Automatic phase diversity, in which signals from two space-diversity antennas are combined in phase, is used for the overwater path. Full standby facilities are provided for both systems with automatic switching of the telephone base band in case of unsatisfactory performance of the equipment in use.

In two years of telephone operation, circuit outage for all reasons was 0.02 percent, none of which was attributable to the radio apparatus. In two and a half years of television operation, the total outage was 0.04 percent, of which 0.032 percent was for abnormal fading during



Figure 10—Precision oscilloscope using 14-inch (36-centimeter) cathode-ray tube.

Recent Engineering Developments

September 1959 and only 0.0004 percent was attributable to the radio equipment.

*Standard Telephones and Cables
Le Matériel Téléphonique*

Television Transmitters—At the end of 1961, the television transmitter at Hoher Bogen in Bavaria started operation in Band V. The transmitter is a prototype using a tetrode power amplifier stage and modulating at an intermediate frequency in the frequency-multiplying chain. It is rated at 10 kilowatts for video and 2 kilowatts for sound, being designated a 10/2-kilowatt installation.

The Deutsche Bundespost received 1 transmitter of 20/4 kilowatts, 3 transmitters of 10/2 kilowatts, and 3 transmitters of 2/0.4 kilowatts for second-program installations during 1961.

In addition, another 2/0.4-kilowatt transmitter for first-program service in Band V was supplied to Norddeutsche Rundfunk.

Standard Elektrik Lorenz

Flight Simulator Color Film—A color film, "Mirages in Action," was presented in Paris to an audience of military, civilian, governmental, and foreign diplomatic personnel. It was produced in collaboration with the French Air Force when the first flight simulator for the Mirage III fighter plane was placed in operation. This equipment is described elsewhere in this issue.

After a trip of over 550 kilometers (350 miles) by road, the simulator was placed in operation within an hour. It has operated for thousands of hours with no outages for equipment failure, a tribute to conservative design and high uniformity of manufacture of its 2000 transistors and 30 000 other components.

Le Matériel Téléphonique

Telephone Switching on the "France"—Three independent telephone systems are installed on the new French liner "France."

The main network uses the first Pentaconta crossbar exchange aboard ship and provides for 1300 subscribers' sets. Two special circuits for use in ship-to-shore radiotelephone calls may be connected to 140 of these subscribers' sets.

Serving both passengers and ship personnel, the lines can be assigned readily to any of 30 classifications. The commanding officer, for instance, can call any line but cannot be called from passenger extensions. Special numbers provide for news bulletins, time checks, and other information in both French and English.

A manual switchboard provides for the second service. It serves 60 security telephone booths and 80 wall outlets into which ship's personnel can plug handsets when making their rounds.

The third service is made up of 16 independent point-to-point links installed permanently for special purposes.

Le Matériel Téléphonique

United States-Bermuda Telephone Cable in Service—Commercial operation was started in January 1962 over a new telephone submarine cable linking Bermuda and the United States. The cable is owned jointly by Cable and Wireless Limited and the American Telephone and Telegraph Company. It terminates at Manahawkin, New Jersey, and Flatts, Bermuda.

The cable is capable of providing 80 both-way channels. The Bermuda Telephone Company reports that it is now using the cable for 14 channels to the United States and 4 to Canada from where service may be extended to the United Kingdom over the new North Atlantic telephone cable.

This is believed to be the first complete submarine cable system terminating in the United States that has been wholly manufactured elsewhere. Standard Telephones and Cables supplied 750 nautical miles (1389 kilometers) of cable, 34 submerged repeaters, 3 submerged equalizers, and terminal equipment.

Standard Telephones and Cables

Eglin Gulf Test Range

HARRY ALTMAN

ITT Federal Laboratories, A Division of International Telephone and Telegraph Corporation; Nutley, New Jersey

1. Introduction

The Eglin Gulf Test Range is a facility that was designed to support research, development, and operational testing of Air Force short-range guided missiles and, in addition, for the training of Air Defense Command missile squadrons. Surface-to-air, air-to-surface, and air-to-air missiles can be accommodated by the range facilities.

Figure 1 shows the major sites of the range, which extends for 450 miles (724 kilometers) from Eglin Air Force Base in northwest Florida to Key West.

The range is unique in that it was designed with an integrated capability to support the launching of 3 missiles against 3 target drones. The instrumentation provides for tracking and acquiring high-precision data from all the airborne vehicles and, in addition, remotely controlling the missiles or drones in flight.

In contrast to other missile test ranges that

came into existence by a process of evolution, the Eglin Range was planned and designed as an integrated facility to provide a high degree of operational flexibility. Careful consideration was given to future capabilities to protect against early obsolescence. The major facilities at each of the sites shown in Figure 1 are as follows.

A-3, DRONE CONTROL CENTER

3 AN/MPS-9 Radars

3 AN/FRW-2 Ultra-High-Frequency Command Systems

Optical Trackers

Communications

A-6, TELEMETERING AND FREQUENCY MONITORING

3 Missile Telemetry Systems

3 Drone Telemetry Systems

Frequency Monitor and Interference Control

Communications

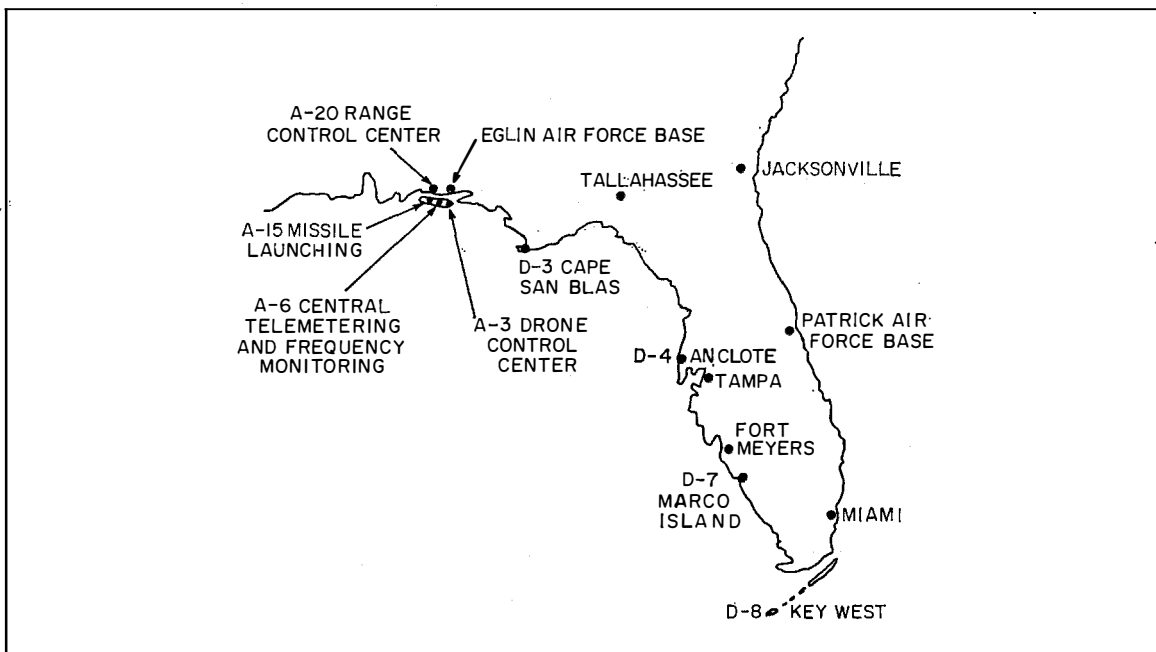


Figure 1—Geography of the Eglin Gulf Test Range.

Eglin Gulf Test Range

A-15, MISSILE LAUNCH FACILITY

Beacon Check
Telemetry Check Out
Timing Count Down
Communications

A-20, RANGE CONTROL CENTER

3 *AN/FPS-16* Radars
3 Phototheodolites
3 Skyscreens
Communications

D-3, CAPE SAN BLAS

3 *AN/FPS-16* Radars
2 *AN/MPS-9* Radars
1 *AN/MPQ-31* Radar
3 Missile Telemetry Systems
3 Drone Telemetry Systems
Communications
Frequency Monitor and Interference Control
3 *AN/FRW-2* Ultra-High-Frequency Command Systems

D-4, ANCLOTE

3 *AN/FPS-16* Radars
2 *AN/MPS-9* Radars
1 *AN/MPQ-31* Radar
3 Missile Telemetry Systems
3 Drone Telemetry Systems
Communications
Frequency Monitor and Interference Control
3 *AN/FRW-2* Ultra-High-Frequency Command Systems

D-7, MARCO ISLAND

2 *AN/FPS-16* Radars
1 *AN/MPS-9* Radar
1 *AN/MPQ-31* Radar
2 Missile Telemetry Systems
2 Drone Telemetry Systems
Communications
Frequency Monitor and Interference Control
3 *AN/FRW-2* Ultra-High-Frequency Command Systems

D-8, KEY WEST

1 *AN/MPS-9* Radar
1 *AN/MPQ-31* Radar
2 Missile Telemetry Systems
2 Drone Telemetry Systems
Communications
Frequency Monitor and Interference Control
3 *AN/FRW-2* Ultra-High-Frequency Command Systems

2. Site A-20

Site *A-20* is the range control center and is therefore normally responsible for the conduct of test missions. This site contains the major range control consoles, facilities for range safety, optical and radar instrumentation, and the various required support systems.

Figure 2 shows a portion of the range control room including some of the primary-control consoles. The console for the mission commander is shown in the right foreground. The mission commander has over-all responsibility for the proper conduct of a mission. To perform his functions, his console is provided with the necessary indications, displays, and communications so that he may have for evaluation all factors that might contribute to the failure of a mission.

Immediately to the left of the console for the mission commander is that for the mission coordinator, who performs his duties under the supervision of the mission commander. The mission coordinator is responsible for the control of the count-down system and to notify the range sites through the public-address system of announcements and alert notifications. There are 3 independent count-down systems because of the 3-missile firing capability.

The range safety officer occupies the console in the center of the control room. He is provided with the necessary indications, displays, and controls to insure that proper precautions are taken to prevent injuries to personnel or damage to property.

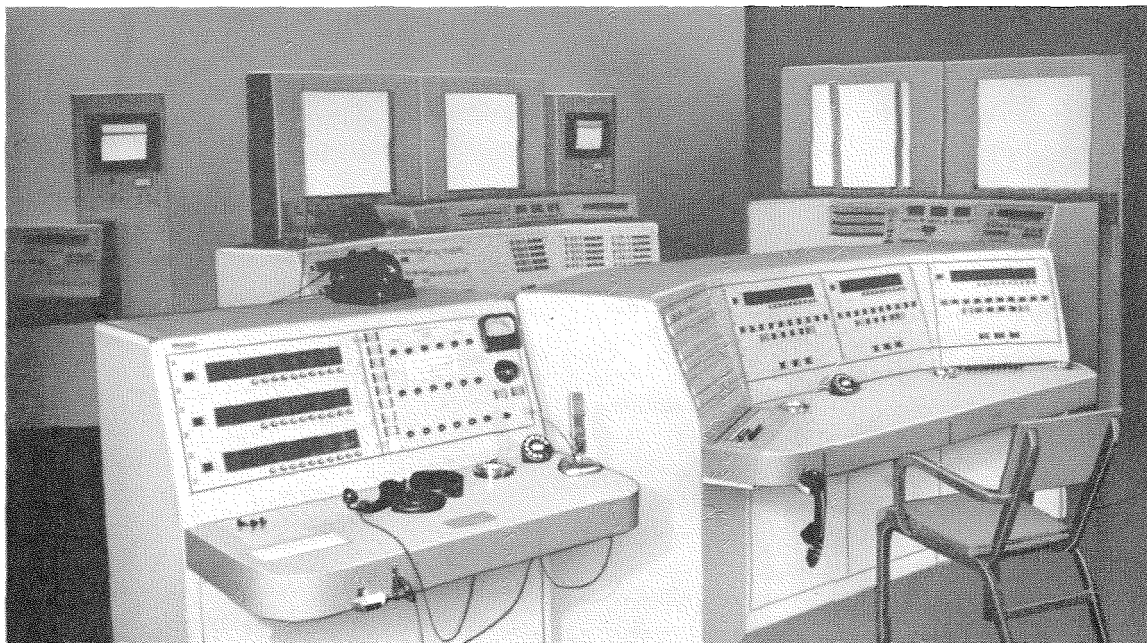


Figure 2—Range control room at A-20. In the foreground, the right and left consoles are for the mission commander and the mission coordinator, respectively. The range safety officer uses the center console. At his right is the data selector's position. At the rear are the missile safety consoles.

Seated next to the range safety officer is a data-selecting operator. This individual has the duty of deciding, on the basis of indications on his panels, which site of radar data to connect to the communication buses so that the best information available may be utilized by the various sites for remote acquisition and for the plotting-board data used for range safety purposes.

In the background of Figure 2 are 2 of 4 missile safety consoles. A console is required for each of the 3 missile complexes. A fourth identical console was furnished to provide a future capability; each console may be employed for any of the 3 missile complexes.

The missile safety officer is responsible for monitoring the performance of the missile from the prelaunch period until it has completed its mission. He is given the capability of preventing the launching from taking place and of

destroying the missile at any time in its flight.

To perform these functions, the missile safety officer is provided with several visual displays including two vertical plotting boards placed at the rear of the consoles. One board plots the missile position in XY and XH (altitude above the earth) cartesian coordinates over the entire test range. The second board shows an expanded or folded display for the A-20, D-3, D-4, D-7, or D-8 areas. These plotting boards are always provided with the best data available on the range as chosen by the data selector.

During the launch period, indications are received from each of the optical trackers at 3 sites including A-20 showing the azimuth of the missile at this critical phase of the mission. The missile-safety officer has the capability of transmitting destruction signals in case of malfunction of the missile and, during the flight of the missile, he will select the site to be utilized for

this transmission and whether ultra-high-frequency radio or radar will be the transmission means.

3. Site A-3

Site *A-3* is the drone-control center of the range and is provided with radars, ultra-high-frequency command guidance equipment, and optical equipment for tracking and controlling as many as 3 drones. The site is also provided with several control consoles. The most significant of these consoles from an operation standpoint is that for the drone control officers. As in the case of the missile safety console, four identical consoles were supplied with the fourth providing a back-up capability for the others. Figure 3 is a photograph of the drone control console. The function of the drone controller is to fly his assigned drone along the path described for a particular mission and to perform the safety functions required when the drone ceases to respond to the command signals.

The drone controller is presented with flight performance data such as heading, altitude, engine rotational speed, et cetera, and with information defining the spatial position of the drone. The spatial information is presented on plotting boards in a manner similar to that for the missile. The flight performance data are obtained from the telemetering ground stations. A chain telemetering control system selects for

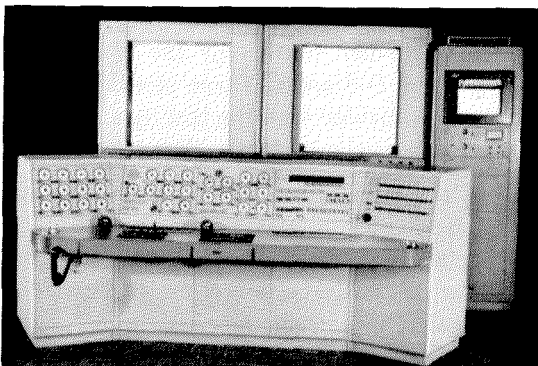


Figure 3—Drone control console and plotting boards at site *A-3*.

display on the drone controller's console the data from the site receiving the "best data". The drone controller, utilizing both the telemetering and radar data, initiates commands for changing the flight path of the drone. The drone controller can also select the site through which the command or destruction signals will emanate. The drone complexes include various voice communication facilities including an air-to-ground link.

4. Site A-6

Site *A-6* is the master telemetering station providing facilities for the reception of telemetering signals from 3 drones and 3 missiles. This station performs the important function of monitoring the performance data of the missiles and drones as well as selecting the best data available for presentation to the drone controllers.

5. Down-Range Sites

The down-range sites *D3*, *D4*, *D7*, and *D8* contain tracking radars and telemetering receiving stations as well as secondary range safety and drone control facilities. These facilities are similar to those described for *A-20*, *A-3*, and *A-6*, except that the remote control and select features are not present. Each down-range site is capable of performing all the range functions on a local basis and therefore if failure of the remote-control features occurs, control can be turned over to the local site. The handover from site to site can be accomplished by simple voice communication.

6. Radar

The primary function of the radar system is to obtain high-precision data of the flight paths of the airborne objects for the purpose of range safety, performance evaluation, and command control and destruction of the airborne objects. The three radar types utilized are *AN/FPS-16*, *AN/MPQ-31*, and *AN/MPS-9*.

The *AN/FPS-16* is a high-precision instrumentation radar operating in the *C* band. Three



Figure 4—Range control building and phototheodolite building at site A-20. The three AN/FPS-16 radar antennas are visible on the roof.

AN/FPS-16 pedestals and antenna structures are shown on the roof of site A-20 in Figure 4. The other two radars are modified versions of van-mounted S-band radars.

The radars provide data consisting of slant range, azimuth, and elevation. The AN/FPS-16 and the AN/MPQ-31 generate these data in digital form (primary data) and in analog form (secondary data). The AN/MPS-9 provides only analog data. Each of the radars has the capability of accepting remote acquisition data in analog synchro form.

The radar sites were strategically located so that the airborne vehicles would be continuously tracked and, if required, guided over the range with at least 2 sites tracking the target simultaneously.

As previously mentioned, the range was designed to track and control 3 drone and 3 missiles simultaneously. In addition, it was required that as many as 3 adjacent sites be capable of tracking a given target simultaneously to provide backup for range safety, guidance, and remote acquisition. Therefore, there can be as many as 6 radars tracking and interrogating

different targets from a given site location as well as radars at different sites attempting to interrogate a given target.

A radar synchronization system was developed to permit the radars to perform properly under this environment.

The two major functions that the synchronization system must perform are as follows.

(A) Prevent interference between the radars at a given site location.

(B) Prevent interference at the airborne beacon caused by the interrogation of radars at different sites before the beacon has had adequate time to recover.

The first function was accomplished by the synchronization of all the radars at a given site so that their transmitted pulses are emitted simultaneously. The second function required not only synchronization of the radars between sites but also the insertion of a fixed delay at each of the sites relative to a master site.

The interference-free range obtainable with a system of this type is a function of the range geometry, the pulse-repetition frequency, and

the beacon recovery time. When a radar at each of 3 adjacent sites is actively tracking a given beacon, an interference-free range of 200 miles is available from each radar if 341 pulses per second are transmitted and the beacon recovery time is less than 250 microseconds.

One method of synchronizing all the radars at a single site is to supply each with a common 82-kilocycle-per-second reference signal from which a pulse-repetition-frequency trigger signal is developed.

This method is not used to synchronize between sites because the communication system can transmit only in the voice-frequency band. Instead, a sine-wave signal at the pulse repetition frequency is transmitted between sites and controls by phase-lock loops a local oscillator of approximately 82-kilocycles per second through which the radar pulses are synchronized. All of the radars at the site are so synchronized. A return path is provided from each site to the master site to determine the delay in transmission through the communications system. Half this loop delay must be subtracted from the total delay required at that site. The synchronizer unit has provision for inserting the required calibrated delay.

7. Radar Data System

Primary and secondary forms of space coordinate data are generated. The primary data generated by the *AN/FPS-16* and the *AN/MPQ-31* radars consist of 3 words: azimuth, elevation, and range. These words are converted by optical and mechanical disc encoders to binary code within the radar. A word of 17 bits each is produced for azimuth and elevation and of 20 bits for range.

The 3 words go to a data converter that adds 2 more words, identification and time. Identification is a 34-bit word encoding radar number, site, object tracked, mission, year, month, and day, which is generated internally in the converter. Time in hours, minutes, seconds, and milliseconds is a 27-bit word that is supplied to the data converter from the timing system.

The 5 words are converted to a serial parallel *IBM-704* format. Lateral and longitudinal parity checks are added by a parity-generator circuit. There are 5 sampling rates available between 10 and 100 pulses per second. Figure 5 is a photograph of the data converters and magnetic tape recorders. The data, which is multiplexed on 7 parallel recording lines, is applied through a buffer to the 7-channel magnetic-tape recorder. The 7-channel data also goes to a data control unit, converted to nonreturn-to-zero format and applied to the intersite communication bus. If chosen by the data selector, the primary data are transmitted to a master recorder at the computation center. In this way, each site has a local recording in *IBM-704* format of its own data obtained during a mission and the computation center has a master recording of the best data available from the different sites as the mission progressed. These tape recordings are utilized in the performance evaluation of the missile.

The transmitted primary data may also be supplied to an *IBM-704* computer in which real-time computation may be performed.

The radar secondary data are generated in the form of polar analog voltages derived from precision sine-cosine potentiometers and a slant-range (linear) potentiometer within the tracking radars.

The data are converted from polar to cartesian form for application to local plotting boards, height recorders, and data transmitters. The data transmitters convert the *XYH* data to time-multiplexed binary words at the rate of 10 frames per second. Each of the 3 data words (*XYH*) is represented by 13 binary bits; therefore, 39 of a total of 48 bits are assigned to the analog information. The remaining 9 bits are comprised of control and synchronization information. The output of the transmitters is applied to the communication lines when chosen by the data selector and transmitted to the other sites. The receiving sites utilize data receivers that convert the data back into analog form. The remote secondary data can be applied to

plotting boards and height recorders or it can go through cartesian-to-polar converters and supply synchro information to facilitate target acquisition by the radars.

Correction circuits for parallax and earth-curvature are contained in the polar-to-cartesian and cartesian-to-polar converters as well as in the plotting boards and height recorders so that the plotted data are referenced to the local site.

The facilities provided for both the *S*-band and *C*-band radar chains are essentially the same.

To transmit that primary or secondary data that represents the best information on the range, a signaling and control system is utilized. A radar group leader at each site obtains data quality information in the form of indications from the local radar operators and by observation of the local plotted data. From this information, the radar group leader indicates the quality by selector buttons. This indication from each of the sites is sent up-range to the respective data selectors at sites *A-20* or *A-3*. The data selector is then able to select the best data by pressing a button that operates relays connecting the data transmitter at the selected site to the communication data bus so that it can be received by the other sites. If remote selection fails, data can be placed on the communication lines at the local sites using voice communication.

In most instances, a fourth set of primary and secondary data equipment exist at each site to provide a spare or back-up capability.

8. Optical System

The optical system provides a facility for the observation and recording of the behavior of missiles or other airborne vehicles under test. Flight performance during launch, lift off, the first part of the flight trajectory, and the region of target interception can be documented with range time for evaluation.

In addition, the optical equipment provides data for range safety, radar target acquisition, and radar tracking calibration and error correction. The recorded space position and attitude data

contain range time for correlation with the various other types of data obtained on the range.

The optical system has a capability for tracking and photographically documenting 3 simultaneous flights as in the case of the other systems.

The equipments used to obtain the outlined capability are phototheodolites, optical trackers, boresight cameras, and a telescopic photographic recorder. Each optical installation includes the necessary communication facilities, count-down indicators, and timing terminal equipment.

During early phases of a missile flight, radar tracking may not be possible due to ground clutter. The optical data, therefore, serve as the only accurate record of performance at this time.

A missile-launching site is located at *A-15*. Appropriately located around it, are sites *A-13*, *A-18*, and *A-20*, where phototheodolites are used. Model *IV* boresight cameras and the *M2* optical trackers are installed at site *A-20*. In addition to their normal tracking function, *M2* trackers are used to supplement the range safety trackers installed at sites *A-13* and *A-18*, which are adjacent to the launch site. Mark *51* optical trackers and model *IV* boresight cameras are located at sites *A-3*, *D-3*, *D-7*, and *D-8*. The telescopic photographic recorder is located at *D3* as this site is the expected interception vicinity of the drone and missile for certain

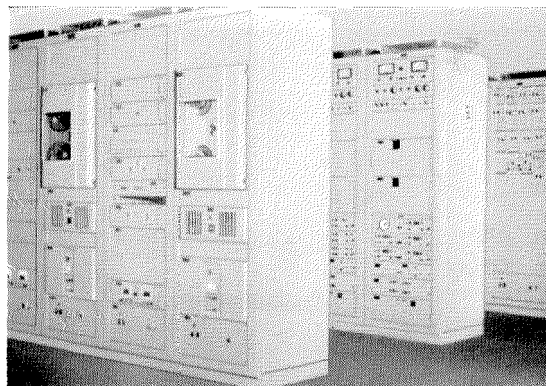


Figure 5—Data converters and magnetic tape recorders.

evaluation test programs. The telescopic photographic recorder is basically a long-focal-length telescope and motion-picture camera designed to record objects in flight. It is capable of distinguishing an object 2 inches by 6 inches from a distance of approximately 4 miles. The recorder is slaved to the *AN/FPS-16* or *AN/MPQ-31* radar for target acquisition, and can be switched to manual tracking when the target comes within telescopic range. Manual tracking is accomplished by 2 operators using individual controls, one for azimuth and the other for elevation. The *M2* and *Mark 51* optical trackers were adapted to provide target acquisition data for the radars. Azimuth and elevation synchro data are directed to the radars, enabling them to acquire and begin tracking during the portion of a flight when the radar return is obscured by ground clutter.

The phototheodolite is basically an optical measuring device with an associated 35-millimeter motion-picture camera. It is employed in the precision measurement and recording of motion in space and provides a continuous record of attitude, position, and trajectory of moving objects for documentation and evaluation. Azimuth, elevation, and time are simultaneously recorded on the film to provide data correlation. The equipment is also utilized for the checking and dynamic calibration of *AN/FPS-16* radars. Figure 4 shows the phototheodolite building at site *A-20*.

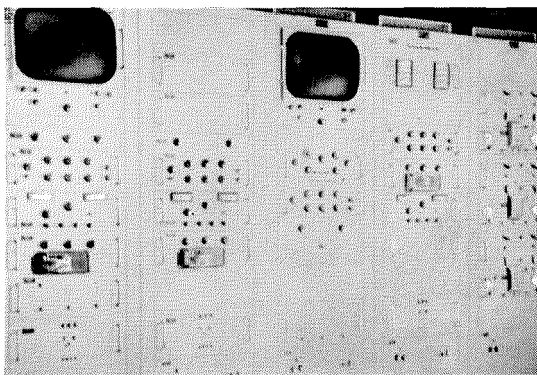


Figure 6—Section for demodulating the pulse-duration-modulated signals.

The timing system provides timing information to be recorded on film with the picture and pulses to operate camera shutters and flash or strobe lamps. The timing information is given once per second and consists of a 17-bit code word at a 1000-pulse-per-second rate. The shutter and strobe-lamp pulses are supplied at rates of 1, 5, and 10 pulses per second.

9. Telemetry

The telemetry system provides the simultaneous reception of data from 6 airborne objects at sites *A-6*, *D-3*, and *D-4* and from 3 objects at sites *D-7* and *D-8*. The sites are positioned along the range so that at least 2 sites can receive data at any time. A nearly complete back-up system is provided at each site in the event of equipment failure.

The telemetry system provides separate equipments to support the missile and drone functions. However, the equipment and patching facility is arranged so that any desired configuration is realizable.

The major function of the missile section is to monitor and record the missile telemetry data. There are 4 antennas and receiving systems provided with one being available as a back-up facility. At each site, 2 magnetic tape recorders are supplied to record the composite missile signals. There are 16 fixed and 3 band-switching discriminators and a decommutator station is provided to demultiplex pulse-duration-modulation or pulse-amplitude-modulation missile signals. An oscilloscope monitor for pulse-duration or pulse-amplitude modulations and an oscillographic recorder are provided for monitoring the missile data. Figure 6 is a photograph of the demodulator section for pulse-duration modulation.

The major function of the drone section is to receive data from 3 drones for presentation to the drone controllers throughout the range. Each site has 2 magnetic tape recorders for the composite signals.

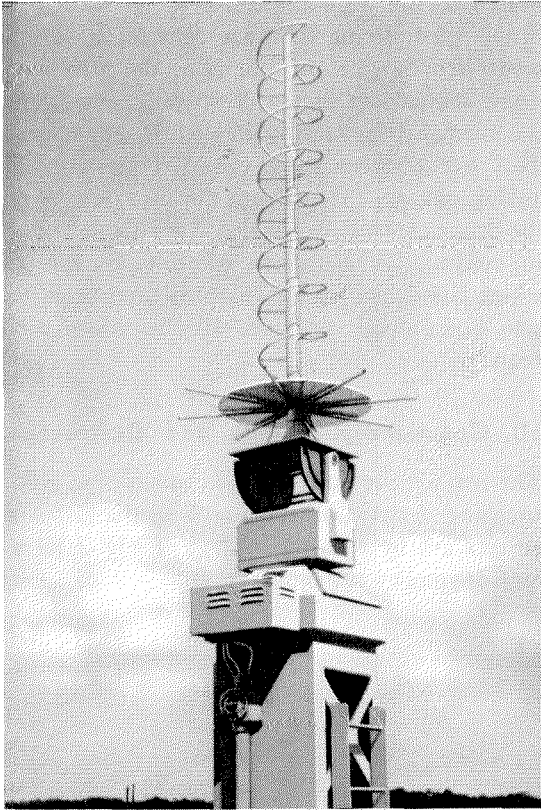


Figure 7—Single-helix telemetering antenna.

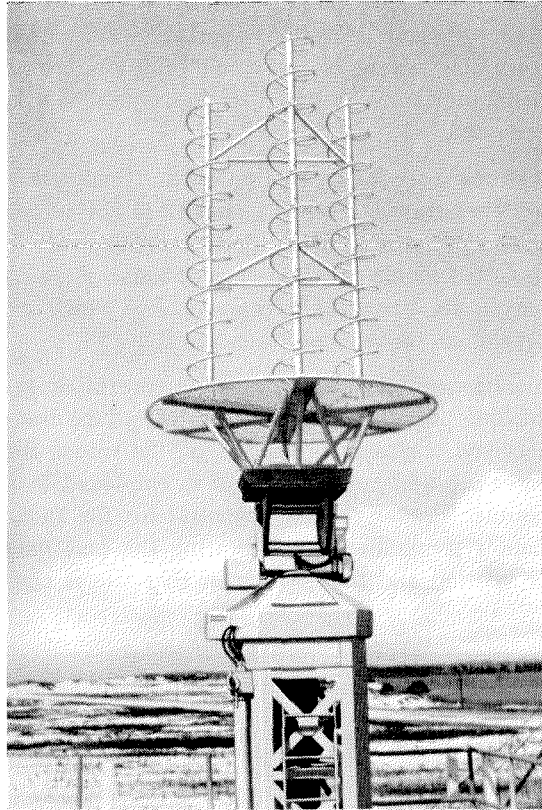


Figure 8—Trihelix telemetering antenna.

There are several types of drones contemplated for use on the Eglin Range. Typical of these are the *QB47*, *QF80*, *Regulus*, and the *Q2*. In an attempt to satisfy the various requirements, each of the 3 drone telemetering stations consists of 12 discriminators. The data-transmission encoders accept the 12 outputs representative of such functions as heading, air speed, attitude, et cetera and convert them to a time-multiplexed digital train. Each output is sampled 10 times per second and is converted to an 8-bit-plus-sign digital code. Because the resulting pulse repetition is too high for reliable transmission over a standard voice channel, the output bits of the encoder go alternately to 2 parallel voice lines. By this method and the use of a nonreturn-to-zero binary code, the

maximum pulse repetition rate is held to 500 pulses per second, which can be handled reliably on a standard voice channel.

The missile data transmission telemetering method is essentially the same as the drone system with the exception that only 6 channels of information are transmitted for each missile.

Each major telemetering site has a total of 7 helical antennas, of which 6 are single-helix types and one is a trihelix. Figures 7 and 8 are photographs of the single helix and the trihelix antennas, respectively. The single helix has a gain of 13 decibels and a beam width of 40 degrees. The trihelix has a gain of 19.5 decibels and a 20-degree beam width. The antennas are remotely positioned from control positions in

Eglin Gulf Test Range

the telemetering building shown in Figure 9. Azimuth and elevation synchro information from the radars is presented on the control-panel indicators. A signal-strength meter is also provided.

The radio-frequency section of the telemetering system covers the range from 215 to 260 megacycles per second. A 20-decibel preamplifier is mounted inside each antenna pedestal. At each major site, there are 9 receivers, 7 of which are crystal controlled and 2 are tuneable.

To transmit the data for drone control or recording purposes that is obtained from the best-received telemetering signals on the range, the signaling and control system is employed in a manner similar to that described for the radar data system. The site indicating the best data is selected and the encoder at that site is con-

nected to the communication bus. The digital drone telemetering data are sent to the drone controller consoles at site A-3, the auxiliary drone controllers at the down-range sites, and the master telemetering site A-6. The digital data are converted by the decoder into 12 analog outputs that actuate the instruments on the drone controller consoles. This display, used in conjunction with the plotting boards on which the drone position is presented in cartesian coordinates, provides all the information required to control a drone.

10. Command Guidance and Destruction

The two primary methods of transmitting guidance and destruction commands to the airborne objects are by radar or by *AN/FRW-2* ultra-high-frequency transmitters.

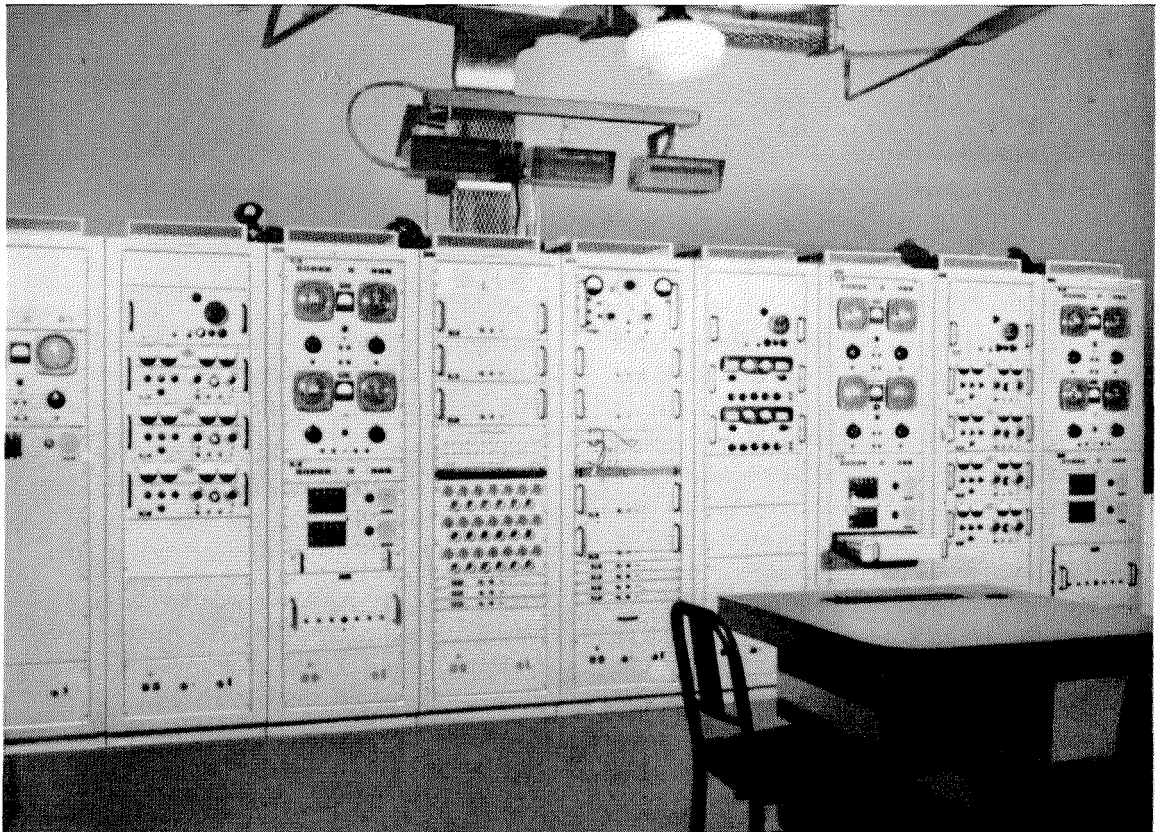


Figure 9—Telemetering receiver section and antenna control positions.

Radar command guidance is performed through various beacon encoders by time modulating the beacon pulse code by single or multiple tones or by changing the pulse code.

Command guidance by means of the ultra-high-frequency transmitter is accomplished by coders that provide tones that either frequency modulate or frequency-shift-key the radio-frequency carrier. The missile and drone control or destruction commands are initiated from the missile safety consoles and drone control consoles, respectively.

The missile safety officer or drone control officer may select a central or local mode of operation. In the local mode, decisions to transfer control from site to site are done aurally. In the central mode, the officer selects the command source, defining the site at which the radar or radio-transmitter coders are keyed and the signals transmitted. The mode to be used: radar, *AN/FRW-2*, or a combination of both, can also be selected. In the central mode, the down-range sites are locked out and cannot initiate commands unless this restriction is removed by the drone controller at *A-3*.

By the information presented and the control techniques described, an operator at a console in the Eglin Air Force Base area can control an airborne vehicle over the entire length of the range through the facilities at each of the sites.

11. Timing System

The timing system provides the means of obtaining high-accuracy time correlation of the various forms of data generated on the range and, in addition, generates the various synchronized sampling rates and the time base for the count-down system.

Extremely high accuracy of timing signals is achieved by means of a 1-megacycle-per-second frequency standard incorporated in the master time generator at site *A-20* and in the slave time generators at each of the down-range sites. The stability of the frequency standard is 1 part in 10^9 per day. The system makes provision for calibration against the timing signals of *WWV*.

Figure 10 is a photograph of the master time generator.

Another feature of the system is the high degree of accuracy of time correlation between signals produced by timing equipment at all sites of the range. This accuracy is obtained through use of a synchronizing signal, produced by the master time generator, that is transmitted via land lines, microwave, and forward-scatter communication systems to all the slave time generators. Timing signals generated by the slave time generators are synchronized to within 50 microseconds of those produced by the master generator. Should the synchronizing signal be lost, the system will maintain accuracy to within better than a $\frac{1}{4}$ millisecond over an 8-hour period.

The system includes provision for the transmission of a 1-pulse-per-second timing signal between each slave and the master generator. This permits the measurement of transmission delay,

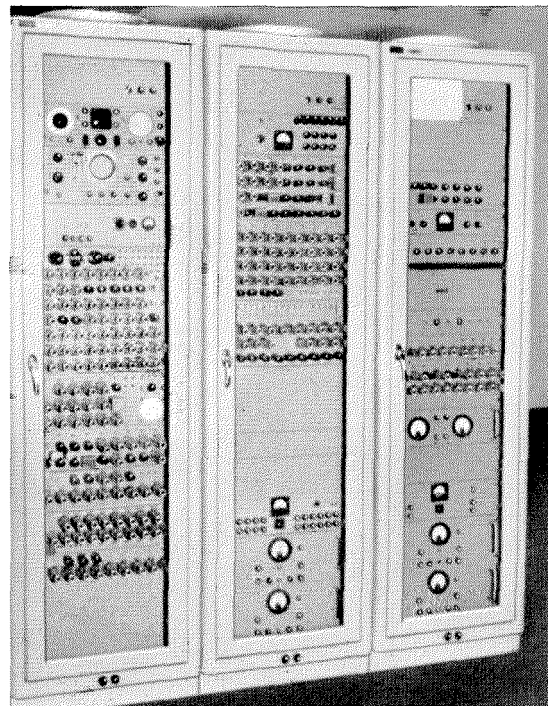
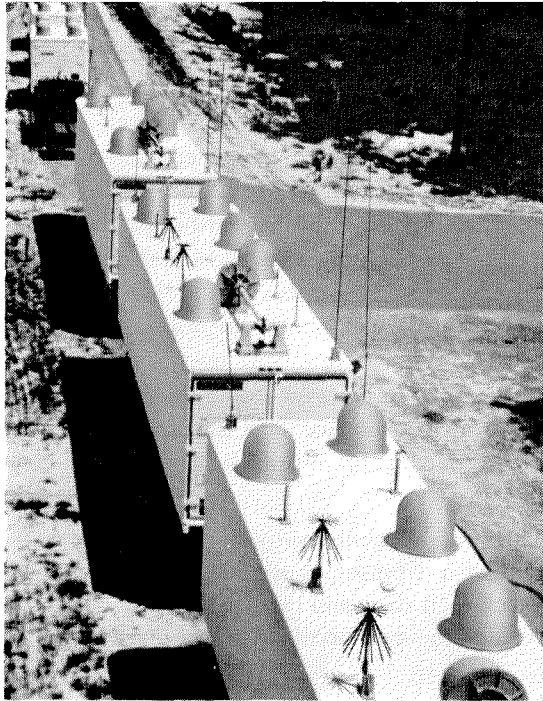


Figure 10—Master time generator.

Figure 11—Frequency monitoring and interference control installations in semifixed vans.



which can be compensated for in each slave generator.

In the previous discussions, several of the timing signals utilized by the various instrumentation equipments have been mentioned. The master and slave generators control terminal units that generate the specific time codes for the plotting boards, cameras, tape recorders, and the various paper recorders.

12. Frequency Monitoring and Interference

A frequency-monitoring and interference-control system was developed. As indicated by its name, one of its functions involves the monitoring, recording, and evaluating of guidance and destruction signals pertinent to an operational mission, and the other involves the detection, analysis, location, and recording of signals that may possibly interfere with any part of the mission operation.

Figure 12—Chase vehicles used for frequency monitoring and interference control.



Frequency monitoring helps prevent serious shifts in carrier frequencies, drops in carrier strength, changes in radar pulse-repetition frequency and pulse width, and deviations in other areas of importance. Control functions can be recorded as a function of range time during a test, thus providing a permanent record for future reference if the need arises to determine the cause of a malfunction.

Interference control is fundamentally a safety measure to guard against the generation and existence of undesirable radio-frequency radiations. The high concentration of transmitting, receiving, and general electrical and electronic equipment in the range area places a high degree of importance on interference control because of the possibly serious consequences of spurious signals.

Various equipments are utilized to monitor the radio-frequency spectrum in the vicinity of the range. These equipments and the supplementary facilities that comprise the system can detect and locate radiation on all frequencies between 15 kilocycles per second and 10.75 gigacycles per second.

Three types of installation are used at various sites. There is the fixed type, which is located in the building at site *A-6*; the semifixed type, which is installed in semitrailer vans located at down-range sites; and the mobile support, which is furnished the sites by chase vehicles containing monitoring equipment.

Figures 11 and 12 are photographs of the semifixed vans and the chase vehicles, respectively.

The basic receivers get their signals from suitable antennas or direction-finder systems. The signal is tuned and converted into several different useable forms. One of these is an audio-frequency signal that can be directed to a loudspeaker, headphones, or a tape recorder. Another form is the automatic-gain-control voltage produced by the signal. It can actuate a graphic recorder to represent signal strength. Intermediate-frequency or video-frequency outputs can be connected to panoramic spectrum analyzers and the resulting displays can be

photographed with an oscilloscope camera. Radar receivers are connected to signal analyzers, which are used to display characteristics such as pulse width, pulse-repetition frequency, and signal-to-noise ratio. Motion-picture cameras are used to document displays on this instrument. Range-time data are simultaneously recorded on the various tape and graphic recorders along with the receiver outputs.

13. Communication System

The entire communication system was specifically designed to support the requirements of the range. Both microwave and forward-scatter systems are used. The forward-scatter system is required between sites *D-3* and *D-4* and between sites *D-7* and *D-8*.

The microwave system operates in the band from 7125 to 7750 megacycles per second. Paraboloidal antennas and tower-mounted reflectors are used for the antenna systems. Dual frequency diversity is provided on all paths since reliability of the highest order is required.

The forward-scatter system operates between 1700 and 1785 megacycles per second. It achieves 4-fold diversity by the use of 2 separate power amplifiers operating at different frequencies energizing 2 antennas at the transmitting end and 2 antennas in space diversity supplying signals to 4 receivers at the receiving end.

Table 1 indicates the number of voice-quality channels assigned to the various range functions. The channel bandwidth is 250 to 3100 cycles per second. On all the data channels, the information is in digital form.

In addition to the voice-quality channels, there are several channels having special characteristics. The timing and synchronizing signals could not use the standard voice channels because the phase and frequency error produced by the reinsertion of the carrier at the receiving site in the single-sideband transmission could not be tolerated. This problem was corrected by placing these signals on a double-sideband frequency-modulated carrier channel.

Eglin Gulf Test Range

Function	Number of Channels	
	Up Range	Down Range
Missile Secondary Data	3	3
Drone Radar Data	3	3
Drone Telemetry Data	6	6
Missile Telemetry Data	3	3
Signal and Control	12	9
Count-Down	—	3
Missile Fixed Network	3	3
Drone Fixed Network	3	3
Frequency Monitor Network	1	1
Air to Ground	3	3
Operational Intercommunication	6	6
Public Address	1	1
Dial Telephone	9 Duplex Trunks	

The primary data utilizes 21 frequency-shift-keyed channels, 7 for each system, which were equalized and broadened in bandwidth to satisfy the requirements of the digital information rates.

14. Signaling and Control

In the preceding discussion, some of the functional uses of the signaling and control system have been mentioned. This system provides the necessary indication and remote control for the various range functions.

These functions can be divided primarily into quality indications, data-source selection, range status, and command guidance and destruction.

Functions that are critical to the operational support and safety of a mission are equipped with confirmation paths to indicate that the transmitted control function has taken place at the remote site.

The major components of the signaling and control system consist of tone equipments for signal transmission between sites with a variety of relay circuits for performing switching functions.

Frequency-division-multiplex equipment provides 23 channels on a standard voice-frequency

line. Frequency-shift keying is used on these channels with the transmission of one frequency indicating a mark signal and transmission of another frequency indicating a space. In addition, time-division-multiplex equipment is used on several of the frequency-division channels. This was done primarily to obtain more-efficient utilization of the available communication spectrum. Each time-division channel will provide a maximum of 32 functions on each frequency-division channel.

15. Support Systems

There are several support systems that play important roles in an integrated range including the count-down system and various voice communication systems.

The count-down system provides accurate visual time displays simultaneously at every site. It is divided into 3 independent identical systems as a result of the multiple-missile-firing requirements.

The count-down system is based on a digital logic operation. A 6-digit indication of time in hours, minutes, and seconds is presented from minus time (prelaunch) running downward through zero, then in a positive direction (post-launch). The master count-down generator receives 1-pulse-per-second signals from the timing system. The signal is encoded and transmitted to the remote slave units. The remote units receive the coded signals and convert them into closures for the visual time displays.

The count-down system can be preset and started at the master generator or remotely from the mission-coordinator console. The visual indicators also display "hold fire" and "lift off". Hold-fire signals initiated by designated personnel will stop the count-down. The system can be programmed so that on command from a missile-launch sequencer it will recycle to a preset condition.

The range has several voice communication systems, which include a public-address installation, a command control system, operational intercommunication equipment, dial telephone,

party line for local equipment operators, and an air-to-ground system. Each of these voice systems has a prescribed function in the operation of the range.

The command control or fixed networks provide the primary intersite voice communication used during operational missions. At critical positions, loudspeakers are installed to permit constant automatic monitoring when the headset is removed or when an operator is using another voice system.

There is a total of 7 fixed networks, 3 for the missile complexes, 3 for the drone complexes, and one for frequency monitoring and interference control. The fixed networks are effectively range-wide party lines that are continuously monitored and controlled by designated operational personnel.

The operational intercommunication system is key operated and provides communication between the buildings and between the various consoles at each site.

The air-to-ground system provides communication with piloted aircraft in controlling a drone, air launching of a missile, or other flight testing. The air-to-ground communication system at each site is designed so that the drone-control officer at the control site can select one or more sites for transmitting or receiving. The press-to-talk switch also keys the transmitter at the selected site. The received signals are transmitted to all the sites via the range communication system.

16. Conclusion

The Eglin Gulf Test Range was designed and built to be an integrated facility having a high degree of versatility and flexibility in handling a vast variety of range requirements. It has been in operation for well over a year supporting single and multiple missile firings.

Like the world around us, a range is in a state of continuous evolution so that it may fulfil not only the present mission requirements but those of the progeny of the existing missiles and space vehicles.

17. Acknowledgment

The program was accomplished under Air Force Contract AF01(601)-21123. ITT Federal Laboratories was the prime contractor for the instrumentation of this range. As systems manager, it had responsibility for the design, development, fabrication, procurement, and integration of the system as well as for the installation, maintenance, and operation of the range. It was supported by two other International System organizations, Federal Electric Corporation and ITT Kellogg.

There are many individuals who are important contributors to a program of the magnitude of the Eglin Gulf Test Range. I would like to acknowledge the support and cooperation of Dr. A. M. Levine, A. Smolen, C. Elbert, and C. Maasik for the major roles they played in this activity.

Flight Simulator for Mirage III

S. M. POOLE

Le Matériel Téléphonique; Paris, France

Aircraft flight simulators used for flight crew training represent a rather special application of the electronic art and of analog computing. While embodying many of the classical features of analog computing, the simulator uses various electric and electronic systems to achieve faithful synthesis of all aspects of aircraft performance. A flight simulator is designed to train members of a flight crew in all matters relating to the operation of the aircraft from the starting of the engine on the ground before take-off to final shutdown after landing.

Target detection by radar and interception by guided missiles or gunfire have also been incorporated in the simulator. A synthetic sound system reproduces engine noises as well as sounds made by generators, converters, hydraulic pumps, undercarriage, flaps, and dive-brake operation, including the effects of wind, rain, and other weather conditions.

Figure 1 shows a block diagram of a typical simulator. The use of electronic or electro-

mechanical computing in a simulator is a relatively recent innovation. Early training devices, such as were pioneered by Link Aviation, were not flight simulators for a specific aircraft but were simply very generalized trainers based on a typical airplane. They frequently employed hydraulic or pneumatic devices. The effects of radio aids were introduced manually by the instructor.

Another limitation was the inability to simulate engine and auxiliary equipment with any degree of realism. The imitation of flying qualities of the early machines left much to be desired.

In 1939, Le Matériel Téléphonique was granted a patent in which for the first time the application of electronic devices to flight training equipment was suggested. The patent described the application of electric devices to the flight system, track recorders, and radio aids together with a primitive visual system for training in bombardment. In 1947, the prototype L.M.T. 141 flight trainer shown in

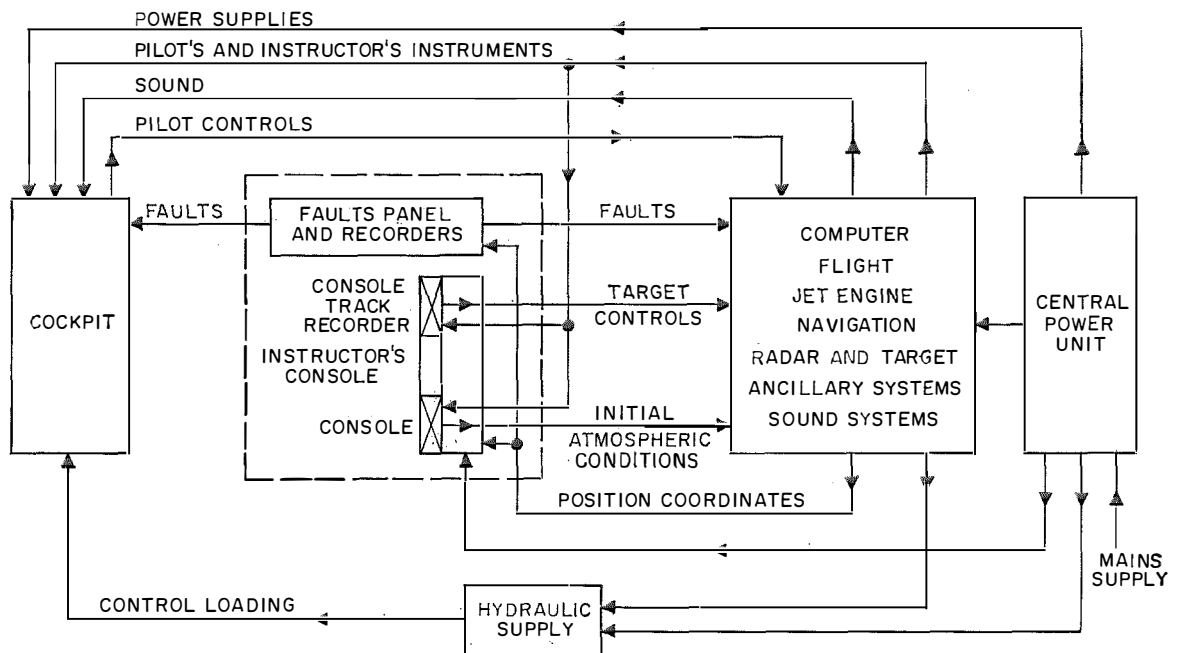


Figure 1—Flight simulator for Mirage III aircraft. The individual power supplies, derived from the alternating-current mains, have been omitted for clarity.

Figure 2 was completed. About 60 of these were manufactured.

Since the war, the growing complexity of aircraft and of navigational and combat systems has had a corresponding impact on flight simulators. The simulator for the Mirage III has more than a thousand transistors and fifty servomechanisms despite the use of every modern technique to minimize the volume of material and the number of components.

1. Technical Considerations

The Mirage III is a single-seater single-engined fighter-interceptor aircraft. The simulator for it is equipped with artificial airborne radar and guided missiles and may be considered to be a typical example embodying the latest technical features of the art.

Figure 3 shows the typical arrangement of this simulator as installed in a semitrailer. The main items are the cockpit, which is at the extreme left in the compartment with the instructor's console, various track and other pen

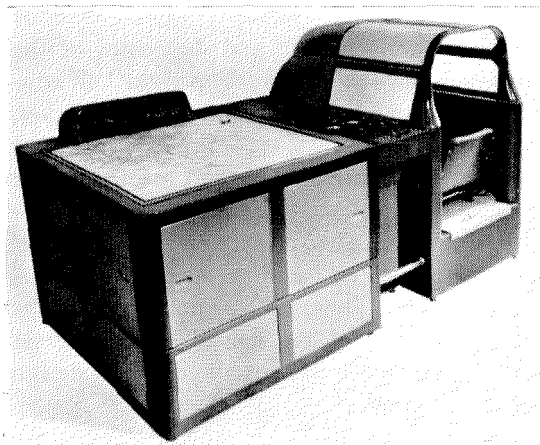
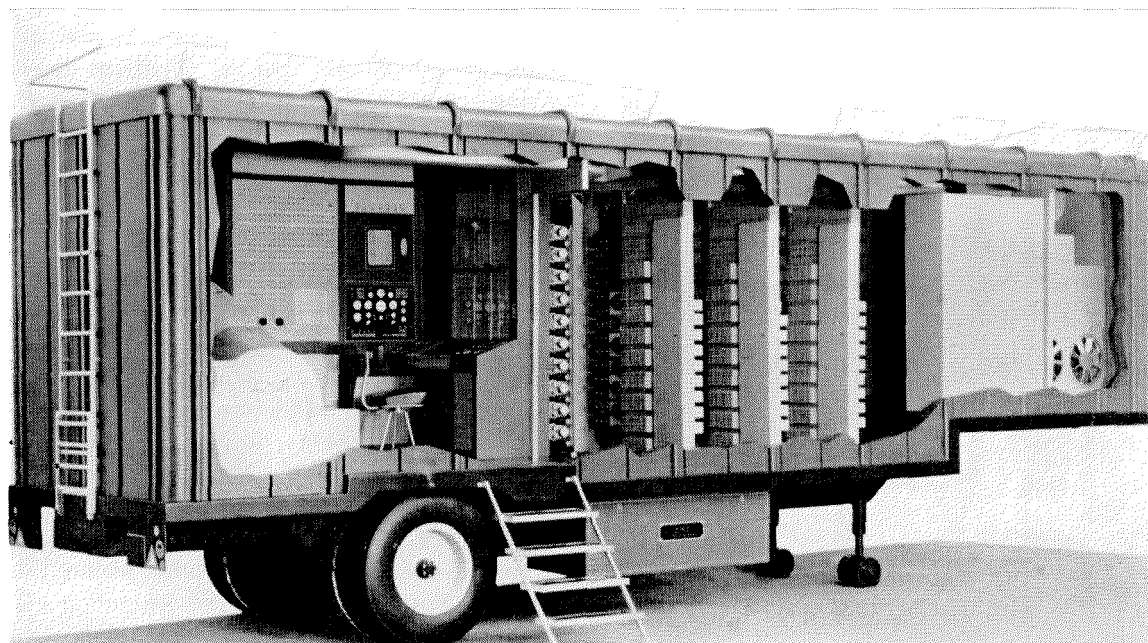


Figure 2—Prototype flight trainer of 1947.

Figure 3—Mirage III simulator. The student's cockpit is at the left next to the instructor's controls and recorders. The computer and the power and air-conditioning plants occupy the right half of the trailer.



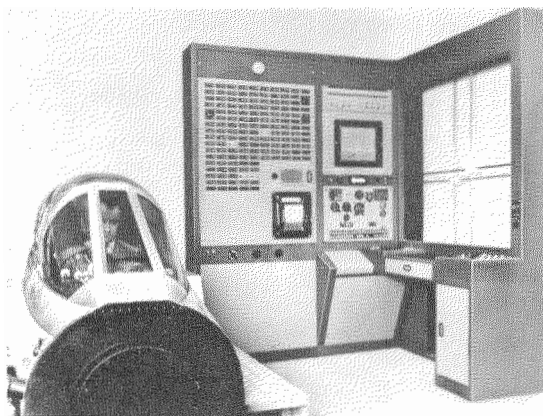
Flight Simulator for Mirage III

recorders; panels to set up troubles, exterior conditions, and targets; and duplicates of the instruments in the cockpit. The right half contains the computer for flight, engine, rocket, hydraulics, electronics, radio aids, radar, et cetera, and at the extreme right are the power supplies, air-conditioning plant, and its automatic controls. The trailer is about 31 feet (9.4 meters) long and about 8 feet (2.4 meters) wide. The relative smallness of the vehicle is proof of the considerable progress that has been made in over-all computer design and minification.

2. Cockpit

The interior of the simulator cockpit is an exact replica of that of the real aircraft. However, the majority of cockpit components are drastically modified behind their seemingly familiar outer appearances. For example, gyroscopic and barometric mechanisms are replaced by selsyn-type repeaters. The feel of all controls is faithfully simulated and in the case of the flying controls, it is often convenient to reconstitute the entire electrohydraulic servo system of the aircraft.

Figure 4—Cockpit and instructor's console. The fault panel at the center permits the instructor to confront the student with any of 120 troubles. The track recorders for the positions of the aircraft and the fictitious target are at the extreme right.



Loudspeakers hidden behind the pilot reproduce all aircraft noises normally heard throughout the full range of operation of the real aircraft. To simulate jet-engine noise, a harmonic analysis was made of magnetic recording of the sounds of the real aircraft from starting the engine on the ground (or in flight) to full power at all speeds. The factors governing each harmonic were determined as functions of engine speed, flight speed, altitude, Mach number, et cetera. In the simulator, each harmonic is reproduced faithfully such that the sum of all these harmonics automatically reproduces the correct sounds.

3. Instructor's Console

The instructor's console, shown in Figure 4, allows the instructor to follow all actions of the pilot by means of duplicate flight and engine instruments, various indicators, and lights. The instructor plays the part of the control-tower, airport traffic controller, ground-controlled-approach operator, et cetera.

The main parts of the instructor's console are a double-track recorder for the simulated aircraft and the fictitious target, repeated radar scope, trouble or fault panel to provide for some 120 different faults, radio-aids and atmospheric-conditions panels, fictitious-target flying controls, repeated instrument panel, ground-controlled-approach recorder, and radar recorder.

4. Computer

The requirement that the simulator be capable of being housed in a semitrailer prompted the development of thin open equipment racks mounted vertically as shown in Figure 5. Servomechanisms, amplifiers, relays, selectors, and other components are mounted on each side of the rack. The rack itself is 6 feet (1.8 meters) high, 2.5 feet (0.8 meter) wide, and 3.25 inches (8.3 centimeters) deep. The extremely complex wiring is placed within this shallow, upright box form, the computing elements themselves being mounted on the two

outer surfaces by means of quick release fasteners or vertical hinges. This structure gives complete access to all elements and requires a minimum of space.

5. Power Supply

The location of air force bases at substantial distances from industrial centers often results in their having poorly regulated mains supplies so the trailer has been equipped with its own 3-phase regulators.

Some 15 different power supplies are required, and vary from direct current to both 50 and 400 cycles per second.

6. Semitrailer

The whole simulator is mounted in a fully air-conditioned semitrailer. The air-conditioning problem is a severe one despite the fact that the fully transistorized simulator dissipates only 4 kilowatts.

The technical specification calls for an internal

temperature of 65 degrees fahrenheit with the trailer placed either in full sunlight under sub-tropical conditions or under subzero blizzard conditions.

The whole trailer is thermally insulated with 6 inches (15 centimeters) of glass-wool in the roof, 4 inches (10 centimeters) in the walls and 2 inches (5 centimeters) in the floor.

Depending on external conditions, one or two 10-horsepower electric motors are switched on to drive the refrigeration plant and 10-kilowatt magnetic amplifiers energize heating elements to compensate for excessive cooling.

7. Computer Elements

The ultimate success of any computer depends on the computing elements of which it is composed. For the flight simulator, these must be very flexible in use, easy to manufacture, and extremely robust.

A complete range of computing elements have been developed. They include 6 basic electric

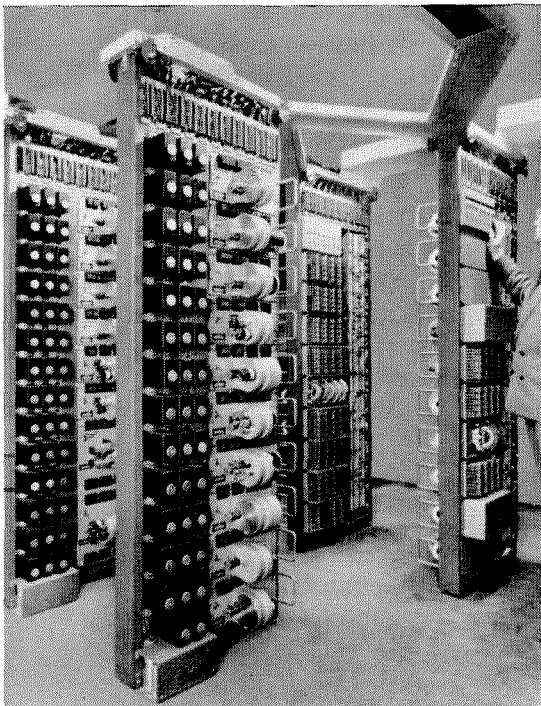
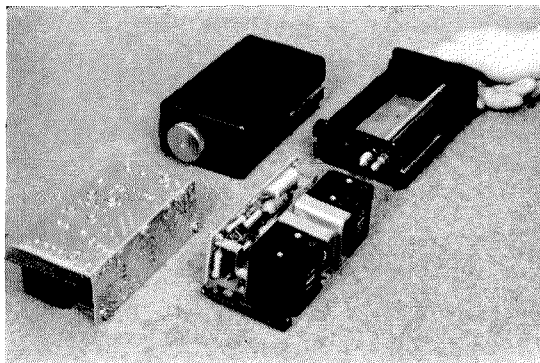


Figure 5—Computer racks have equipment mounted on both sides with quick-release fasteners for rapid servicing.

Figure 6—General-purpose transistor amplifier.



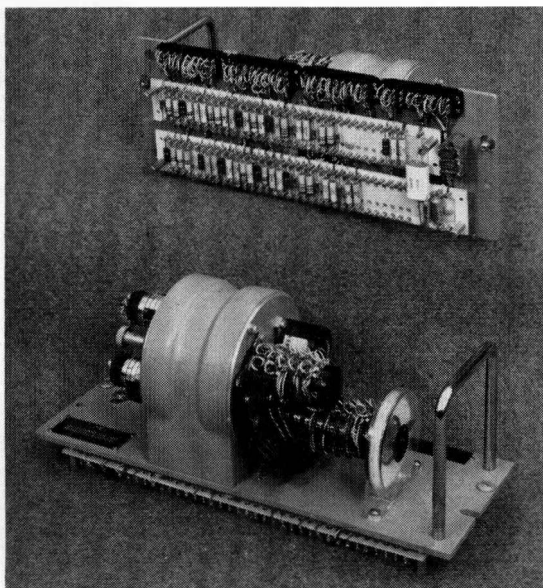


Figure 7—Computer servomechanisms.

circuits all mounted in the same manner in a cast duralumin box and a basic range of mechanical parts for constructing any type of servomechanism.

8. Electronics

The first of the 6 basic electric circuits is the transistor amplifier shown in Figure 6, which is used either as a summing amplifier with a center-tapped push-pull output of 5 watts or as a 400-cycle-per-second servo amplifier delivering 5 watts at 20 volts.

Secondly, there is the switching amplifier, which closes a relay in its output circuit for 2 or 3 millivolts of in-phase 400-cycle-per-second signal at its input.

Thirdly, there is a modulator that linearly modulates a direct-current signal with a 400-cycle-per-second input.

The fourth unit is a differentiator that mathematically differentiates a direct-current signal. The fifth basic circuit is a demodulator. It is a phase-sensitive amplifier producing plus or

minus direct current from an in-phase or out-of-phase 400-cycle-per-second signal. Finally there is a low-frequency random-noise generator.

All these circuits use only transistors, are very sturdily constructed, and are virtually 100 percent reliable.

Among the advantages of transistors can be counted a reduction in total power consumption of about 90 percent; a considerable space saving allowing the simulator to be housed in a relatively small vehicle; and complete freedom from tube failures, which in the case of ordinary simulators in the past have caused considerable down time especially after 1000 or 2000 hours of operation.

9. Servomechanism

To simulate aircraft having exceedingly fast response rates, as in the case with the modern high-performance fighter, the computer servomechanisms must have a large dynamic range, good high-frequency response, and in some cases only 1 part in 5000 of backlash. The motor-generators are 2-phase, 400-cycle-per-second machines. The servo gearbox is machined with extremely high tolerances. Center tolerances are quoted at 0.0002 inch (0.005 millimeter) and radial tolerances on gears, mounting flanges, ball-races, et cetera, are held to +0 and -0.0005 inch (-0.013 millimeter).

Servomechanisms are used for converting signals into angular movement or for integrating. The servo output shafts drive potentiometers, synchronous motors, selsyns, switching sectors, et cetera, used to generate signals for all parts of the computer and for driving the various instruments found in the cockpit of an aircraft.

10. Relays

About 500 relays are used to modify the various computer circuits to simulate the effects of whether the aircraft engine is running or not, whether the aircraft is on the ground or in flight, whether electrical generators are running or are shut down, whether the instructor

by controls on the faults panel has called for the blowing of any of dozens of fuses, and so on.

11. Conclusions

The flight simulator, despite its initial cost, is a great money saver. It costs at least \$200 to \$300 per hour to put the modern military or civil aircraft in the air. This figure would be much too low in the case of the new giant 4-engined jet transports. In the case of civil aircraft used for training purposes, there is also the profit that otherwise would have been earned. On the other hand, the cost of running a simulator is about \$50 an hour. This figure includes amortization over 5 years at 2000 hours a year, maintenance costs, instructor's salary, and power consumption.

Apart from these financial considerations, which are far from lacking interest, the flight simulator has other practical advantages. Exercises can be carried out in the simulator that would be unthinkable in the air. Engine fires, engine failures at take-off or landing, engine overspeed, dangerous hydraulic and electric failures, among many other dangerous conditions, can all be safely simulated.

For a single-seater fighter aircraft, all pilot actions and decisions, in face of the many difficult and hazardous conditions of wartime flying, can be closely followed. It is universally recognized that a pilot attains the highest degree of perfection and the ability to make split-second decisions only when the majority of his actions have become conditioned reflexes.

This is the ultimate role of the simulator.

Potential Application of Recent Advances in Communication Technology *

L. A. deROSA

ITT Communication Systems, Inc.; Paramus, New Jersey

E. W. KELLER

Radio Corporation of America; Camden, New Jersey

1. Introduction

The success of future communication systems will depend to a large degree on the exploitation of new communication technologies. When these technologies have been reduced to operational concepts that are feasible in practice, communication system design can then advance. It is the purpose of this paper to discuss such potentially applicable communication technologies.

Communication requirements and trends in traffic patterns have a significant impact on how well any system will satisfy both present and future demands. Utilization of new techniques for expansion is generally a compromise between economics and ability to meet future demands.

The first section of this paper discusses broad communication requirements, operational concepts and philosophy, and future trends. No attempt will be made, however, to specify definitive communication requirements since the presentation of global-system designs is not within the scope of this paper.

Subsequent sections in the paper discuss the potential application of technological advances to advanced communication problems. Some of the areas discussed are:

- A. New media, transmission modes, and extension of frequency ranges
- B. Improvement in terminal devices
- C. Advances in modulation, coding, and data-processing
- D. New switching technologies.

Fundamental limitations of various modes of communication are discussed, and spectrum windows that appear most useful are pointed out. The frequency range of interest is extended beyond the ultraviolet region.

New technologies in terminal devices such as parametric amplifiers, tunnel diodes, and masers are discussed. Basic concepts are used to develop the expressions for noise figures to provide the basis on which to compare these devices and to discuss potential applications. In addition, advances in data-processing techniques, modulation, coding, and decoding are discussed.

To compare these technologies, the effective noise temperature T_e is developed for each and plotted as a function of frequency. Applicability of these technologies can be determined by comparison with cosmic and atmospheric noise temperatures.

2. Requirements, Philosophies, and Trends

The demand for communication has been estimated as doubling within the next five years. This increase is predicted as holding not only for civilian but also for military communication needs. The communication engineer must utilize every available technological advance to meet this rapidly increasing requirement.

The increased demands for communication are expected to be particularly large between subscribers at geographically remote positions. There have been no significant technological developments except for a limited wide-band cable facility in overseas communications in the past fifty years and, perhaps for this reason, overseas telephone messages have been only approximately one percent of our domestic long-lines messages. This small overseas traffic has been caused by high cost, poor quality, and the long waiting times that the subscriber en-

* Presented at Institute of Radio Engineers Fifth National Symposium on Global Communications in Chicago, Illinois, on 22 May 1961.

counters when attempting to use these facilities. It is certainly apparent that all technological developments that can improve and increase global communication facilities are of particular importance. The rapidity with which the limited overseas communication channels have been saturated is an indication that the main deterrent to increased global communication is the paucity of suitable facilities.

Large proportions of the expanding communication needs are required by complex military systems that depend for their operations on the reliable transmission of huge volumes of data between centers and peripheral points. Sources producing and sinks operating on and utilizing huge quantities of data are already in existence; the only remaining void is the wide-band communication links to connect these collection and data-processing centers. Accordingly, more and more demands will be made for such links having high reliability and low cost.

It might be well to consider first the manner in which the basic characteristics of communications have changed during recent years.

If there were equal interchange of information between all members of a population, the communication requirements would be given by a binomial coefficient of n people taken two at a time with repetitions allowed. The communication requirements under these conditions would, even for a small population, increase enormously. This equal interchange, however, would serve no useful purpose unless the data flow did not saturate the subscriber, and if all subscribers possessed the same intellectual standard and educational background. Since this situation is a highly improbable one, organizations must find other means for producing results requiring a coordinated effort on the part of many individuals. This quest, which is the very basis for proper organizational management, is of particular concern to all military and large-scale civilian efforts.

Organizations are able to produce results through the coordinated efforts of many in-

dividuals and the use of facilities that can be economically justified only by such large-scale ventures. A further characteristic of an organization is that the functions must be selected so that there is no duplication, or only an intended duplication, of any two individuals. This is a principle of management. A second principle, and also an important one, is that the decisions made by members of an organization must be weighted so that the most-capable people make the most-important decisions. As soon as we subscribe to this latter principle, we immediately introduce into communication the concept that certain bits of information are more important than others.

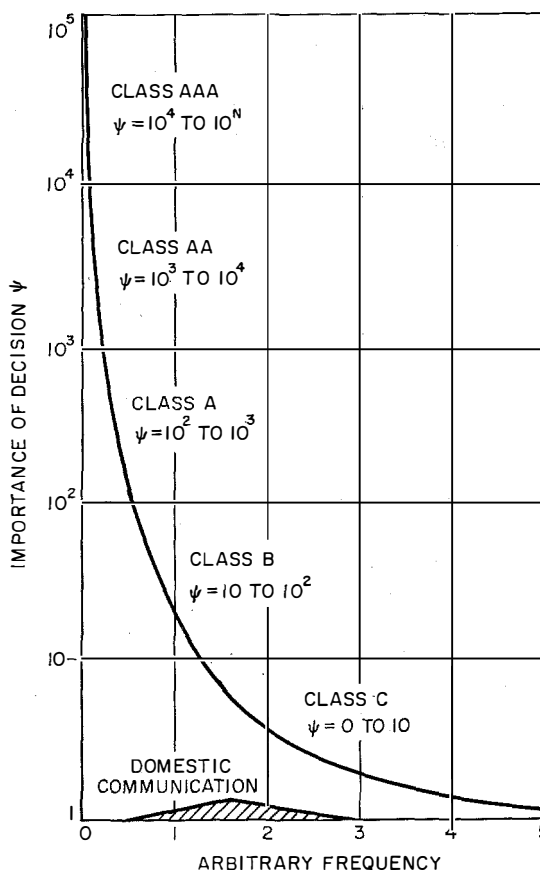


Figure 1—Relative importance and frequency of transmitting bits of information in a large organization.

The relative frequency of transmission and relative importance of bits of information in a large organization is shown in Figure 1. The difference between the distribution for a large organization or a military service may be compared with the distribution for a small unit or family shown at the bottom of the figure. In the past, the common-carrier attack on the communication problem has been, in general, that of providing communication for the unit or individual user. It has been assumed that one communication is as important as another and a telephone system does not discriminate among subscribers of various intelligence quotients (IQ).

Indeed, organizations are arranged by talented management so that the breakdown by divisions or departments and the allotment of tasks to units or individuals is accomplished with a view to minimizing the communication links that must be provided across the organizational barriers.

As a consequence, future communication requirements must consider more and more the supply of facilities with various orders of reliability or at least permit the consumer to select by suitable control over modems and terminal encoding processes the reliability commensurate with his requirements. Arrangements such as Telpak, offered by the American Telephone and Telegraph Company, are particularly suited for this latter purpose.

Another requirement is to supply wide-band facilities so that organizations can utilize and share central data-processing machinery not otherwise economically justifiable. To meet at least the two requirements of variable reliability and large transmission capacity, not only over domestic facilities but on a global basis, the communicator must consider what technological changes may be expected and how best they may be used in solving his problems. Some of the technological advances will be discussed in this paper. Techniques and proposed future efforts are also considered.

3. Transmission Media

In communication, the ratio of signal to noise at the receiver determines the quality or error rate. The design parameters are optimized to achieve and maintain a predetermined quality. Economically, it may be better to reduce the noise, where possible, rather than attempt to increase the transmitter power. Therefore, it is important to determine how new techniques can be applied to maintain the predetermined quality over a wide latitude of distances, bandwidths, and frequencies.

The composite effect of noise (and possible interference) can be represented by an equivalent noise temperature T_e , which includes the effects of line losses, antenna temperature, and receiver noise factor. Consequently, with this equivalent noise temperature, the noise in watts per cycle of bandwidth B is kT_e watts per cycle per second or $1.380 \times 10^{-23} T_e B$, watts.

Several reasons for using the concept of effective noise temperature instead of a noise factor are:

A. Temperature, which is power normalized with respect to kB , can easily be added to other temperatures as long as they all are transferred to the same part of the system. For linear networks, superposition applies.

B. Temperatures in high-performance systems are easier to measure than noise factors. Radiometric techniques are used.

C. In high-performance systems, small errors in noise factor F result in very large errors in temperature since at low temperatures $T \propto 70 F$, for T in degrees Kelvin and F in decibels. Thus small contributions to F , which may not seem important, may be the most-important system limitation.

The purpose of this discussion is to determine some of the fundamental limitations to system performance and how new techniques may improve this performance.

Convenient points of reference at which to express T_e are at the antenna terminals, at the

input to the receiver, or at the output of the receiver, all contributions to T_a being transferred to the reference point by the methods discussed in Section 7.2.

The communication model chosen is shown in Figure 2 and consists of three lossy passive networks and one active circuit, which is the receiver. The noise at the receiver output is determined by all external sources (T_g and T_{SL}), and by internal sources resulting from Johnson noise, system losses, and system gains. The reasons for choosing this model will become clear after a brief discussion of each element of the model.

3.1 NOISE SOURCES FROM OUTER SPACE T_g

The following sources contribute to T_g , the noise sources from outer space.

A. Thermal or black-body radiation from the sun, producing equivalent antenna temperatures T_a of 6000 degrees Kelvin. Some nonthermal quiet radiation (≈ 100 degrees Kelvin) should be added.

B. Burst and Cerenkov radiation from the sun, with T_a from 10^4 to 10^5 degrees Kelvin in the region from 10 to 1 gigacycles per second.

C. X and Lyman radiation in the ultraviolet region.

D. Thermal or black-body radiation from the planets and the moon. Measured values are shown in Table 1.

Except for the moon, radio black-body temperature T and equivalent antenna temperature

T_a are related by $T_a = TG (\Omega/4\pi)$, where G is the receiving-antenna gain and Ω is the solid angle subtended at the antenna by the source. (See Section 7.1.) For the moon, since $\Omega = 0.5$ degree, an integral can be used giving approximately $T_a = T$.

Radiation of this type has a continuous spectrum except at visible frequencies and above, where it decreases rapidly. (See Section 7.1.)

E. H_I radiation from our galaxy at a wavelength of 21 centimeters.

F. Nonthermal radiation from discrete sources, yielding T_a from 10^3 to 10^6 in the range between 1 and 10 gigacycles per second, and the galactic corona.

G. Nonthermal radiation from the planets, occurring in lightning-like bursts.

H. Thermal radiation from H_{II} sources such as Cygnus χ .

Body	Infrared Black-Body Temperature in Degrees Kelvin	Antenna Temperature T_a in Degrees Kelvin	Frequencies in Gigacycles per Second	Radio Black-Body Temperature T in Degrees Kelvin
Moon	—	150	1 to 30	150
Venus	240	2.0	9.5	600
Jupiter	130	<0.4	9.5	140
Mars	260	0.24	9.5	218
Saturn	—	<0.10	8.0	<100

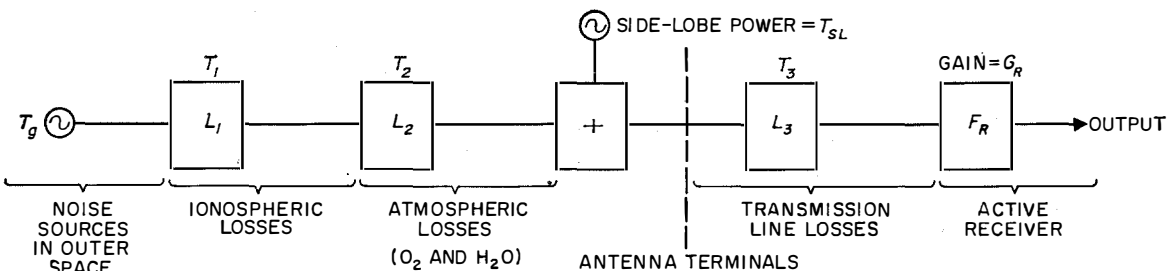


Figure 2—Communication system model.

3.2 IONOSPHERIC LOSSES

Losses in the ionosphere are caused by a transfer of energy from the propagating wave to the electrons. Generally, these losses are less than 0.3 decibel at 21 degrees Kelvin for frequencies above 100 megacycles per second. Faraday losses, however, are approximately 3 decibels at 1.4 gigacycles per second and become smaller as the frequency is increased. Above 7 gigacycles per second, Faraday losses are considered negligible. All calculations given

in Section 7.1 have already assumed a 3-decibel loss.

3.3 ATMOSPHERIC LOSSES (TROPOSPHERE)

These are due to molecular absorption by oxygen, uncondensed water vapor, and scattering by precipitation particles.

3.4 SIDE-LOBE POWER

This indicates the effect of the terrestrial temperatures of 300 degrees Kelvin through the

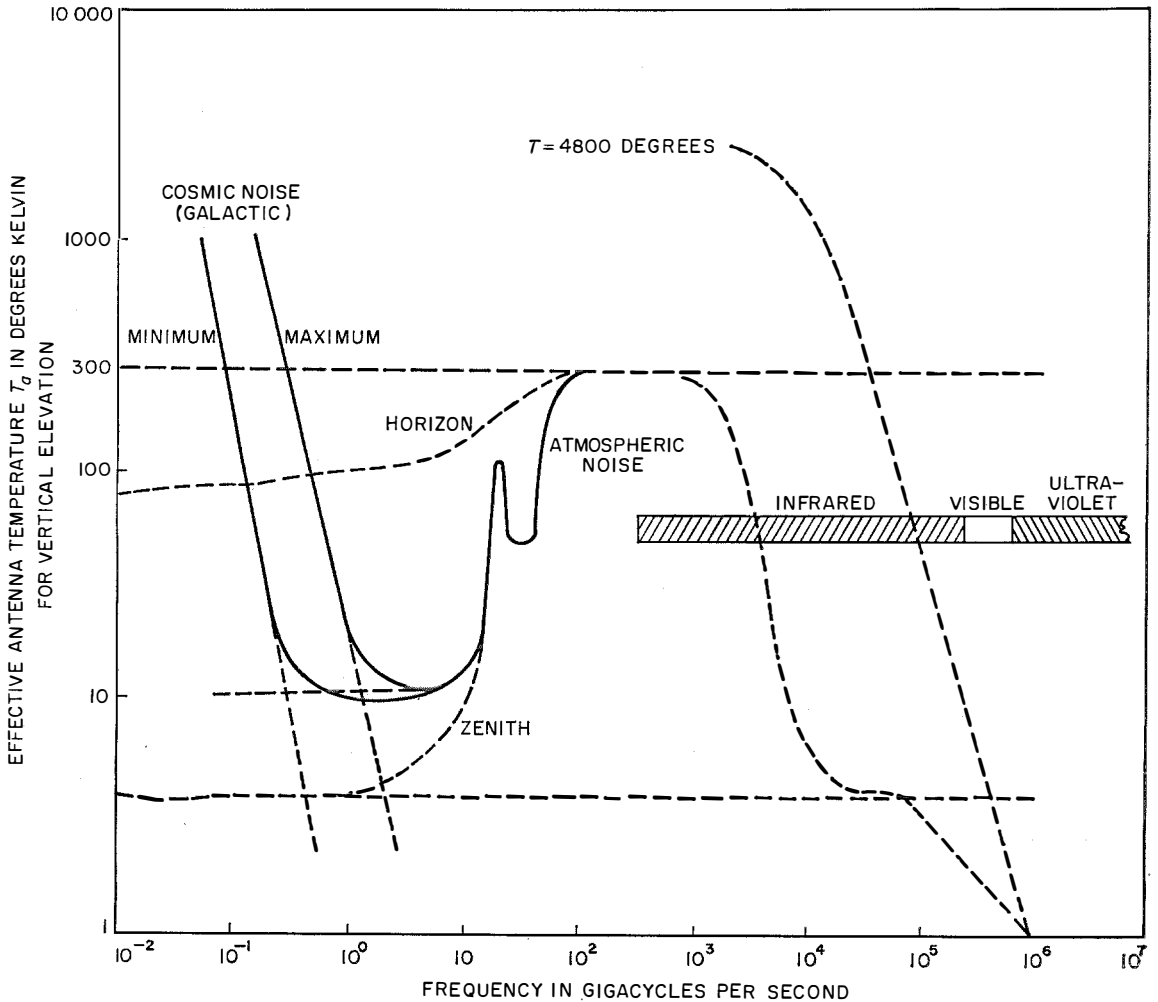


Figure 3—Galactic corona, ionospheric, and atmospheric noises as a function of frequency.

side lobes of the antenna and may increase T_a from 2 to 200 degrees Kelvin depending on the elevation angle of the antenna and its design.

3.5 TRANSMISSION-LINE LOSSES

See Section 7.2.

The model chosen represents a linear combination of sources and networks, each of which has gain or loss and at the same time contributes noise by virtue of its temperature. Figure 3 shows a composite of galactic corona noise and ionospheric and atmospheric noise. Noise from the sun, planets, and moon, and noise from H_I and H_{II} can be added as needed. However, each propagation path will, in general, differ, so only those noises common to all are shown. The upper infrared decay of atmospheric noise is based on scattered experimental data, but a reduction is expected as the frequency increases. Also shown is a $T = 4800$ degrees Kelvin source, which has a flat spectrum until reaching 10^4 gigacycles per second at which point it reduces rapidly. This latter is a prediction based on the use of Planck's exact radiation law and is yet to be verified experimentally. (See Section 7.1.) As shown, two general windows appear useful: 1 to 10 and above 10^5 or 10^6 gigacycles per second, the latter appearing more useful in outer space. The knee of the curve in the latter function moves toward lower frequencies as T reduces.

3.6 OVER-ALL TEMPERATURE

To obtain the over-all effective noise temperature referred to the input of the receiver, one can use the results described in Section 7.2 as applied to the system model shown in Figure 2. The loss $L = 1/G = F$. The over-all effective noise temperature, referred to the input to the receiver is

$$(T_{e1})_{\text{Eff}} = (T_{e1})_{\text{Rec}} + \frac{T_a}{L_1 L_2 L_3} + \frac{T_1(L_1 - 1)}{L_1 L_2 L_3} + \frac{T_2(L_2 - 1)}{L_2 L_3} + \frac{T_3(L_3 - 1)}{L_3} + \frac{T_{SL}}{L_3}$$

Letting $L_1 L_2 L_3 = L = 1/G_0$ and assuming $T_1 = T_2 = T_3 = T_0$, the above expression becomes

$$(T_{e1})_{\text{Eff}} = G_0 T_g' + (T_{e1})_{\text{Rec}} + (1 - G_0) T_0 \quad (1)$$

where $T_g' = T_a + (T_{SL})L_1 L_2$. However, when $T_1 \neq T_2 \neq T_3$, the component terms given above must be added together as indicated. Note that the effective antenna temperature, referred to the antenna terminals, is

$$(T_a)_1 = \frac{G_0 T_g' + (1 - G_0) T_0 + (T_{e1})_{\text{Rec}}}{G_3} \quad (2)$$

and the effective noise temperature, when referred to the receiver output terminals, is

$$(T_{e2})_{\text{Rec}} = G_r [G_0 T_g' + (T_{e1})_{\text{Rec}} + (1 - G_0) T_0]. \quad (3)$$

Therefore, the amplifier noise output becomes

$$N = k B (T_{e2})_{\text{Rec}} = k B G_R [G_0 T_g' + (T_{e1})_{\text{Rec}} + (1 - G_0) T_0] \quad (4)$$

from which the predetection signal-to-noise ratio can be determined for a given transmitter power. Note that in some instances, some of the terms in (4) may be omitted. As an example, consider the following system parameters.

Frequency = 5.65 gigacycles per second.

B = bandwidth = 25 megacycles per second.

G_R = gain = 35 decibels.

$G_0 T_g' = 5.95$ degrees Kelvin. (This corresponds to an exceptionally well designed system operating in a quiet sky.)

$(T_{e1})_{\text{Rec}} = 10.5$ degrees Kelvin. (Traveling-wave maser.)

$(1 - G_0) T_0 = 2.0$ degrees Kelvin.

Therefore, the noise $N = -107$ decibels referred to 1 watt, and the required signal at the detector input for $S/N = 20$ decibels is -87 decibels referred to 1 watt.

3.7 COMMUNICATION PATHS

The fundamental limitation in being able to communicate efficiently is consequently determined by the noise at the receiver, as given

by (4). Consider the system just discussed used for the following communication paths.

3.7.1 Earth and Moon

When the receiver is on the moon pointing at the earth, N increased by $316/18.5 = 17$ because of the noise temperature of the earth. When the receiver is on the earth, N increases by $166/18.5 = 9$, because of the noise temperature of the moon. To maintain the same S/N ratio would require corresponding increases in transmitter powers.

3.7.2 Earth and Venus

When the receiver is on Venus pointing at the earth, the term $G_0 T_g'$ in (4) will be about 2 or 3 degrees Kelvin because the earth is a discrete black-body radiator ($T = 300$ degrees) observed from Venus. Similarly, when the receiver is on the earth, (4) indicates $G_0 T_g'$ will be about the same since Venus contributes T_e of only 2 degrees or less. Thus, the noise

N would not increase appreciably over the value of -107 decibels referred to 1 watt.

3.7.3 Earth and Satellite

For earth to satellite, N will be determined by other sources that may fall within the field of view. When the receiver is on the earth, $G_0 T_g'$ could increase to 10^5 degrees Kelvin if and when the sun appeared in the field of view. Similarly, other discrete thermal and non-thermal sources could raise $G_0 T_g'$ and thereby raise N by 40 or 50 decibels. When the receiver is on the satellite, the black-body radiation from the earth will increase $G_0 T_g'$ by an amount depending on the receiving beam angle. A 10-decibel increase can be expected. If the latter is too large, other discrete and continuous sources of noise may appear. To reduce the effect of thermal and nonthermal radiation in satellite-to-satellite communication, infrared, visible, ultraviolet, gamma, and X-ray modes are suggested. (When the sun is in the field of view, however, its own Lyman, ultraviolet, Gamma, and X-radiation would probably disrupt any communications.) As indicated in Section 7.1, black-body radiation from most sources decreases rapidly at these high frequencies and, as indicated in the preceding general noise discussion, nonthermal radiations tend to reduce rapidly so that at 1 gigacycle per second, they are negligible.

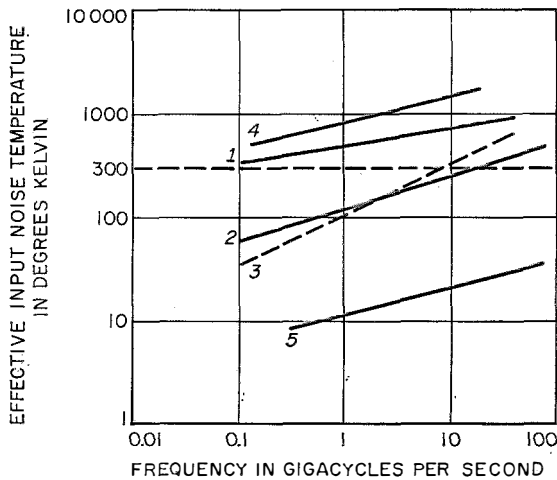


Figure 4—Effective input noise temperatures in degrees Kelvin of low-noise amplifiers. These temperatures include the effects of connecting hardware and do not represent the intrinsic T_{e1} . The numbered curves are for the following amplifiers. 1—Parametric (traveling-wave and helix). 2—Parametric (cavity). 3—Traveling-wave tube (estimated). 4—Tunnel-diode. 5—Maser (traveling wave).

4. Terminal Devices and Distribution

The previous discussion is useful in determining radio windows in the spectrum for use in communication. With the windows established, the terminal devices can be optimized to yield a predetermined degree of performance. The particular terminal devices of interest are transmitters, antennas, receivers, and terminal-area distributors.

4.1 TRANSMITTERS

Based on existing development rates, the maximum available peak power output from a single device will be of the order of 50 mega-

watts in the 1970 period. Between 100 and 5000 megacycles per second, this value of power is relatively independent of frequency. Above 5000 megacycles per second, the available peak power decreases with frequency, giving approximately 10 megawatts at 10 000 megacycles per second. No major breakthroughs are expected in the next few years, except in the field of lasers, irasers, and masers.

4.2 ANTENNAS

No major breakthroughs are predicted for the 1970 period. However, for high-performance systems, continued effort is being applied to increase antenna accuracy and to reduce side lobes and spillover to a negligible amount. It should be noted that, in addition, a synthesis of antennas for satellite applications is progressing rapidly. The use of circular polarization or diversity is suggested.

4.3 RECEIVERS

The most-fruitful developments in the next ten years will probably be in operational receiver design and general utilization of the spectrum above the infrared. By using the broad spectrum window above the infrared coupled with irasers, lasers, or masers, some of the congestion at lower frequencies can be relieved and generally better performance established.

As an indication of receiver-amplifier performance in the frequency range of the lower spectrum window, Figure 4 shows the effective input noise temperature, including the effects of connecting hardware. These experimental data reflect the advances in receiver design in the last few years.

Figure 5 is a superposition of Figures 3 and 4, indicating that 10-degree-Kelvin amplifiers are indeed needed in the window shown. A reduction in noise temperature from 1000 to 10 degrees Kelvin is equivalent to a 20-decibel reduction in transmitter power, maintaining the same S/N ratio. Note the dependence of T_{e1} on frequency. (See Section 7.2 for a dis-

cussion of T_{e1} .) Also, curve 6, the estimated intrinsic noise temperature for the laser, is based on extrapolation of the low-frequency performance. Some experimental results indicate laser noise temperature in excess of 10 000 degrees Kelvin. Curve 6 is intended to be a lower bound.

It may appear that error-correcting codes could retrieve the information when the S/N ratio becomes -30 or -40 decibels. When the message rate is maintained constant, it can be shown that error-correcting codes based on spread-spectrum techniques are of little value since the fundamental limitation is thermal noise. If the message rate can be reduced, some form of iteration, coded or uncoded, may be helpful.

From (4), the impact of T_{e1} is clear. Until recently, it has been the fundamental limitation in system performance. With present techniques, T_{e1} can be made equal to or smaller than the sum $G_0 T_g' + (1 - G_0) T_0$.

4.4 TRANSMISSION ABOVE 10^5 GIGACYCLES PER SECOND

For the other window in the spectrum above 10^5 or 10^6 gigacycles per second, new techniques will have to be developed. Some of those recommended for consideration follow.

4.4.1 *Black-Body Radiators*

The plasma resulting from an electrically exploded wire approximates a black-body radiator.¹ For digital use, one millisecond explosions can be generated having temperatures ranging from 20 000 up to 350 000 degrees Kelvin, sufficient for transmission throughout our solar system.

4.4.2 *Coherent X-Ray Generators, Suitable for Modulation*

Present high-power X-ray designs may be inadequate to produce enough quanta for long-range communication, even outside the atmosphere of earth. Coherent X-ray generators could

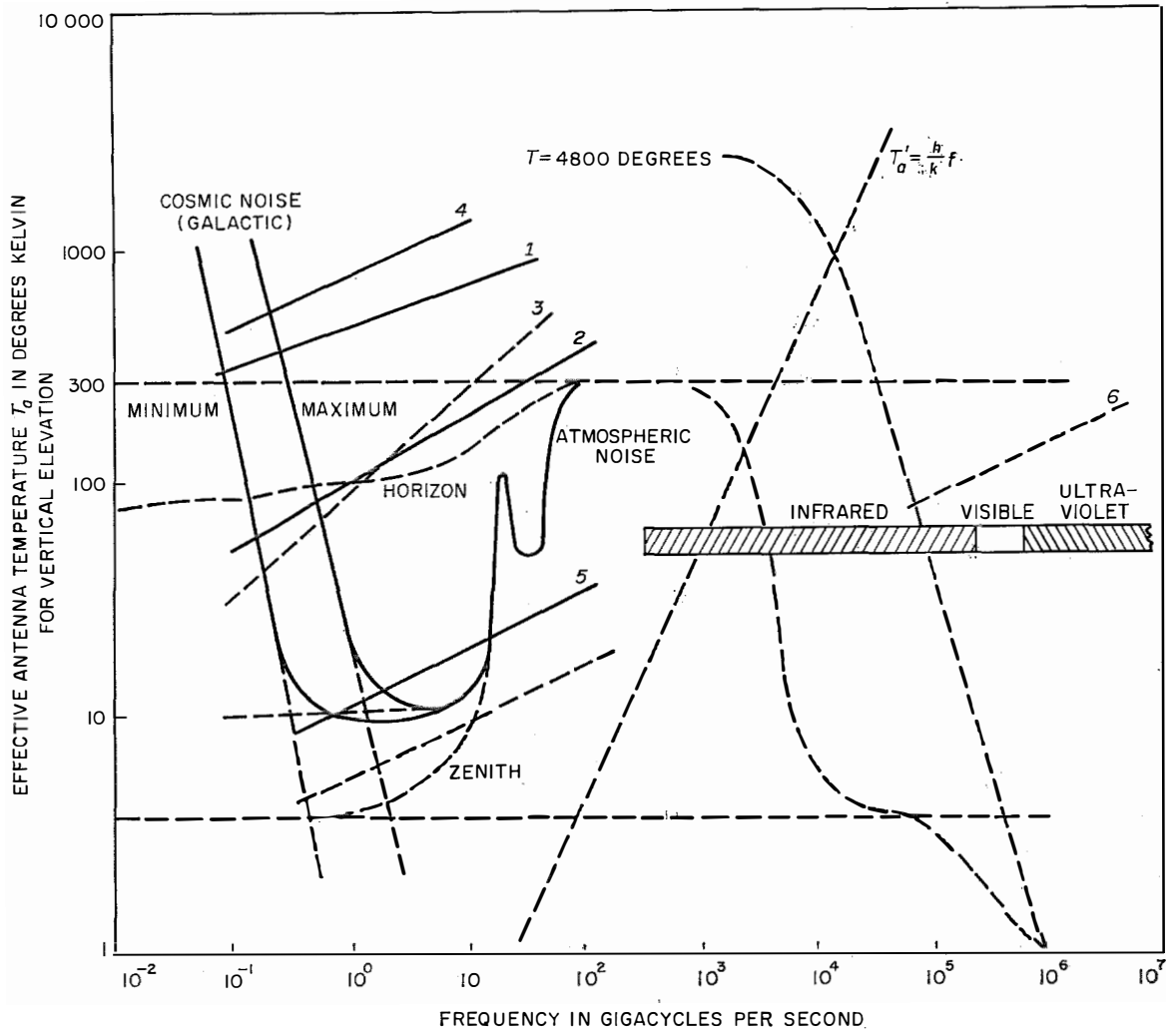


Figure 5—Superposition of Figure 3 and 4. Curve 6 is estimated for the laser.

relieve this situation. (The cosmic-ray noise background for this mode is severe and must be carefully analyzed.)

4.4.3 Coherent Gamma-Ray Generators

Present schemes are based on the disintegrating nuclei of atoms, produced in a nuclear-fission reactor. Sizes, powers, and weights are now excessive and, in addition, incoherent radiation results. A coherent source would assist in resolving this problem. (The cosmic-

ray noise background for this mode is severe and must be carefully analyzed.)

4.4.4 Coherent Ultraviolet Generators

Present continuous optical masers use, for example, a gas discharge in a helium-neon mixture. A typical wavelength is 11 530 angstrom units (near infrared) at a power of 15 milliwatts. Extension of these principles into the ultraviolet regions would generally produce more favorable S/N ratios.

For communication at these frequencies, new modulators and receivers will have to be developed. Undoubtedly, amplifiers based on the same principle as the oscillator can be developed to replace the quantum counters currently in use at these frequencies. There is little argument that coherent radiation will produce a much more favorable S/N ratio at the receiver than incoherent radiation, because the noise is greatly reduced by the use of selectivity similar to that in lower-frequency receivers. However, the fundamental limitation² that determines the minimum detectable signal for a given bandwidth at these frequencies is not clear. If it is assumed that photon or quantum uncertainty determines the lower bound in detection, such as in photon counters, an equivalent temperature representing the lower bound on receiver noise temperature will be

$$T_a' = (h/k) f = (4.8 \times 10^{-2} f) T$$

where the frequency f is in gigacycles per second and the temperature T is in degrees Kelvin.

This curve is plotted in Figure 5 and indicates that the upper window is wiped out. However, if it is recognized that the photon representation of a signal is better suited for representing a random function than a sine wave, since a photon by definition is impulsive in character and, therefore, cannot represent a sine wave, the fundamental limitation in reception must be other than T_a' . It may be said that "well ordered" or "coherent" photons can be used to represent a sine wave and, if so, the latter argument is strengthened. In any case, additional experimental and theoretical work will resolve this fundamental point.

Also, optical devices, by virtue of their potentially narrower beam angle with coherent radiation, require less power than a microwave system. For example, the transmitter power P_t required to communicate between two points separated by a distance R is given by

$$P_t = \left(\frac{P_r}{f} \right) c \frac{\lambda R^2}{A_1 A_2}$$

where P_r = required receiver power

f = operating frequency

c = velocity of light

λ = wavelength

A_1, A_2 = transmitter and receiver antenna areas.

If one assumes that P_r/f is constant, then

$$\frac{(P_t)_{\text{light}}}{(P_t)_{5 \text{ cm}}} = 10^{-5}$$

or the power required by a laser system is 5 orders of magnitude less than that required by a 5-centimeter system. In practice it may be even less, except where the transmitter is located on a hot thermal source such as Venus ($T = 600$ degrees Kelvin). In an optical receiver, the beam angle can be less than the angle subtended by Venus at a point on the earth (beam angle = 2×10^{-4} degree and the angle subtended by Venus is 10^{-2} degree). Thus $T_a = T = 600$ degrees Kelvin. (See (18) in Section 7.1.) In general, T_a is small, of the order of several degrees.

5. Modulation and Coding

The demand for increased communication may be met, as has been indicated previously, by the utilization of a wider portion of the electromagnetic spectrum. Another attack is to utilize more effectively that part of the spectrum now in common use. This suggests new types of modulation and encoding to accommodate greater amounts of information per cycle per watt of power. In this type of study, there are two major considerations. The first is an investigation of modulation and encoding processes that, from a theoretical viewpoint, offer promise. The second is a critical examination to determine at an early stage which offer promise of practical realization.

From a theoretical viewpoint, there is an almost inexhaustible number of new encoding processes and new proposals for novel modulation schemes. However, few of these can be realized as practical equipments because of

component unreliability. It is also possible to show that encoding methods can be and have been conceived to permit signaling at rates arbitrarily close to the capacity of a channel and with an arbitrarily small probability of error. Nevertheless, few of these encoding processes are attractive from the practical point of view for the large bulk of communication traffic. Many of the special codes, such as the parity-check codes, are extremely useful for the higher-priority messages where an increased cost of monitoring and maintenance is justifiable.

Until such time as the reliability inherent in components is increased substantially, many communication engineers believe that they must revert to time-honored solutions such as reiteration. This retrogression philosophy is a result of considering the error-reduction problem on a global basis and the additional capital expenditures necessary to introduce complex encoding equipment on a large-scale basis.

In addition to the reliability and cost considerations, one must realize that the premises on which theoretical considerations are often based are derived from simplifying assumptions as to the statistics associated with the error-producing sources. As an illustration, consider a transmission link using the tropospheric-scatter phenomenon. A 1-kilowatt installation will cost in the neighborhood of \$25 000 for the transmitter, including power supply. A 10-kilowatt installation will cost approximately \$75 000 to \$100 000 more. The variation in signal strength which may be encountered in one week of operation in a typical Mediterranean area installation is 40 decibels, while seasonal variations of as much as 70 decibels are possible. This requires an encoding process that will improve the operation under certain levels of ambient noise and propagation anomalies of 70 decibels. Since the capacity of the channel under these extremes of signal-to-noise ratio is subject to wide variation, it is difficult to conceive of an encoding process that will substitute for reserve

power in the transmitter. In most considerations of encoding and operation in large ambient noise backgrounds, the disturbances are considered to be Gaussian in nature. Further gains in combatting noise and in minimizing errors due to propagation phenomena must rest in obtaining more precise statistics relating to the perturbing influences and in devising methods of modulation for operation in this environment. The operation and encoding methods should be selected so that they can be physically realized without complex circuits or loss of reliability.

It might be well to consider briefly one or two methods of attack on this problem. In a given bandwidth ΔB filled with noise and signal, the only means to separate the signal from the noise lies in determining the differences between the complex portions of the Fourier spectrum. If the noise is considered to have a normal distribution, which in many cases is contrary to the facts, modulation and encoding devices are unnecessarily limited. Consider a transmission band ΔB wherein certain phase relationships between noise components are more probable than others. In other words, certain wave forms are characteristic. This is the case for atmospheric noise from nearby sources. For communication against such an ambient, a selection should be made of uniform band-limited power spectra whose complex phase spectra are sufficiently different so that the correlation function of the noise with the signal approaches zero.

These functions are encountered in network analysis when lattice networks are excited by impulse-type functions and under these conditions produce orthonormal functions. As an example, the lattice network of Figure 6 leads to the generation of Legendre functions when excited by an impulse function while that of Figure 7 leads to the generation of Laguerre functions. A set of real and continuous functions $L_1(X), L_2(X) \dots$ is considered to be orthonormal in the range $0 < X < \text{infinity}$

if

$$\int_0^\infty e^{-x} L_n(X) L_m(X) dX = \begin{cases} (n!)^2 & (n = m) \\ 0 & (n \neq m) \end{cases}$$

In each of the lattice networks, the polynomials provide the properties for the admittances of the various branches and may be derived by using the current in the *n*th branch due to the unit voltage applied to the input of the filters. Figure 8 shows the first five Laguerre functions that may be obtained by such a lattice network. Let us now assume that the noise is spike-like in character and is represented by the waveform of the first Laguerre polynomial shown at *A*. Let us, in addition, assume that the next four functions are used as symbols in an alphabet. Further, if we assume that the signal-separating device is a correlator, we would find that with a practical correlator a signal-to-impulse-noise discrimination for the second Laguerre function operating against the first Laguerre function is of the order of 15 decibels. Correlating the third against the first yields a discrimination of about 18 decibels and similar values are obtained for the fourth and fifth, correlated against the first.

Many other interesting relationships can be found with other orthonormal functions serving as modulation matrixes. Suitable functions may be found and generated that are particularly suited for use against noise and distortions due to propagation through dispersive media.

6. Switching

Introducing switching techniques that operate more rapidly than the conventional mechanical types, such as step-by-step and crossbar, offers some possibility for more-effective utilization of existing facilities.

It is possible to obtain a more-rapid user-to-user connection, that is, provide a short reaction time, by rapid switching. This has not been considered an important factor in the past since not many communication networks would be handicapped if this reaction time

were longer than 5 to 10 seconds. However, with the coming of wideband switched circuits transmitting huge quantities of data and operating between data-processing centers, a switching time of 5 to 10 seconds may make it mandatory to assign lines to avoid such switching.

A second objective of high-speed switching is to increase the trunk efficiency or the utilization of trunking facilities. The efficiency with which a trunk is used is determined by the ratio of

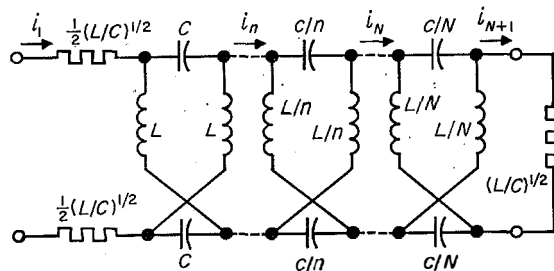


Figure 6—Lattice network for Legendre polynomials.

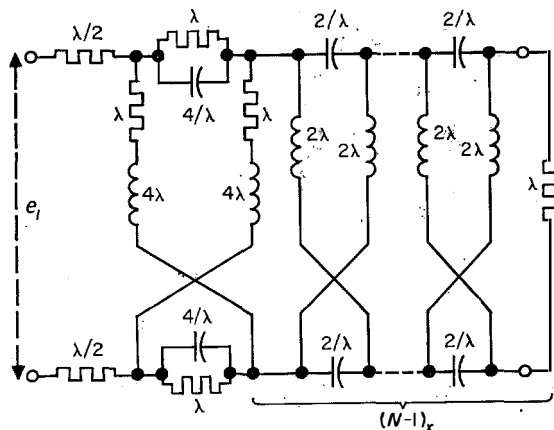


Figure 7—Lattice network for Laguerre polynomials.

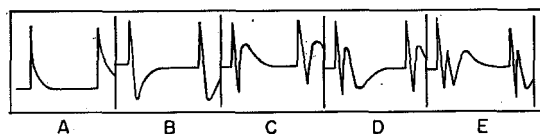


Figure 8—Laguerre polynomials.

the effective communication time to the setup time, that is

$$\eta = \frac{t_m}{t_m + n_c(t_{si} + t_{sw})}$$

where t_m = mean message time
 n_c = number of centers in tandem
 t_{si} = signaling time
 t_{sw} = switching time of one center.

The denominator in the formula for efficiency may average approximately 120 seconds when using crossbar switching. For voice transmissions, this is satisfactory, but when operating with wideband data, large quantities of messages may be involved with holding times of 1 second or less, so that the efficiency with which trunks are used would be decreased to a point where high-speed switching would be economically justifiable. A high trunk efficiency may also be obtained by proper traffic regulation by utilizing better queuing programs or store-and-forward techniques.

The utilization efficiency of the network can also be affected by the rapidity with which internal control is performed. Crossbar systems may have a total switching time long enough to make it impossible to use a single control marker, thus necessitating the use of several markers. In a fast matrix system, such as those using reed relays or semiconductor crosspoints, the speed is such that a single marker will suffice. Calls may thus be handled one at a time. This enables much-more complex control operations to be performed and increases the flexibility of the system. With representative message lengths, signaling times, and switching times for a three-center over-all setup, and with representative marker holding times, a simple crossbar marker may handle about 30 calls per minute. A reed relay marker may handle about 1000 calls in that time.

The implementation, therefore, of more-rapid switching apparatus will be particularly effective in increasing the efficiency of utilization of existing facilities for the transmission of data and wide-band and short duration messages.

7. Appendixes

7.1 BLACK-BODY RADIATION

An adequate representation of galactic and other extraterrestrial sources of noise that influences communication is in terms of equivalent black-body radiators. The equivalence is adopted for representation only and does not imply that the mechanism by which the noise is generated is similar to that found in a black body.

Heated bodies emit radiation, the quantity and quality of which depend, for a given body, on the temperature of that body. Thus, the rate of radiation and the spectral distribution of that radiation are functions of the temperature of the body. The term thermal radiation is used here in its widest sense, that is, including all low-temperature phenomena as well as all high-temperature phenomena.

By way of definition, let

p_λ = noise power radiated per unit radiator surface area per unit solid angle at the wavelength λ in the spectral range λ to $\lambda + d\lambda$. Units are watts per square meter per unit solid angle.

$\Psi_\lambda d\lambda$ = radiant energy per unit volume in a stream of radiation such as that found in a totally enclosed cavity resonator in an isothermal spherical shell, contained in the spectral range λ to $\lambda + d\lambda$. Units are joules per cubic meter.

$p_\lambda = (c/4\pi)\Psi_\lambda d\lambda$ is the black-body relation between the radiated power and the energy source,^{3,4} where c is the velocity of light.

From the theorem of the equipartition of energy, the Rayleigh-Jeans formula for the spectral energy distribution can be derived.

$$\Psi_\lambda d\lambda = \frac{8\pi kT}{\lambda^4} d\lambda, \quad \text{joules per cubic meter} \quad (5)$$

where k is the Boltzmann constant = 1.38×10^{-23} joules per degree Kelvin. Equation (5)

results from recognizing that whatever may be the nature of the radiating and absorbing mechanism in the black body, each degree of freedom of the entire system should have associated with it an average amount of kinetic energy $kT/2$. Each degree of freedom also has an equal amount of potential energy, yielding a total energy of kT for each degree of freedom. For electromagnetic waves in an enclosure, the number of degrees of freedom is $8\pi (d\lambda/\lambda^4)$, leading directly to (5).

However, the radiation expression given by (5) is not adequate for the entire spectrum, particularly at the higher frequencies (above 60 000 gigacycles per second) since it does not agree with experimental data at high frequencies. Radiation in part of the infrared, all of the visible, and all of the ultraviolet spectra is thus not adequately described by (5), indicating the failure of the classical principle of the equipartition of energy.

Planck resolved the difficulty just indicated by means of a quantum hypothesis which led to

$$\Psi_\lambda d\lambda = \frac{8\pi ch}{\lambda^5} \frac{d\lambda}{\exp[ch/\lambda kT] - 1} \quad (6)$$

where h = Planck's constant. Note the asymptotic values of (6).

For large λ , $\Psi_\lambda d\lambda \approx \frac{8\pi}{\lambda^4} kT d\lambda$.

For small λ , $\Psi_\lambda d\lambda \approx \frac{8\pi ch}{\lambda^5} \exp\left[\frac{-ch}{\lambda kT}\right] d\lambda$. (7)

Note that (5) becomes zero for infinite λ and that (7) becomes zero for zero λ . Equation (6) is plotted in Figure 9 for two different temperatures.

Applying the relation $p_\lambda = \frac{c}{4\pi} \Psi_\lambda d\lambda$ to (6)

$$p_\lambda = \frac{2c^2 h}{\lambda^5} \frac{d\lambda}{\exp[a/T] - 1}$$

watts per square meter (8)

where $a = (ch/\lambda k)$. But since $\lambda = c/f$, $\Delta\lambda = \lambda^2 \Delta f/c$, where only magnitudes are

indicated. Thus, letting $p_\lambda = p$ and $d\lambda = \Delta\lambda$,

$$p = p_\lambda = \frac{2ch}{\lambda^3} \left\{ 1 \frac{\Delta f}{\exp[a/T] - 1} \right\} \quad (9)$$

expressed in watts per unit of area of radiation surface in bandwidth Δf per unit solid angle.

The equivalent antenna temperature and noise power received can be obtained from (9). Figure 10 shows the relationships between the black-body radiator and the receiver.

The power received by the antenna from dS depends on the amount of power radiated from dS in a unit solid angle that is intercepted

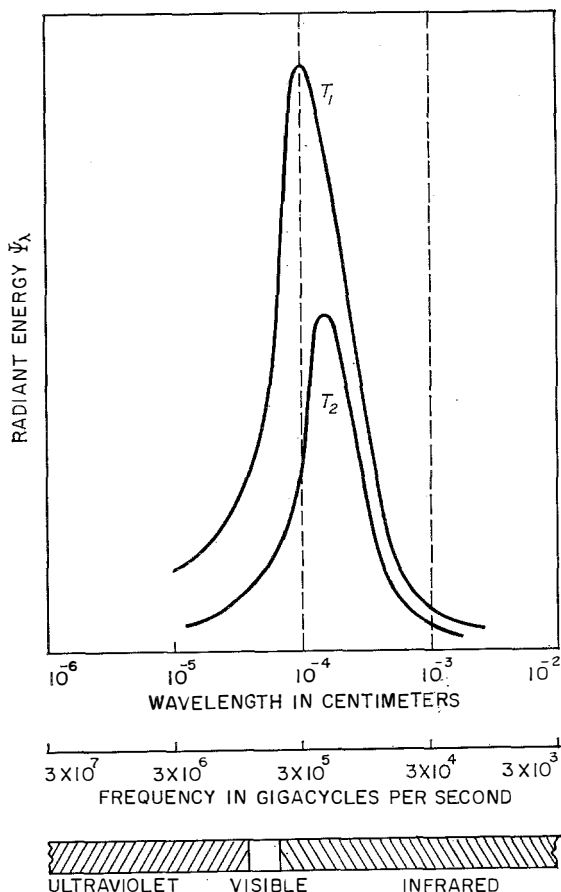


Figure 9—Black-body radiant energy for unit volume as a function of wavelength at two temperatures, $T_1 \approx 2940$ and $T_2 \approx 1470$ degrees Kelvin. $\lambda_{max} = 0.294/T$ centimeters.

by the antenna. Assuming that no losses between the radiator and the antenna or other sources exist, the power received from dS is

$$dP = \frac{p}{2} dS \frac{A_e}{r^2} \quad (10)$$

where the $p/2$ represents the power received with a linearly polarized antenna and A_e/r^2 is the solid angle subtended by the antenna at the source located at dS . But

$$(dS/r^2) = d\Omega \quad (11)$$

which is the differential solid angle subtended by the differential surface area of the elemental source being considered. Using (11) in (10), (10) becomes

$$dP = \frac{p}{2} A_e d\Omega. \quad (12)$$

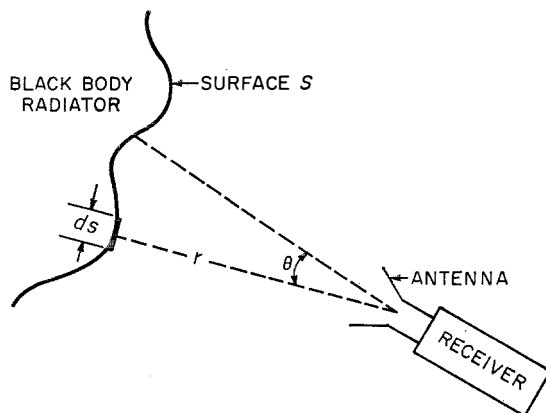
The antenna cross-section A_e is, however, related to the antenna gain by the following expression

$$A_e = \frac{\lambda^2}{4\pi} G(\theta, \varphi). \quad (13)$$

The total noise power received by the antenna then becomes

$$P = \int_{\Omega} \frac{p}{2} \cdot \frac{\lambda^2}{4\pi} G(\theta, \varphi) d\Omega. \quad (14)$$

Figure 10—Equivalent antenna temperature.



With (9) and replacing df with $\Delta f = 1$, (14) becomes

$$P = (hf) \int_{\Omega} \frac{1}{\{\exp[a/T] - 1\}} \frac{G(\theta, \varphi)}{4\pi} d\Omega \quad (15)$$

in watts per unit bandwidth. Note that each quantum of radiant noise energy has the magnitude hf .

In (15), $a = hf/k = T_a$ and the effective antenna temperature is $P/k = T_{ea}$ or (15) becomes

$$T_{ea} = T_a \int_{\Omega} \frac{1}{\exp[T_a/T] - 1} \frac{G(\theta, \varphi)}{4\pi} d\Omega. \quad (16)$$

The quantity $T_a = a = 4.8 \times 10^{-11} f$ in degrees Kelvin. Since $G(\theta, \varphi)$ will be assumed independent of frequency, T_{ea} depends on frequency in accordance with T_a . This dependence is shown in Figure 11.

$X = 1$ corresponds to $f = \frac{T}{4.8 \times 10^{-11}}$ cycles per second,

$X = 2$ corresponds to $f = \frac{2T}{4.8 \times 10^{-11}}$ cycles per second,

$X = 3 \times 10^{-5}$ corresponds to $f = 3$ gigacycles per second and $T = 4800$ degrees Kelvin

$X = 10^{-4}$ corresponds to $f = 10$ gigacycles per second and $T = 4800$ degrees Kelvin.

The low-frequency region (up to 100 gigacycles per second) indicates no significant change in power as the frequency changes, thus reflecting the Rayleigh-Jeans approximation to the Planck radiation equation. However, at higher optical frequencies, the noise power due to black-body radiation decreases as the frequency increases.

For low frequencies, (16) becomes

$$T_{ea} = \int_{\Omega} T \frac{G(\theta, \varphi)}{4\pi} d\Omega. \quad (17)$$

For the case when T is independent of Ω (or when $G(\theta, \varphi)$ has a beam angle equal to or

smaller than the angle subtended by a black body at the receiver), (17) becomes

$$T_{ea} = T \tag{18}$$

since

$$\int_{\Omega} \frac{G(\theta, \varphi)}{4\pi} d\Omega = 1.$$

When the black-body radiator, on the other hand, is small so that the angle subtended at the source is small with respect to the antenna beam angle, (17) becomes

$$T_{ea} = \frac{TG(\Omega_s)\Omega_s}{4\pi}. \tag{19}$$

The above arguments apply only to the thermal type of spectrum. However, there is in nature a nonthermal spectrum in which the intensity of noise decreases as the frequency increases, while the thermal type has a spectrum that is independent of frequency, at least up to 100 gigacycles per second. These different spectra arise from different physical processes of radio radiation.

It is generally accepted that the mechanism of the thermal process involves free-free transitions in the ionized interstellar hydrogen gas, while the nonthermal process involves the synchrotron radiation from relativistic electrons moving in the galactic magnetic field. Over nearly all the sky, the observed radiation at frequencies below 300 megacycles per second is mainly dominated by the nonthermal component. At higher frequencies, the thermal component begins to dominate the rapidly decreasing nonthermal component.

Thus, the resulting effective antenna temperature becomes

$$T_{ea}' = \sum (T_{ea})_{th} + \sum (T_{ea})_{nth} \tag{20}$$

where $(T_{ea})_{th}$ is the thermal type and $(T_{ea})_{nth}$ is the nonthermal type of source. The summations include discrete as well as continuous or extended radiators.

7.2 NETWORK RELATIONS

The immediate discussion is intended to provide some basic tools required in evaluating

the performance of a communication system. When high performance (low noise) is intended, small perturbations in noise, such as might result from an error in calculation, could make the performance appear better or worse than it actually is. Another problem is that of understanding how noise powers can be represented as equivalent sources in one part of a network, whereas in reality they are generated in an entirely different network. Also, the different methods of representing noise will be considered, with the transformations from one to the other discussed. As indicated, these tools will assist in correctly representing many diverse sources of noise in a complex system.

7.2.1 General Two-Terminal Pair Networks

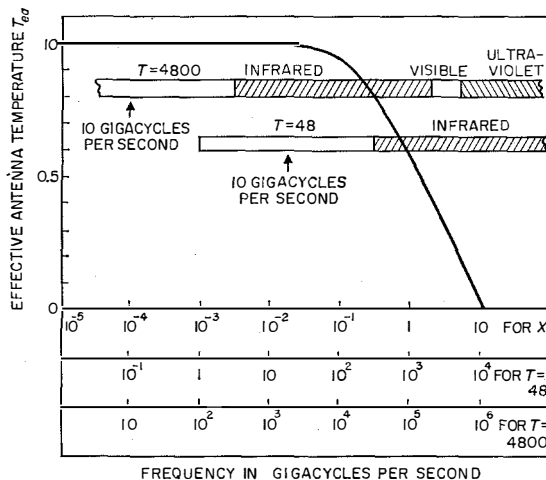
7.2.1.1 General Concepts

For the network shown in Figure 12, the noise factor F is defined^{5,6} as

$$F = \frac{(S/N)_{input}}{(S/N)_{output}} = \frac{S_1/N_1}{S_2/N_2} = \frac{S_1N_2}{S_2N_1} \tag{21}$$

Figure 11—Frequency dependence of T_{ea} for two values of T , 4800 and 48 degrees Kelvin.

$$\frac{x}{e^x - 1} = \frac{T_{ea}}{T}, \quad x = \frac{T_a}{T} = \frac{4.8 \times 10^{-11} f}{T}$$



Application of Advances in Communication

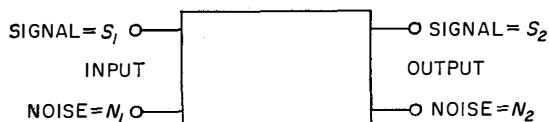


Figure 12—General two-terminal pair network.

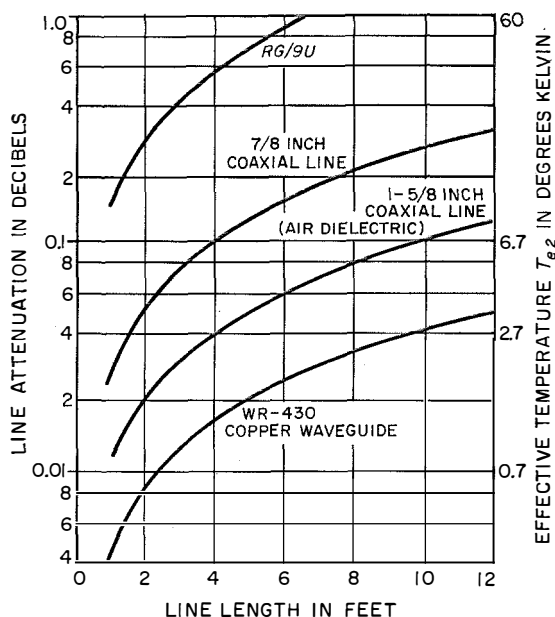


Figure 13—Contribution of line loss to effective temperature T_{e2} referred to the output of the line. Line temperature is assumed to be 290 degrees Kelvin. $T_{e2} = T_e (1 - G)$, where $T_e = T_e$ and $G =$ attenuation.

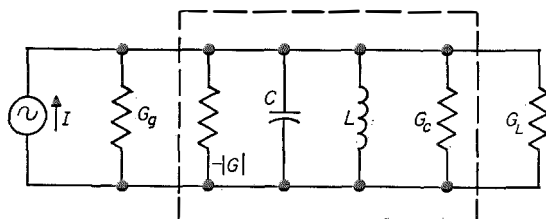


Figure 14—Basic circuit of a negative-resistance amplifier referred to the input terminals of the amplifier.

But S_2/S_1 is the power gain G , and $N_1 = kT_1B$, so (21) becomes

$$F = \frac{N_2}{GkT_1B} \quad (22)$$

where $G =$ average network gain, calculated at some f_0

$k =$ Boltzmann's constant, 1.38×10^{-23} joules per degree Kelvin

$T_1 =$ noise temperature of source noise in degrees Kelvin

$B =$ effective noise bandwidth of network in cycles per second.

Note that, contrary to some arguments, T_1 need not be equal to T_0 , the standard ambient noise temperature of 290 degrees Kelvin.

Strictly speaking, $GB = \int_0^B g(f)df$, where G is the average power gain over bandwidth B such that the area of GB is equal to the area under the actual gain curve $g(f)$. To obtain N_2 , the noise generated within the network is needed.

Let P_n represent the noise generated in the network by an equivalent generator located at the input terminals of the network. This internal noise is thereby referred to the input terminals of the network. Then, $N_2 = GP_n + GN_1 = GP_n + GkT_1B$ and (22) becomes

$$F = 1 + \frac{P_n}{kT_1B} \quad (23)$$

which can be rewritten as

$$P_n = (F - 1)kT_1B. \quad (24)$$

But $P_n = kT_{e1}B$, where T_{e1} is the effective noise temperature of the network referred to the input terminals. Using (24), T_{e1} becomes

$$T_{e1} = (F - 1)T_1. \quad (25)$$

When referred to the output terminals of the network, the effective noise temperature becomes

$$T_{e2} = GT_{e1}. \quad (26)$$

Thus, by means of effective noise temperature, noise sources within the network can be represented by means of equivalent noise

generators located at either the input or output terminals. Care must be used, however, to specify which terminals are being used. With (26), (25) becomes

$$T_{e2} = (F - 1)GT_1 \quad (27)$$

where GT_1 may be taken as T_0 if the output termination of the network is at room temperature. Thus T_1 may be defined as T_0/G and may become equal to T_0 only when $G = 1$.

7.2.1.2. Passive Network

A passive network, in general, operates at finite temperature and, because of its losses, contributes noise power to its output terminals. The network may be lumped, distributed, or combinations of both. As shown above, the effective noise temperature may be referred to either of the two terminal pairs.

For the passive network, it is convenient to obtain the noise factor or effective noise temperature as a function of the network gain or loss.

Assume for the moment that the network has no losses. Then noise power output is $N_2 = kT_1B$.

When the network has losses and, therefore, a finite nonzero temperature T_n , the noise power output is still given by (22) when $T_n = T_1$ because of network equilibrium conditions. Half of the source noise power terminates in network losses, the other half in the output termination. Similarly, for the noise power generated by T_n , half is lost in the input termination and the other half in the output termination. However, a part of $N_2 = kT_1B$ comes from the input noise source

$$(N_2)_1 = GkT_1B \quad (28)$$

where G is the network gain as defined above. The network, therefore, contributes the rest, or

$$(N_2)_2 = kT_1B(1 - G). \quad (29)$$

The total output then becomes

$$\begin{aligned} N_2 &= (N_2)_1 + (N_2)_2 \\ &= GkT_1B + kT_1B(1 - G) \end{aligned} \quad (30)$$

when $T_n \neq T_1$, (30) becomes

$$N_2 = GkT_1B + kT_nB(1 - G) \quad (31)$$

from which the effective noise temperature of the network alone referred to the output can be obtained by letting $N_2 = kTB$, where $T = GT_1 + T_{e2}$

$$T_{e2} = T_n(1 - G). \quad (32)$$

For a passive lossy network, the gain G is usually less than 1. Since $T_{e2} = GT_{e1}$, the effective noise temperature of the network alone referred to the input becomes

$$T_{e1} = T_n[(1/G) - 1] \quad (33)$$

and the noise factor for this network becomes

$$F = 1/G \quad (34)$$

by using (25).

Equation (32) has been plotted in Figure 13 for several types of distributed-parameter networks showing the influence of line length and the general kind of line on T_{e2} .

7.2.1.3. Active Network

Generally, active networks^{7,8,9} such as masers, parametric amplifiers, and tunnel diodes can be described by the noise factor F of (21), (22), and (23). However, to gain some insight into the dependence of F on frequency, temperature, circuit loading, et cetera, the general equivalent circuit of Figure 14 proves useful.

From the basic definition of F in (22)

$$F = 1 + \frac{T}{T_1} \left(\frac{G_c - |G| + G_L}{G_g} \right) \quad (35)$$

$$T_{e1} = T \left(\frac{G_c}{G_g} - \frac{|G|}{G_g} + \frac{G_L}{G_g} \right) \quad (36)$$

where T_{e1} = effective input temperature
 G_c = conductance due to circuit losses
 $-|G|$ = negative conductance contributed by amplification
 G_L = load conductance
 G_g = source conductance
 C = total capacitance of circuit
 L = total inductance of circuit.

For the maser, an approximate expression for $|G|$ is

$$|G| = \frac{\omega_s}{\omega_i} G_g \quad (37)$$

so that

$$T'_{e1} = -T \frac{|G|}{G_g} = -T \frac{\omega_s}{\omega_i} \quad (38)$$

where T'_{e1} = effective input temperature due just to the quantum mechanical equilibrium conditions in the amplifying device and is negative

ω_s = signal frequency
 ω_i = idler frequency = $\omega_p - \omega_s$
 ω_p = pump frequency.

(This result also follows from the application of the Manley-Rowe equations to a multiport network as a whole⁹.)

$$T_{e1} = T \frac{G_c}{G_g} + T \frac{G_L}{G_g} - T \frac{\omega_s}{\omega_i} \quad (39)$$

where, to reduce T_{e1} , it becomes advantageous to use isolators and circulators to minimize the contributions of the first two items; to use a small T ; and to make the ratio ω_s/ω_i large enough to reduce (39) to (38) by overcoming the residual due to the first two terms.

The parametric amplifier can be described by the same over-all equivalent circuit and temperature equations. The tunnel diode can be described by the same equivalent circuit, but the mechanism for producing noise is shot effect and therefore (37) and (38) do not apply.

7.2.14. Networks in Cascade

With two networks in cascade (Figure 15), the effective noise temperature at the input is

$$T_{e \text{ in}} = (T_{e1})_1 + \frac{(T_{e1})_2}{G_1} \quad (40)$$

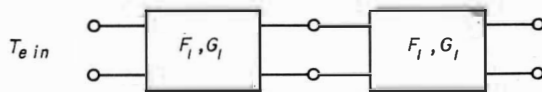


Figure 15—Two networks in cascade.

where $(T_{e1})_1$ = the effective noise temperature of network 1, referred to its input terminals

$(T_{e1})_2$ = the effective noise temperature of network 2, referred to its input terminals.

With (25), (40) becomes

$$F_{(1+2)} = F_1 + \frac{F_{2-1}}{G_1} \quad (41)$$

Note the effect of interchanging the networks on $F_{(1+2)}$, particularly when active and passive networks are used. The results of (40) and (41) may be generalized to

$$(T_e)_{N \text{ in}} = \sum_{i=1}^N \frac{(T_{e1})_i}{\prod_{k=1}^{i-1} G_{(i-k)}} \quad (42)$$

$$F_N = 1 + \sum_{i=1}^N \frac{(F_i - 1)}{\prod_{k=1}^{i-1} G_{(i-k)}} \quad (43)$$

where N is equal to the number of networks in cascade.

8. References

1. C. B. Ellis, "Use of Optical Frequencies for Space Communications," *IRE Transactions of Professional Group on Communication Systems*, volume CS-8, number 3, pages 164-168; September 1960.
2. A. E. Siegman, "Thermal Noise in Microwave Systems," *Microwave Journal*, volume 4, number 5, pages 93-104; May 1961.
3. D. B. Harris, "Microwave Radiometry," *Microwave Journal*, volume 3, number 4, pages 41-46; April 1960.

4. F. K. Ritchmyer and E. H. Kennard, *Introduction to Modern Physics*, McGraw-Hill Book Company, New York, New York; 1942; pages 155-162.
5. "IRE Standards on Methods of Measuring Noise in Linear Twoports," *Proceedings of the IRE*, volume 48, pages 60-68; January 1960.
6. "Representation of Noise in Linear Twoports," *Proceedings of the IRE*, volume 48, pages 69-74; January 1960.
7. L. S. Nergaard, "Amplification—Modern Trends, Techniques, and Problems," *RCA Review*, volume 21, number 4, pages 485-507; December 1960.
8. H. Heffner, "Masers and Parametric Amplifiers," *Microwave Journal*, volume 2, number 3, pages 33-40; March 1959.
9. G. Herrmann, "Idler Noise in Parametric Amplifiers," *Proceedings of the IRE* (Letter to Editor), volume 48, pages 2021-2022; December 1960.

Understanding Digital Computers

Paul Siegel of the International Electric Corporation, an associate of the International Telephone and Telegraph Corporation, is the author of this new book. The following statements appear in the preface.

"The book is written primarily for the technician who is thinking of entering the digital computer field. But anyone with a basic understanding of electronics—a 'ham' for instance—can read it with complete understanding. Not a design handbook, it is about principles, and each principle is illustrated by means of examples."

The contents are arranged in three major sections, the chapters being on the subjects given below.

1. Introduction

Logic and Arithmetic

2. Word and Number Languages

3. Arithmetic Processes

4. Machine Logic

Building Blocks

5. Mechanical and Electromechanical Components

6. Vacuum-Tube and Related Components

7. Electromagnetic Components

8. Germanium Diodes and Transistors

9. Other Devices and Circuits

10. Logical and Functional Building Blocks

Functional Units of a Digital Computer

11. Machine Language

12. Memory Unit

13. Input-Output System

14. Arithmetic Unit

15. Control Unit

16. A Specimen Computer

Its 381 pages of text are followed by a short bibliography, a 9-page glossary, and a cross index of similar length, making a total of 403 pages. The book is 6 by 9¼ inches (15 by 24 centimeters).

Understanding Digital Computers is available from the publisher, John Wiley & Sons, 440 Park Avenue South, New York 16, New York, at \$8.50 per copy.

Dewdrop Communication System Performance*

WILLIAM G. DONALDSON

JAMES P. BARBERA

Federal Electric Corporation; Paramus, New Jersey

Dewdrop is a single-sideband suppressed-carrier quadruple-diversity communication system operating between 350 and 450 megacycles per second and employing tropospheric scatter propagation. This 691-mile (1112-kilometer) link, the longest operational single-hop tropospheric scatter system in existence, connects Thule, Greenland, and Cape Dyer, Canada. Many problems and anomalies have been encountered. Some of these were expected but most were not. Military operational requirements have placed more-stringent transmission objectives on the system than those originally contemplated.

TABLE 1
SYSTEM CHARACTERISTICS

Modulation	Single Sideband, Suppressed Carrier
Channels	24 Voice-Frequency
Receiver Output	30 Decibels Referred to 1 Milliwatt for a Normal Talker
Sensitivity	132 to 48 Decibels Referred to 1 Milliwatt
Noise Factor	
Initial	6 Decibels, Maximum
Modified	2 Decibels, Maximum
Transmitter Output	
Initial	3 Kilowatts, Average
Modified	10 Kilowatts, Average
Regulation	Within 1 Decibel, Average
Transmitter Signal Input	10 to 33.5 Decibels Referred to 1 Milliwatt
Antenna	
Paraboloidal Reflector	120 Feet (37 Meters)
Beam Width	≤ 1.5 Degrees at 400 Megacycles per Second
Gain	40 Decibels
Polarization	Horizontal and Vertical

* Reprinted from Institute of Radio Engineers, *Seventh National Communication Symposium Record*, pages 227-232.

Prime responsibility for the design, manufacture, installation, and test of the AN/FRC47, Dewdrop equipment, was held by the General Electric Company under

1. System Description

Table 1 lists the significant system characteristics and Figure 1 is a map of the location of the two terminals of the system.

It is of interest to note that the transmission path is over water that is covered with sheets of ice and icebergs during seasonal changes;

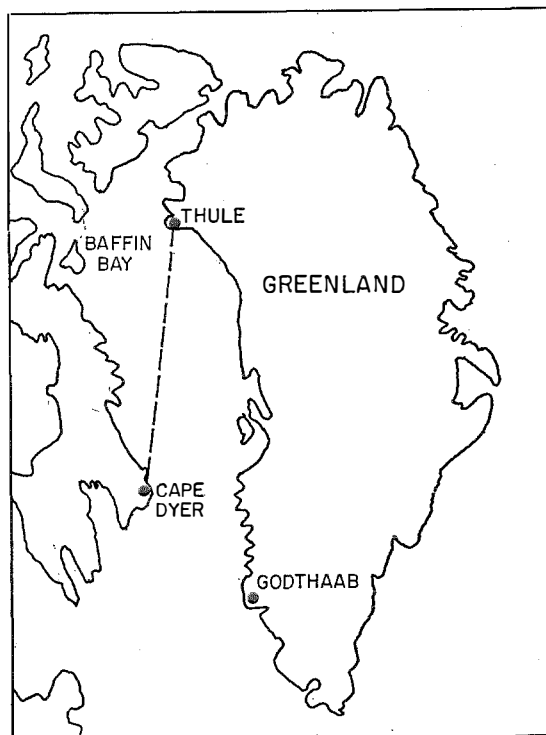


Figure 1—Map of the 691-mile (1112-kilometer) path between Thule, Greenland, and Cape Dyer, Canada.

contract AF30 (635)-7958. Page Communications Engineers, Massachusetts Institute of Technology Lincoln Laboratory, Headquarters GEEIA, Headquarters AACS (AFCS), and Headquarters AFCCDD (formerly AFCRC) actively participated in addition to the General Electric Company in the various phases of testing and evaluating the AN/FRC47 in Dewdrop.

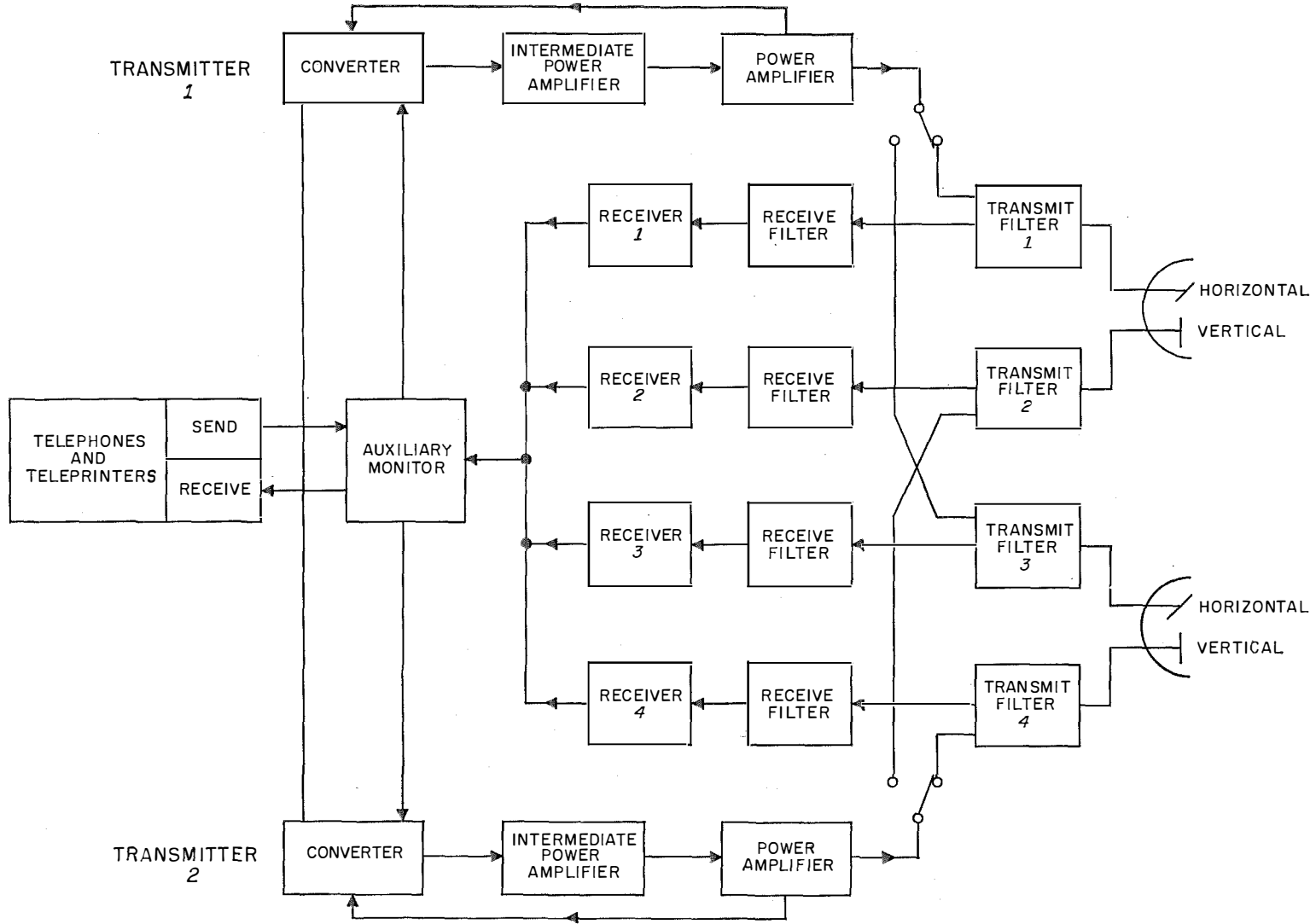


Figure 2—Terminal equipment at each end of the link.

Dewdrop System Performance

this may account for some of the propagation anomalies that were experienced.

The radio installation consists of two transmitters, four branching filters, a radio-frequency patching panel, two antennas, four receivers, system monitor, auxiliary monitor, test set, and six voltage regulators (Figure 2). Each transmitter consists of a converter, intermediate power amplifier, and power amplifier. The two transmitters are operated with the local oscillators of the converters cross-tied (master-slave type of operation) for phase and frequency synchronization.

The nominal radio-frequency power output of each transmitter is 10 kilowatts average and 66.8 kilowatts peak envelope power. A total of 200 kilowatts of power from a 208/120-volt three-phase power source is required for the operation of the radio set and its usual associated terminal equipment. The outputs of the transmitters pass through the radio-frequency patching panel to the branching filters in a configuration that allows the output from one transmitter to be connected to the vertical feed of one antenna while the output from the other transmitter is connected to the horizontal feed of the second antenna. This provides for the transmission of two planes of polarization. In addition, the antennas are physically situated to provide space diversity which, in effect, provides quadruple-diversity operation. Each of the four antenna feeds is connected to one of the four receivers.

2. Operation and Maintenance Problems

2.1 TRANSMITTER POWER

The power amplifier was originally designed to operate at a power output of 3 kilowatts. The power output was subsequently increased to 10 kilowatts. Although the increase in power output changed the distortion figure from 26 to 19 decibels, there was an over-all system improvement.

Klystron tube life has been a problem. The average operating-hours-to-failure for the eight

klystrons replaced was approximately 3000 hours. The largest single cause of failure was heater-to-cathode short, which manifested itself shortly after tube installation. In some cases, the short circuit was cleared by removing the klystron from the power amplifier, inverting it, and energizing the filament. In other cases, the usable life of the tube was extended by operating it without the external filament jumper.

2.2 CHANNEL LEVEL

Channel quality checks were made for a total of 22 days in January and February of 1961. These checks were made by monitoring the signal level of the receiving station for one minute and recording the maximum and minimum signal levels during that period. The data on minimum and maximum channel output levels gathered have been averaged for both ends of the link. It was noted that the spread between the maximum and minimum levels was least at the lowest baseband frequency. Figure 3 is a graphical representation of this spread. While there are some unexplained variations, the curve generally bears out local observations that the lower baseband frequencies have greater level stability than the higher baseband frequencies. This also explains to some degree the fact that teletype channels work much better on lower baseband channels.

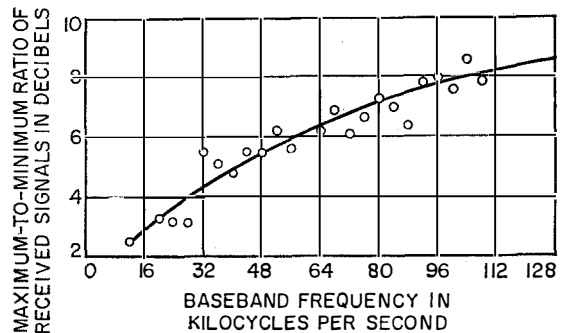


Figure 3—Ratio of maximum-to-minimum received signal levels for 1-minute periods averaged for both ends of the link as a function of baseband frequency.

2.3 PROPAGATION EFFECTS

The vertical polarized signals are received at a consistently lower level than the horizontal polarized signals. Frequency-selective fading has been more severe than anticipated, and at times the receiver slope correction does not appear to be completely effective. This frequency-selective fading causes "holes" in the spectrum in an unpredictable manner. Certain propagation effects have been noticed to cause a 180-degree phase shift of the baseband pilot of one or more of the four receivers. This same effective baseband phase shifting has similarly caused one or more of the receivers to add an out-of-phase baseband signal at the combiner, partially cancelling the baseband output of the other receivers.

Solar effects have caused the total noise to rise above the signal when the sun is at certain critical angles. During the spring, when the sun's rays cross the receiving-antenna beam pattern, periods of up to 10 minutes a day have been encountered when the system has become inoperative due to this solar interference. The severity and duration of the solar noise contribution are somewhat affected by local atmospheric conditions such as clouds, fog, snow, et cetera.

During periods of anomalous propagation, continuous recordings were made of the signal-to-noise ratios of each of the four receivers. These data indicated that 50 percent of the fades occurred essentially simultaneously in all receivers (within 100 milliseconds). Almost all (90 percent) of complete fades occurred together in all four receivers.

2.4 LIMITATIONS DUE TO MULTIPATH

Multipath transmission in conjunction with diversity reception has many advantages, but there are limitations. Because limitations are more evident in wide-band transmission and are directly related to path length, they are of particular importance in this 691-mile (1112-kilometer) 120-kilocycle-per-second multichannel system. It is interesting to note that the same

characteristics of inhomogeneities in the troposphere, as well as reflections from aircraft in the transmission path, produce both the uncorrelated signals in each receiver and the differential path delays. The uncorrelated multipath signals and the random fading characteristics require the use of diversity reception. The differential path delays can be detrimental to system performance.

The calculated differential path delay for the system is 5 microseconds. The differential path delay is based on the difference between the path along the horizontal and the path at an angle to the horizontal equal to one-half the antenna beam width at the 3-decibel-down points. Based on the rather severe case of two paths with a nominally fixed delay and with Rayleigh distributed attenuations of equal means, a maximum bandwidth of 40 kilocycles per second is recommended.¹ This arrangement would reduce the frequency-selective fading to a few decibels throughout the bandwidth.

This 40-kilocycle-per-second bandwidth limitation is conservative because it is based on a severe case and because attenuation and delay of the various possible propagation paths are variables dependent on such factors as inhomogeneities in the troposphere, the number of aircraft in the circuit, et cetera. Considering the fact that the system has a 120-kilocycle-per-second bandwidth, it is not surprising that frequency-selective fading of several decibels has been experienced.

2.5 TOTAL SYSTEM LOSS

Total system loss is defined as the ratio between the transmitted and received power. The factor that contributes the largest variation is the path loss. The variation in the path loss is due to climatological effects. Included in the equation for the path loss is a correction factor resulting from the variation of the mean surface refractive index of air.² A 0.2-decibel increase in path loss per unit decrease in the surface refractive index of air is used to determine changes in path loss. This correction factor has been

Dewdrop System Performance

adopted by the International Consulting Committee on Radio for temperate climates. The average of the mean surface refractive indexes at the two terminals is used. In the Arctic, and where the distance between the terminals is several hundred miles, the correction factor would be of an approximate value but still useful in determining the range of variations. As an example, a change of 30 units from 330 to 300 would cause an increase in scatter loss of 6 decibels. The surface refractivity has an effect on scatter angle and effective scatter volume as well as on scatter loss. These variations in the refractive index are one of the main causes of slow fades.

2.6 PART REPLACEMENTS

Table 2 shows the reported part replacements at the DYE terminal of the system for a six-month period.

These replacements are based on a population of 1500 vacuum tubes and 100 000 electrical

parts. An average of 50 parts was replaced each month.

Of these replacements, 95 percent were the result of corrective maintenance and the remaining 5 percent resulted from preventive maintenance.

Because of the duality of the system, the replacements do not necessarily affect system outage.

An examination of Table 2 reveals that the mean time between failures is 17 hours; however, these were failures of all types: none of them were catastrophic. At most, these failures result in various degrees of reduction in system capability. At first glance, a mean time between failures of 17 hours appears small. But when this figure is related to system population, we find a failure rate of 60×10^{-5} per 1000 hours. This can also be expressed as a mean life of 1.6×10^6 hours.

TABLE 2
REPORTED PART REPLACEMENTS, DEWDROP, 1960

Part Type and Tube Number	June	July	August	September	October	November	December	Total
Filter (Dimineralizer)	0	5	5	12	8	5	3	38
Rectifier, Selenium	7	0	0	0	0	0	0	7
Relay	4	6	3	0	6	0	1	20
Fuse	0	0	0	0	15	10	2	27
Lamp	0	0	0	0	11	6	0	17
5963 Tube	0	0	0	0	0	8	0	8
6X4 Tube	0	0	2	0	8	2	1	13
5Y3GT Tube	0	1	0	0	0	0	7	8
407A Tube	4	3	5	1	1	0	0	14
5879 Tube	0	0	0	1	9	0	0	10
Miscellaneous Parts	12	15	18	29	8	19	10	111
Miscellaneous Tubes	4	2	3	4	9	2	4	28
Total	31	32	36	47	75	52	28	301

2.7 CIRCUIT AVAILABILITY

The bar graph in Figure 4 shows a comparison between all the Dewline communication systems (including Dewdrop) and the Dewdrop communication system for a 6-month period. The Dewdrop system provides about 2 percent of the total Dewline circuits. The outage hours include power failures, equipment failures, and other types of failures such as propagation effects, et cetera; however, failures of the connecting facilities are not included. Although the comparison is not based on equipment failures alone, it is felt that the other elements are essentially common to all Dewline communication systems.

The graph shows that the Dewdrop system has a decidedly lower percentage of circuit availability. One important factor that is not apparent from the graph but is apparent from the raw data is the fact that the Dewdrop system has a very high sensitivity to propagation effects. A good example of this occurred during December 1960 when 90 percent of the Dewdrop outage hours was attributed to propagation. This information supports itself with the previous discussion on propagation effects. The system has an average loading factor of 7 decibels below total power, assuming all assigned channels are used at a nominal activity factor of 25 percent.

2.8 SIGNAL LEVELS AND CHANNEL NET LOSS

In the process of developing a preventive maintenance program for the Dewdrop communication system, it became necessary to determine the inherent capability of the system. Tests were developed to measure important performance areas; among them were received signal levels and channel net-loss stability. These two tests appeared to be most significant for predicting performance inasmuch as they are directly influenced by most other important performance areas.

2.8.1 Received Signal Levels

The levels of received signals were monitored for a period of approximately one month and recorded on an Esterline-Angus recorder. Instead of obtaining continuous recordings, the procedure of sampling in accordance with daily time blocks was employed.³ The signal levels, which appear as random variables, are amenable to a procedure of judicious sampling to predict the total distribution of signal levels. It is desirable to obtain several samples in each time block daily to minimize sampling errors.

Figure 5 is a cumulative frequency distribution of the measured signal levels. It is noted that a low variability ($\sigma = 2.24$) was obtained, which is characteristic of an extremely long tropospheric path. Considerable information on system capability may be obtained from the distribution. For example, signal levels may be compared with system specifications to predict system performance at particular signal levels.

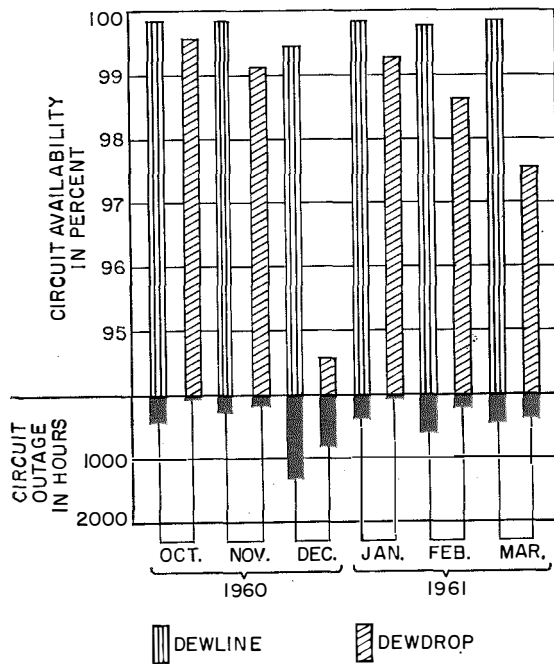


Figure 4—Circuit availability and outage hours for Dewline and Dewdrop from October 1960 through March 1961.

Dewdrop System Performance

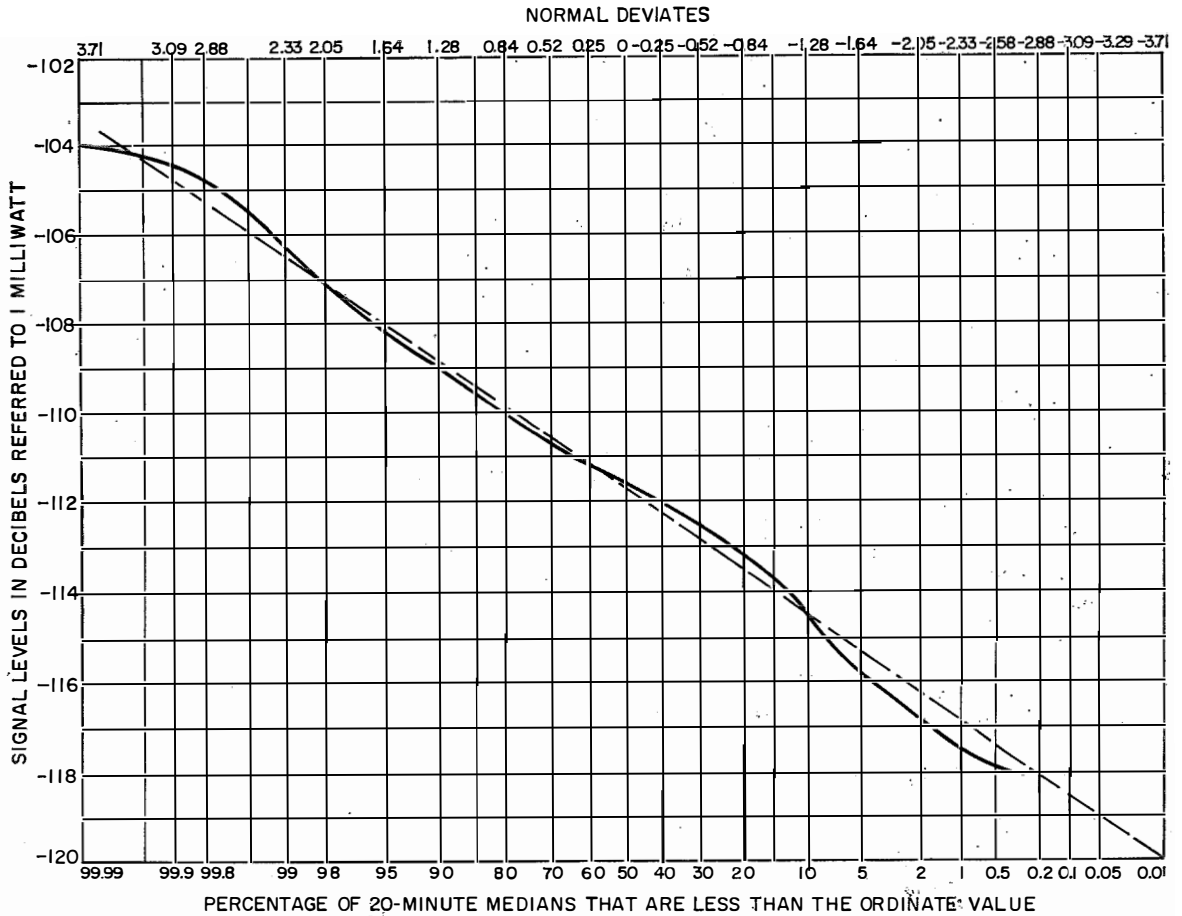


Figure 5—Received signal levels over 691-mile (1112-kilometer) path measured between 24 April 1961 and 25 May 1961 during which 290 measurements of 20-minute intervals gave median values for a standard deviation $\sigma = 2.24$. The solid curve is for the measured distribution and the broken-line curve is for a Gaussian distribution.

Moreover, it is possible to find the percentage of the total time that the system performance will be of a specified grade.

One characteristic of a single-sideband system is that the receivers will operate at low carrier-to-noise ratios without incurring a noise breaking point. This fact is undoubtedly the main reason the facility is able to function at extremely low signal levels. For 50 percent of the time, the signal is less than 9.3 decibels above receiver intrinsic noise. In the case of many frequency-modulation systems, such a carrier-

to-noise ratio could result in total capitulation of the received signal to intrinsic receiver noise.

2.8.2 Individual Channel Performance

The most-striking feature of channel performance is the lack of good stability at drop levels. Distributions of channel receive levels are shown in Figure 6. It is noticed that channels situated high in the baseband spectrum exhibit lower drop levels than channels situated low in the baseband spectrum. In addition, all channel outputs vary in amplitude over wide limits. It

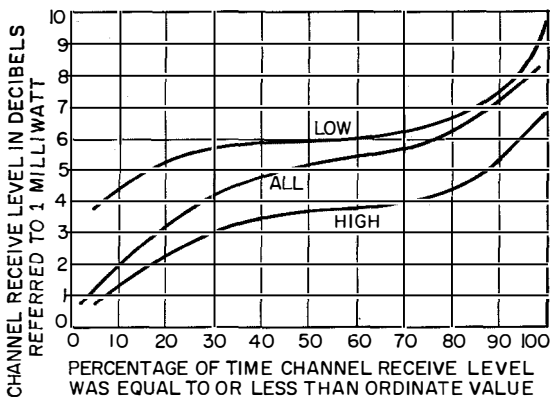


Figure 6—Distribution of channel receive levels. The curve designations are for the low and high baseband frequencies.

is believed that proper application of regulating amplifiers will clean up most of the erratic level changes. To be effective, however, the regulation should be applied on a 12-channel-group basis, rather than regulation of the entire baseband with one amplifier.

3. Conclusions

Two advantages of single-sideband operation of particular benefit in extremely long tropospheric paths are the narrow bandwidth and the absence of a definite threshold above intrinsic receiver noise. The absence of a specific threshold may be an equivocal advantage because to exploit this feature it is usually necessary to tolerate poor voice-frequency channel performance. Narrow bandwidth is of vital importance because of the limitation imposed by the differential path delay of received signals. The lower ultra-high frequencies employed and long distances accentuate the signal delay problems.

A disadvantage of single-sideband modulation, which imposes a definite limitation, is the re-

quirement of operating power amplifiers at very low efficiencies. Inasmuch as a linear amplifier is required to obtain large power outputs, the radiated power is obtained at a large expense of primary power. In addition, the comparatively low output power, which is obtained from a derated klystron of much higher output capability, detracts from one essential source of system gain; that is, transmitter output power.

The 691-mile (1112-kilometer) single hop has stretched the single-sideband system to its design limits and at times of anomalous propagation beyond its design limits. Some improvements will be necessary to bring the Dewdrop system up to par with the other Dewline communication systems.

Based on the information available, it is doubtful that Dewdrop or similar long-path single-sideband tropospheric-scatter systems will be capable of handling reliable high-speed data transmissions.

4. References

1. W. E. Morrow, Jr.; C. L. Mack, Jr.; B. E. Nichols; and J. Leonhard, "Single-Sideband Techniques in UHF Long-Range Communications," *Proceedings of the IRE*, volume 44, pages 1854-1873; December 1956.
2. L. P. Yeh, "Simple Methods for Designing Troposcatter Circuits," *Transactions of the IRE Professional Group on Communication Systems*, volume CS-8, number 3, pages 193-198; September 1960.
3. P. L. Rice, A. G. Longley, and K. A. Norton, "Prediction of the Cumulative Distribution with Time of Ground Wave and Tropospheric Wave Transmission Loss," *NBS Report 5582*, National Bureau of Standards; Boulder, Colorado; July 1959.

Parametric Converter Performance on a Beyond-the-Horizon Microwave Link

JACK HARVEY

ITT Laboratories, a Division of International Telephone and Telegraph Corporation; Nutley, New Jersey

Experimental parametric converters were installed on a quadruple-diversity link of the White Alice system. Two parametric receivers with noise figures of 1.5 decibels were operated simultaneously with two normal receivers of 8.8-decibel noise figures. Comparative measurements showed improvements of 7 decibels in telephone-channel noise and 10-fold improvement in teleprinter error rates.

• • •

1. Introduction

The parametric converter, shown in Figure 1, was developed during 1958 to investigate the characteristics of these devices, particularly the noise figures obtainable in the ultra-high-frequency range. A semiconductor diode [1] having especially favorable characteristics as a voltage-sensitive capacitive reactance was chosen as most suitable for this early use.

In 1959, models of this converter were installed in Alaska on the northernmost beyond-the-horizon link, from Kotzebue to Cape Lisburne, of the White Alice system. Being the longest, this link is the most sensitive to equipment performance. The link normally operates in quad-

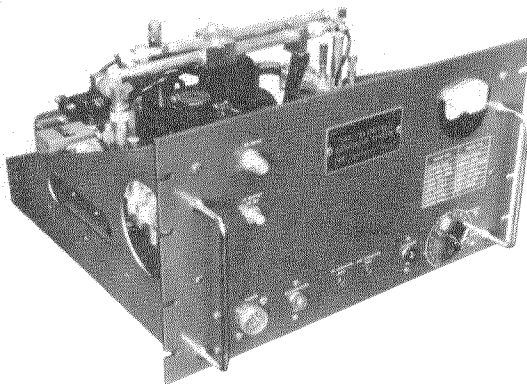


Figure 1—This parametric converter contains all microwave components, pump, local oscillator, and intermediate-frequency preamplifier. The power supply is separate.

ruple diversity. For the test, two of the conventional receivers at Kotzebue were equipped with parametric converters in place of their normal input stages and converters and the other two receivers served as a control group.

2. Details of Parametric Converter

The theory of parametric amplifiers and converters has been thoroughly covered elsewhere [2-7] and it will suffice here to remind the reader of the general principles and operating characteristics.

Briefly, the low-noise performance stems from the absence of resistive devices in the process. A nonlinear reactance can act as a heterodyne

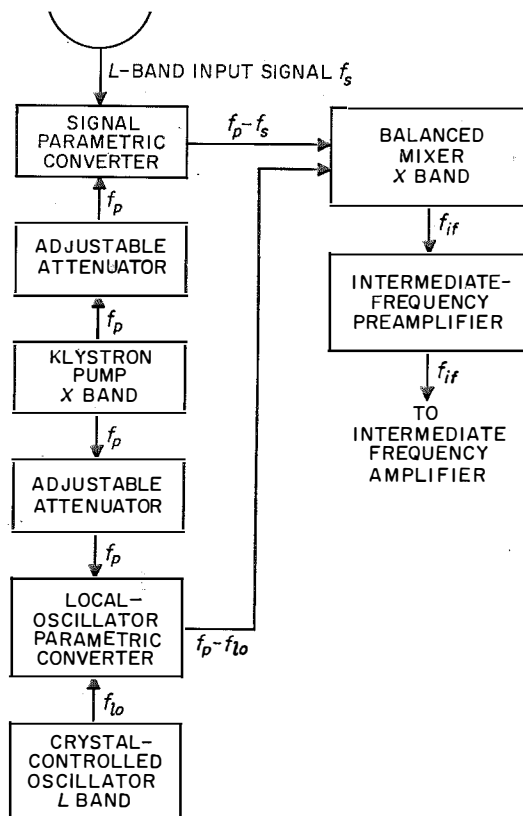


Figure 2—Block diagram of parametric converter system showing method of canceling pump drift.

converter in the same manner as a nonlinear resistance. The sum and difference frequencies of the signal frequency and a locally generated frequency termed the pump, appear in the output.

If the signal is converted in frequency in the usual manner, a power change occurs because the *energy* transfer that occurs for a given change in capacitance of the parametric diode is a constant amount per cycle. Consequently, the *power* transfer is directly proportional to the frequency.

If the signal frequency is converted to a lower intermediate frequency, the power loss would reduce the signal amplitude and the noise figure of the following stage would predominate.

The parametric device used in these tests was a lower-sideband up-converter, shown in block diagram in Figure 2. A klystron was used as a pump to vary the capacitance of the parametric

diode at a 9900-megacycle-per-second rate. The 900-megacycle-per-second input signal mixed with it in the diode produces an output signal at 9000 megacycles per second. Due to the conversion of the input signal upward in frequency and the negative-resistance effect that is present when the output is taken at a frequency of $f_{\text{pump}} - f_{\text{signal}}$, rather than $f_{\text{pump}} + f_{\text{signal}}$, a gain of 20 to 25 decibels accompanies the mixing process.

Since the diode has a very-low equivalent loss resistance, little noise is introduced by the diode. The 20 decibels of gain is therefore sufficient to override the noise figure of 8 to 9 decibels of the *X*-band balanced mixer and give an over-all noise figure of approximately 1.5 decibels. A second parametric converter is used to obtain the local-oscillator voltage for the *X*-band mixer. Using this arrangement, any variations in the klystron frequency cancel and do not appear in the output.

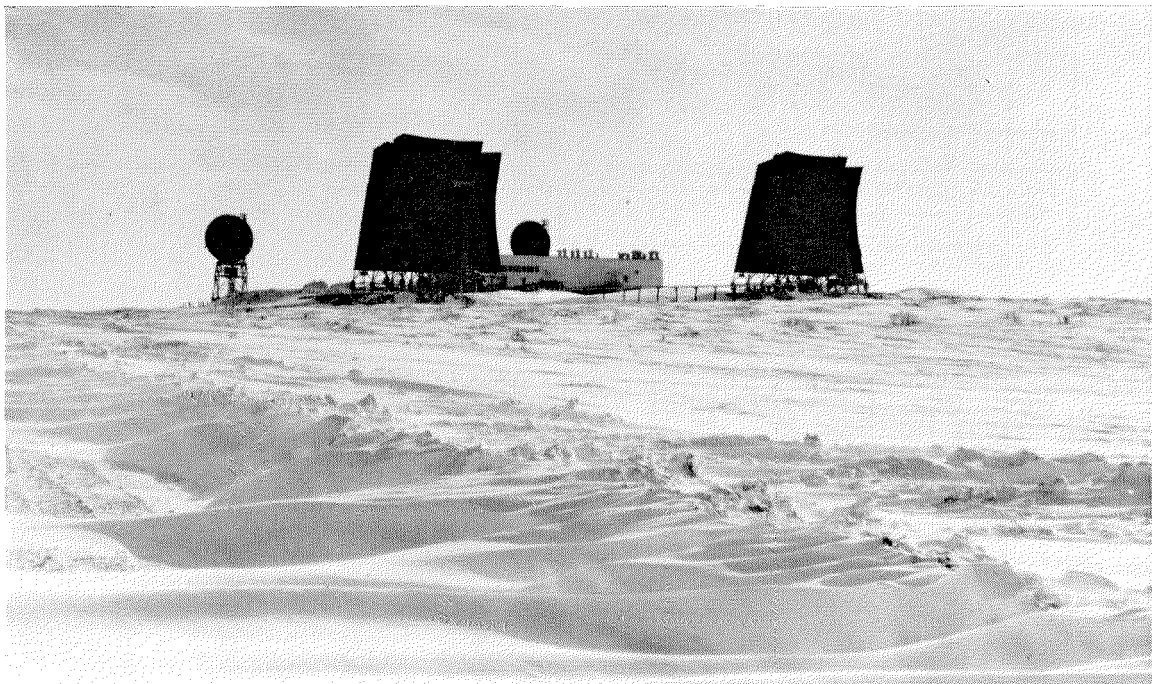


Figure 3—The Kotzebue station. The 60-foot (18.3-meter) paraboloids in the foreground are directed north to Cape Lisburne.

Parametric Converter Performance

3. Kotzebue-Cape Lisburne Link

The radio path between the Kotzebue and Cape Lisburne stations lies almost entirely over land. Much of this area is mountainous and the scatter angle is somewhat larger than for the normal smooth-earth case. The airline distance is about 180 miles (290 kilometers).

In normal operation, quadruple diversity is employed using dual-polarization horns to obtain the four diverse paths with only two paraboloids at each station.

The system uses conventional frequency modu-

lation of the radio-frequency carrier with a 12-voice-channel frequency-division multiplex baseband. The radio-frequency bandwidth is 750 kilocycles per second and the carrier frequency is about 900 megacycles per second.

The antennas are 60-foot (18.3-meter) paraboloids equipped for de-icing. See Figure 3. To get adequate support in the permafrost, they are mounted on piles instead of on a normal concrete foundation. The transmitters use water-cooled klystron amplifiers with 10-kilowatt outputs.

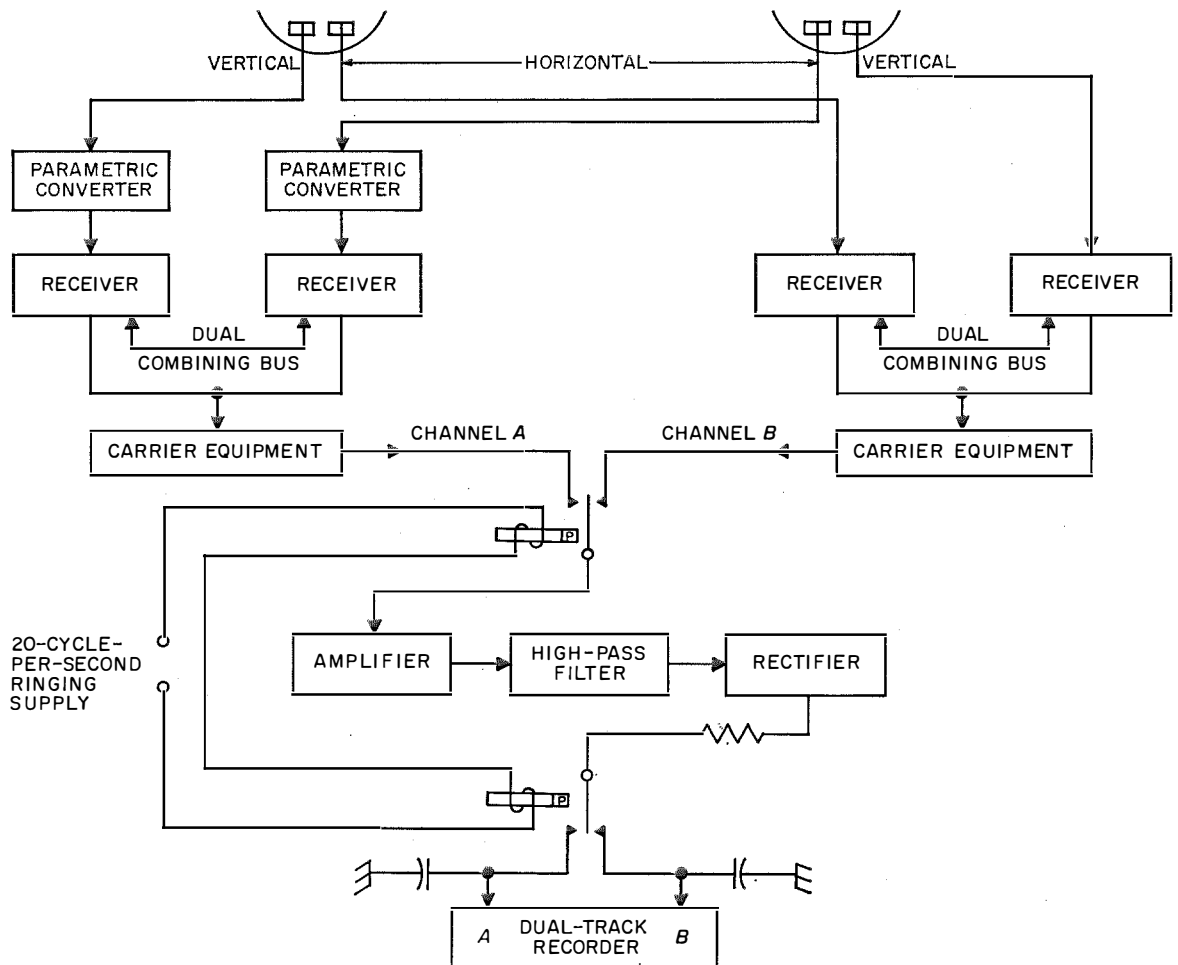


Figure 4—Method for simultaneous measurements of channel noise in normal and parametric systems.

4. Test Methods

To obtain statistical information on the relative performance of the parametric converter, measurements were made simultaneously on two pairs of receivers, each pair connected for dual-diversity operation. One pair of receivers were of existing design and the other pair used parametric converters. Comparative measurements were made on telephone-channel noise and on teleprinter error-rate.

4.1 CHANNEL-NOISE MEASUREMENTS

Noise in a telephone channel was measured as shown in Figure 4. Each pair of dual-diversity receivers, one with parametric converters and one without, was connected to separate sets of

carrier equipment. An unused telephone channel was selected for the test.

A polar relay driven by the 20-cycle-per-second station ringing voltage alternately connected each carrier equipment to its own track of a dual recorder through a common 1200-cycle-per-second-cutoff high-pass filter that rejected spurious hum voltages, and a full-wave noise rectifier. Thus recorder track *A* indicated the channel noise level associated with the parametric receivers, and track *B* that for the normal receivers. Figure 5 is a sample of the recordings. The recorder, which had a 10-second time constant, was calibrated in decibels adjusted (dba) of channel noise by feeding wide-band noise to the input of the carrier equipment and measuring the channel noise with a standard model-43A noise measuring set while noting the recorder pen deflection. This procedure followed a check for proper channel gain made by sending a test tone from Cape Lisburne.

4.2 TELEPRINTER ERROR-RATE TEST

To make a simultaneous check on the teleprinter error-rate in the normal and parametric systems, two model-15 page printers were connected as shown in Figure 6. A "fox message" from a teleprinter distributor at Cape Lisburne was transmitted on a single telegraph channel. At Kotzebue, the normal and parametric receivers actuated demodulating and loop equipment connected to teleprinters.

The teleprinter tests consisted of 10 000-character runs (about 30 minutes) every 2 hours. In all, over a million characters were printed and of this copy 400 000 were analyzed in detail.

4.3 NOISE-QUIETING CHARACTERISTICS

Noise-quieting measurements were made on one receiver using both normal and parametric front ends. A plot of telephone channel noise against signal input is shown in Figure 7. Curve *A* is for the normal 10-decibel-noise-figure front end. Curve *B* is for the parametric front end and shows an 8-decibel improvement over the

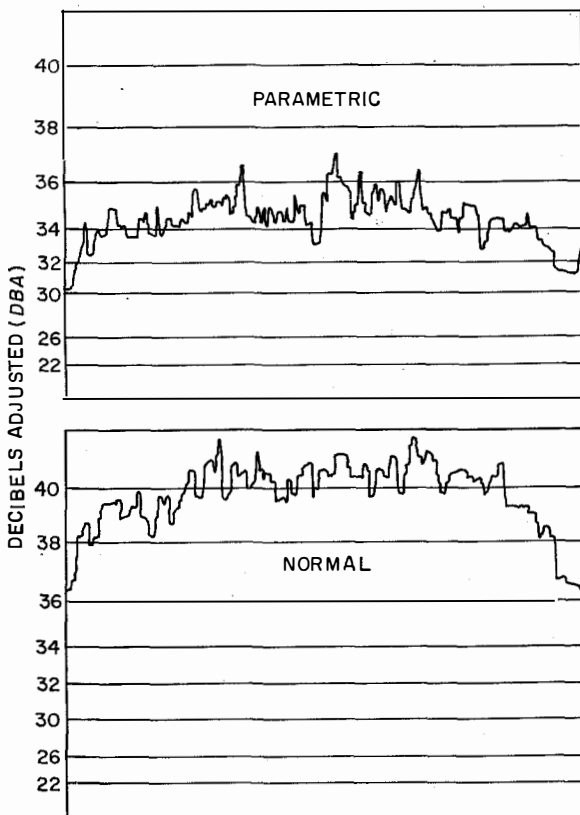


Figure 5—Recordings of simultaneous noise levels on the two channels for 1 hour.

Parametric Converter Performance

normal receiver in the linear portion of the curves.

4.4 ANTENNA VOLTAGE STANDING-WAVE RATIO

The gain of the lower-sideband up-converter at any particular frequency depends on the impedance presented to its input by the antenna and transmission line. If the antenna is not accurately matched to the transmission line, the impedance at the receiver end of the line varies cyclicly across the frequency band. This effect was observed at Kotzebue and is shown in Figure 8A. The satisfactorily uniform response shown in Figure 8B was obtained with a ferrite isolator at the receiver end of the line. It presents a low loss to the signal coming from the

antenna and high loss in the other direction, and thus reduces the magnitude of the impedance variations. Although the particular isolator provided an isolation of about 10 decibels, a 20-decibel isolator would further reduce the impedance variation and give an even-flatter pass-band response. The converter response with a dummy load replacing the antenna transmission line is shown in Figure 8C. Figure 9 shows the voltage standing-wave ratio presented to the parametric converter by the antenna system from 931 to 941 megacycles per second.

4.5 NOISE-FIGURE MEASUREMENTS

The noise figures of the two normal receivers were 8.8 decibels and this value dropped to 1.5

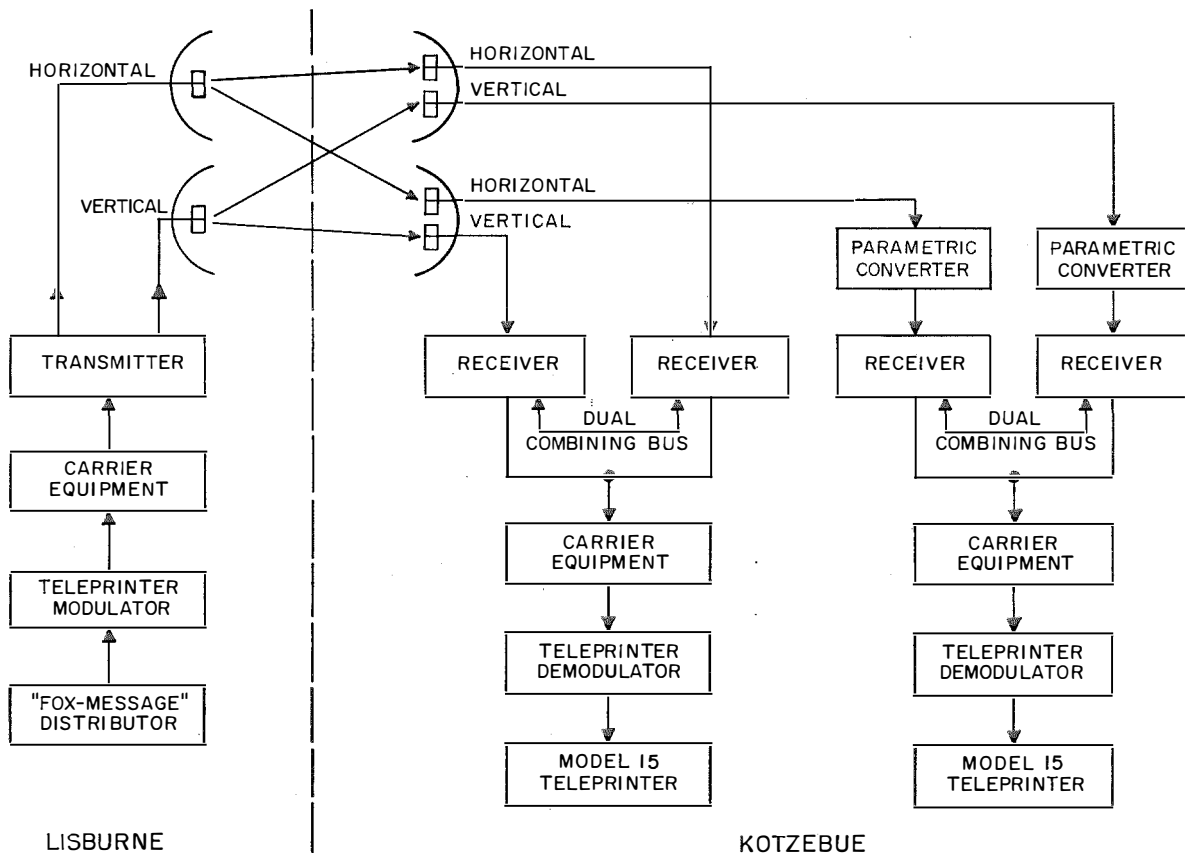


Figure 6—Method of making simultaneous measurements of teletype error rates.

decibels for the two receivers equipped with parametric converters.

4.6 ANTENNA NOISE TEMPERATURE

As the noise contributed by the receiver approaches zero, the noise being received by the

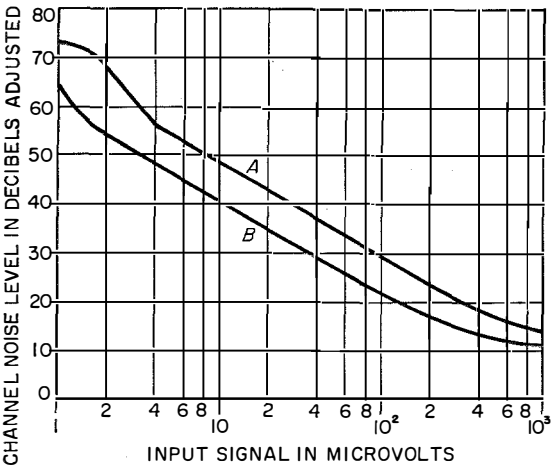


Figure 7—Channel noise versus signal strength. *A* is for a normal receiver and *B* is for the same receiver and a parametric converter.

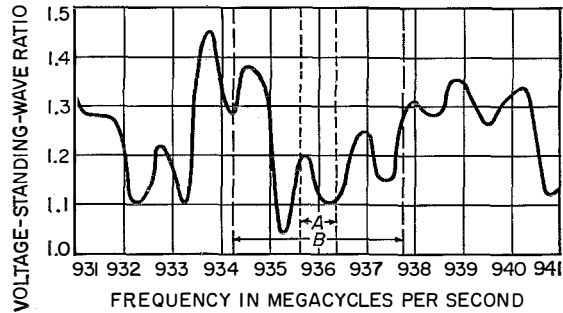
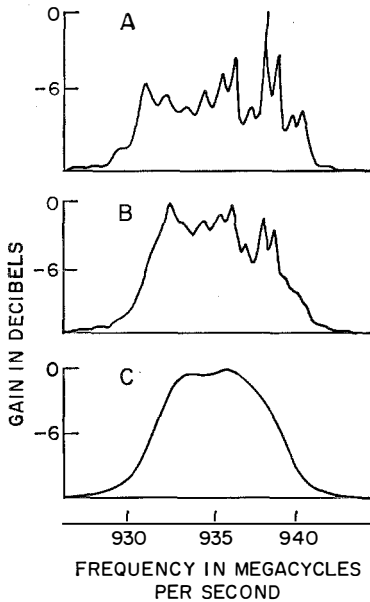


Figure 9—Typical voltage standing-wave ratio at the receiver end of the transmission line from 931 to 941 megacycles per second. Range *A* is for narrow- and range *B* is for medium-band operation.

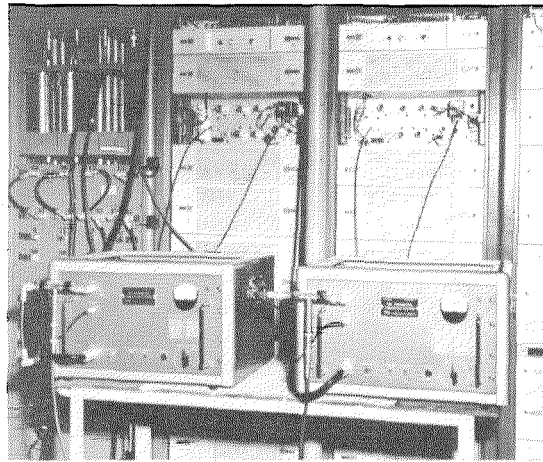


Figure 10—The parametric converters on two receivers of the link. The antenna patch bay is to the left and the two normal receivers are to the right in the picture.

Figure 8—Effect of voltage standing-wave ratio of the antenna transmission line on the gain of the parametric converter. Curve *A* is for the converter connected directly to the transmission line, *B* is for a 10-decibel load isolator between the converter and transmission line, and *C* is with the transmission line replaced by a dummy load.

antenna becomes the limiting factor. This noise can be expressed best as the temperature of a resistor representing the antenna noise. It was measured at the horn of one of the Kotzebue antennas as being about 170 ± 55 degrees Kelvin, which is within experimental error of the expected value.

5. Results and Conclusions

Figure 10 shows the experimental installation, which was made as free of sources of experimental error as possible. The results, however, were biased slightly in favor of the normal receivers because the radio paths to these receivers were parallel while the paths to the parametric receivers were crossed. The fading of signals to the normal receivers had therefore a lower cross-correlation coefficient than those to the parametric receivers [8]. Consequently, the diversity combining was slightly more effective for the normal receivers. It is doubtful, however, that this effect was greater than 1 decibel.

A statistical analysis was made of the channel noise-level recordings. One problem in evaluating these data was that during much of the test period rather strong signals were received so that intermodulation and similar noise predominated in the recorded values. This source of noise is, of course, common to both channels and independent of receiver noise figure. Hence, the improvement appeared to be less when strong signals were being received.

However, by eliminating these periods of strong signals, the statistical analysis of the recorded data showed that the improvement was at least 6 decibels, with a mean value of 7 decibels.

A similar situation occurred in the teleprinter tests. During strong-signal periods, errors that occurred were due to equipment malfunction and transients, which were independent of receiver noise.

The over-all character error rate for the normal channel of 0.75-megacycle-per-second bandwidth was 5.4×10^{-4} and for the parametric channel it was 0.97×10^{-4} . This is a 5-fold re-

duction in error rate. However, by eliminating the strong-signal periods, when equipment errors predominated, the errors were reduced as much as 11-fold.

If the intermediate-frequency bandwidth of a frequency-modulation receiver is increased, the noise power in it and the error rate both increase. To operate 72 voice circuits on this link, it was necessary to increase the intermediate-frequency bandwidth from 0.75 to 3.5 megacycles per second. This increased the noise power by 6.7 decibels, but the parametric converter made up for slightly more than this.

A parametric channel having a bandwidth of 3.5 megacycles per second was compared with a normal channel of 0.75-megacycle-per-second bandwidth. The error rate on the parametric channel was 0.66 that of the normal channel. The parametric converters permitted a substantial increase in circuit capacity with a decrease in noise.

A test was also made with a bandwidth of 3.5 megacycles per second for both channels. As expected, the normal channel then had 8 times as many errors as the channel with parametric converters.

The teleprinter test and channel-noise measurements confirmed the usefulness of the noise-figure improvement. Lowering the receiver noise threshold by 7 decibels reduced teleprinter errors by a factor of 10 (during weak-signal periods) and, of course, lowered the telephone channel noise by 7 decibels. The results predicted from laboratory measurements were fully confirmed in these field tests.

6. References

1. H. Nordlin, "Improved Parametric Diodes," presented at Solid State Device Research Conference of the Institute of Radio Engineers and American Institute of Electrical Engineers, Ithaca, New York; 17 June 1959.
2. T. Warren, "Low-Noise Parametric Amplifiers and Converters," presented at Institute of Radio Engineers National Convention, New York, New York; 25 March 1959.

3. H. Heffner, "Solid-State Microwave Amplifiers," Institute of Radio Engineers, *Transactions on Microwave Theory and Techniques*, volume MTT-7, pages 83-91; January, 1959.
4. S. Weber, "The Mavar: A Low-Noise Microwave Amplifier," *Electronics*, volume 31, pages 65-71; 26 September 1958.
5. J. M. Manley and H. E. Rowe, "Some General Properties of Nonlinear Elements—Part 1, General Energy Relations," *Proceedings of the IRE*, volume 44, pages 904-913; July, 1956.
6. B. Salzberg, "Masers and Reactance Amplifiers—Basic Power Relations," *Proceedings of the IRE*, volume 45, pages 1544-1545; November, 1957.
7. E. Rostas and F. Hulster, "Microwave Amplification by Means of Intrinsic Negative Resistance," *Proceedings of the Institution of Electrical Engineers*, Part B, volume 105, Supplement 11, pages 665-673; May, 1958.
8. A. D. Watt, E. F. Florman, and R. W. Plush, "A Note Regarding the Mechanism of UHF Propagation Beyond the Horizon," *Proceedings of the IRE*, volume 48, page 252; February, 1960.

7. Acknowledgments

Much credit is due to C. Macdonald for designing and making the experimental installation. The work in Alaska was carried out in cooperation with the Federal Electric Corporation. The author is indebted to these for assistance in gathering data for this article.

Experimental Data Transmission System for Switched Telephone Lines *

H. MARKO
H. AULHORN

Standard Elektrik Lorenz AG; Stuttgart, Germany

1. Introduction

Existing world-wide communication networks would be conveniently useful for data transmission. These networks include (A) teleprinter lines, (B) telephone lines, and (C) wide-band transmission paths such as for broadcasting, telephone groups and super-groups, television, et cetera. Connections for (A) or (B) may be either permanent or may be established on order, which are also termed leased and switched connections, respectively. The transmission paths under (C) are generally of the permanent type.

Teleprinter lines operated at the rather low telegraph speed of 50 bauds are suitable only for the transmission of relatively small quantities of information. Transmission speed can be increased 10 to 20 times using telephone lines. If normal switched connections are suitable, then the existing local networks, especially subscribers' lines, as well as the toll network for direct distance dialing may be utilized. As such a data-transmission system would be of great practical and economic importance because subscribers could be interconnected without installing additional transmission lines, the discussion to follow will be concerned with this case alone.

The following specifications would appear to be adequate for this system.

(A) Transmission medium: Conventional telephone channel.

(B) Character error rate $P_{ch} = 10^{-7}$ to 10^{-8} .

(C) Flow of information: 500 to 1000 bits per second.

This specification requires that the system must be able to cope with noise caused by rotary selectors as well as with short-time interruptions not uncommon in carrier-system channels.

* Revision and translation of "Systemtechnik der Datenübertragung auf Fernsprechleitungen", *Nachrichtentechnische Fachberichte*, heft 19, pages 63-69; 1961.

The character error rate $P_{ch} = 10^{-7}$ permits 1 faulty character in 10 million, which is equivalent to not more than one incorrect character in 24 hours of transmission at a speed of 1000 bauds.

Any telephone channel permits a telegraph speed of 1000 bauds. However, the redundancy of the code used should not reduce this flow of information by a factor greater than 2.

Figure 1 is a block diagram of a data-transmission system made up of an input memory, encoder, modulator, transmission channel, demodulator, decoder, and output memory. The return path of the (basically duplex) telephone line can be utilized for backward signals, such as proceed to send or repeat. The number of possible conditions is rather high as consideration should be given to 5 storage means: paper tape, punched card, ferrite cores, magnetic drum, and magnetic tape; 4 coding methods; 4 modulations; and 3×2 transmission systems. Thus, the problem is to select the most

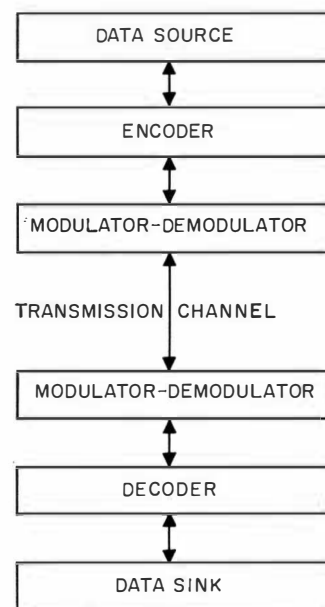


Figure 1—Data-transmission system.

suitable out of $5 \times 4 \times 4 \times 3 \times 2 = 480$ possible combinations. To do this, some of the transmission, modulation, coding, and error-correcting methods will be discussed in general.

2. Transmission

The transmission systems may first be divided on a directional basis for simplex, duplex, and half-duplex operations, corresponding to only one direction of transmission, both directions simultaneously, or both directions alternately. Table 1 shows the important properties of these three types.

In the simplex case, no backward signal can be transmitted; on the other hand, a one-way connection may be utilized in special cases. In the duplex case, the backward signal can be returned without delay as both directions are simultaneously available. However, for a 2-wire circuit in which the two directions are provided by frequency separation, the speed of transmission might be slightly reduced. In

half-duplex operation, the signal in the backward direction invariably causes a loss of time equal to at least twice the line delay plus switching time. Echo suppressors, admissible in simplex and half-duplex operation, must be omitted in duplex operation, thus causing some operational inconveniences. As will be shown later, control signals in the backward direction are indispensable; this eliminates the simplex method. *The duplex method appears most suitable* as backward signals are possible without loss of time and as the omission of echo suppressors is not a serious handicap for they are rarely encountered in the European network.

The second division concerns serial and parallel transmission, (that is, time-division and frequency-division multiplex, respectively). These methods differ in noise and distortion approximately as shown in Table 2.

The signal power is assumed to be the same in both cases and is chosen to avoid overloading the carrier system. Under these conditions, both the serial and the parallel systems have the same sensitivity to random noise; the parallel system has a better performance with respect to impulse noise, and the serial to sinusoidal interference. For n parallel channels, the peak amplitude of a short noise pulse will be $1/n$ that in the serial system because the power is distributed among n channels, each being narrower by that factor. Since, however, the signal amplitude in a parallel channel is $1/n^{1/2}$ that in the serial method, the over-all improvement for parallel operation is only $n^{1/2}$. As to linear distortion, for instance delay distortion at the edges of the frequency band, the parallel system is more favorable because of its longer pulse durations. Nonlinear distortion, such as produced by a compandor, affects the parallel system more. Of particular importance is the fact that for a parallel system the code is practically fixed while there are no restrictions in choosing the code for the serial system. This is of particular advantage for a building-block-type data-transmission system that can be adapted to various applications, *and therefore the serial system was chosen.*

TABLE 1
TRANSMISSION SYSTEMS—DIRECTIONAL

System	Directions of Transmission	Echo Suppressors
Simplex	Forward Only	Permitted
Duplex	Forward and Backward Without Delay	Not Permitted
Half-Duplex	Forward and Backward With Delay	Permitted

TABLE 2
TRANSMISSION SYSTEMS—MULTIPLEX

	Serial (Time Division)	Parallel (Frequency Division)
Impulse Noise	—	Better, $n^{1/2}$
Random Noise	Same	Same
Sinusoidal Interference	Better, $n^{1/2}$	—
Linear Distortion	—	Better
Nonlinear Distortion	Better	—
Code	Any	Inflexible

3. Modulation

Essential operating properties of the most-important modulation systems when used with binary codes are presented in Table 3. Only two of the modulation systems listed need be defined. Direct bipolar transmission means direct transmission in which every information element is represented by two successive elements of opposite polarity to avoid the direct-current component and double-tone modulation is the equivalent of two amplitude-modulation systems.

Reference telegraph speed is the speed for direct transmission if the same bandwidth is assumed for all cases. The gain in signal-to-noise ratio, as compared with direct transmission, is given for white noise at an element error rate¹ of about 10^{-4} . The values given are true for equal density of the noise spectrum. Positive figures mean a gain and negative figures a deterioration with respect to direct transmission. The difference is only a few decibels for all methods, except for vestigial sideband modulation, which requires the carrier to be transmitted to avoid square-law distortion. Some general advantages and disadvantages of the various methods are listed.

The two direct-transmission methods are unsuitable because of the effects of frequency deviation; the received frequency may deviate by not more than 2 cycles per second from the transmitted frequency in a carrier system. For phase modulation, which is most favorable as regards the signal-to-noise ratio, carrier synchronization would be required, involving higher cost and complexity. An advantage of phase and frequency modulations is their insensitivity to level variations. *Frequency modulation has been favored* because of its simplicity of equipment and adjustment and the minor effects of changes in signal-to-noise ratio.⁴

4. Coding and Error Correction

Coding and error correction are the main problems of data transmission maintaining a low error rate. Hence, these problems will have to

be treated in detail. The coding system employs m information elements and k redundant elements for error detection or correction. In a binary system, the total number of possible information combinations being 2^m . The redundant k elements provide for k parity checks of the m information elements. Obviously the error rate will decrease, but the redundancy of this code will increase with increasing k . A code of this structure may be used for both error detection or error correction with various efficiencies as has been described elsewhere.^{2, 3}

Table 4 presents four methods for error correction and error detection. The decision-making stations are shaded. In the error-correcting case, the $n = m + k$ bits of each combination are transmitted in one direction only; hence, a simplex channel can be utilized. In the absence of a backward direction, only an error-correcting code would be useful. The other three methods permit repetition of transmission to correct erroneous material and may employ error-detecting codes. As signals have to be transmitted in the backward direction, a duplex or half-duplex channel is required. Any disturbance will initiate a repetition of the information, the number of repetitions depending on the quantity and duration of the disturbances. For these reasons, the flow of information is discontinuous in all duplex or half-duplex systems employing repetition; a disadvantage compared with the simplex system where without repetition the information flows continuously.

The systems employing repetition can be subdivided into the following three groups.

(A) Error detection in the receiver and decision feedback through the return channel. An error-detecting code is employed, and the receiver decides whether the feedback decision signal q is proceed to send, when no error is detected, or repeat, when errors are detected.

(B) Error detection in the transmitter is provided in an operation where only the m information bits are transmitted to the receiver. The k check bits are derived in both stations

and transmitted from the receiver back to the transmitter where they are compared. This operation is also called redundancy feedback. The decision signal is now issued by the transmitter and instructs the receiver to prepare either for a repetition or for additional material.

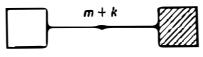
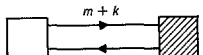
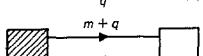
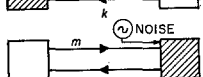
(C) To these two well-known methods, another may be added that permits the abolition of the k check bits altogether. The receiver is

here equipped with a disturbance detector that will indicate the presence of any disturbance, interference, or noise. This disturbance detector may be of several forms: an additional parallel channel conveying no transmitted signals; in a frequency-modulation system, disturbances give rise to an amplitude modulation, which may be used for disturbance indication; a circuit measuring the character distortion of the signal received; or a circuit with some other mode of

TABLE 3
MODULATION METHODS USING BINARY CODES

Modulation Method	Telegraph Speed	Gain in Decibels in Signal-to-Noise Ratio for White Noise	Advantages	Disadvantages
Direct Transmission	1	0	Simplest Equipment	Direct-Current Component; Disturbed by Frequency Deviation
Direct Bipolar Transmission	1/2	+3	—	Disturbed by Frequency Deviation
Amplitude	1/2	-1	Simple Equipment	—
Phase	1/2	+3	Independent of Level Changes	Carrier Synchronization Necessary
Double Tone	1/4	+2	—	Waste of Bandwidth
Frequency	1/2	+2	Independent of Level Changes, Simple Equipment	—
Vestigial Sideband	1/1.5	-6	—	Square-Law Distortion

TABLE 4
ERROR DETECTING AND CORRECTING METHODS

	Code and Method of Operation	Decision Making in	Repetition to Correct Errors	Transmission System	Flow of Information
	Error Correcting	Receiver	No	Simplex	Continuous
	Error Detecting	Receiver	Yes	Duplex or Half Duplex	Discontinuous
	Error Detecting	Transmitter	Yes	Duplex or Half Duplex	Discontinuous
	Disturbance Detecting	Receiver	Yes	Duplex or Half Duplex	Discontinuous

Data Transmission for Telephone Lines

operation. In each case, repetition of the message is initiated by the decision signal q as soon as the output of the disturbance detector reaches a preadjusted value, regardless of whether the character just received has been affected by this trouble or not. The disturbance detector can also be combined with an error-detecting code, repetition being initiated by either device.

The selection of the most suitable error-correcting method must necessarily be influenced by the statistics of noise affecting the transmission.⁵ This requires a brief discussion of typical noise on switched telephone lines and its statistical evaluation.

Figure 2 shows the cumulative frequency of occurrence of noise pulses as a function of receiver response level. This was measured as follows: A telephone connection was established by dialing; both subscriber stations were then disconnected from the line and replaced by proper terminating resistors. At one end of the line, an electronic counter was inserted

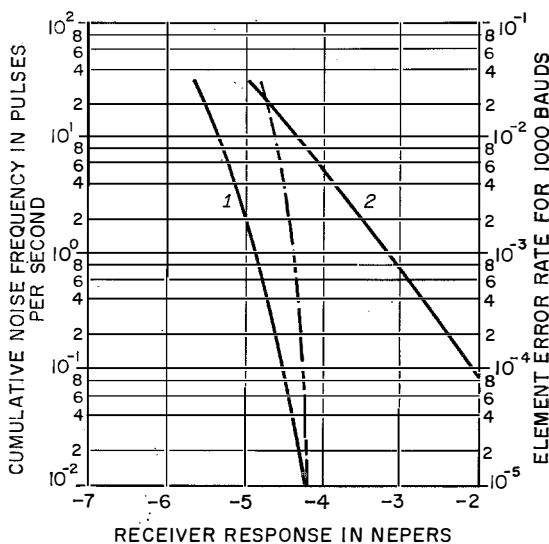


Figure 2—Frequency of occurrence of noise pulses and element error rates for switched telephone lines. Curve 1 is for a private automatic branch exchange using crossbar switches. Curve 2 is for a public network using two-motion selectors. The broken line is calculated for thermal noise of 10 000 picowatts.

by which all noise pulses exceeding the response level were counted. Curve 1 is representative of measurements in the public network of Stuttgart, where two-motion selectors are used, Curve 2 is for the private automatic branch exchange of Standard Elektrik Lorenz AG, which employs crossbar switches. Assuming a telegraph speed of 1000 bauds, the noise-pulse rate (left-hand ordinate of Figure 2) can be converted into the element error rate p (right-hand ordinate) denoting the probability of the occurrence of incorrect elements. It should be noted that the element rate p can be somewhat improved by limiting the receiver bandwidth. For comparison purposes, Figure 2 also shows the element error rate p caused by thermal noise of 10 000 picowatts as calculated.

The noise curve for the local network using two-motion selectors is much less steep than the theoretical thermal-noise curve corresponding to a Gaussian distribution; it does not offer the chance of improving p by several orders through increased transmitter level and the corresponding receiver-response level as in the case of thermal noise. In the receiving level range of interest (-3 to -4 nepers) (-26 to -35 decibels) referred to 1 milliwatt, an element error rate p of 10^{-2} to 10^{-3} will have to be expected.

The most important source of these noise pulses is the modulation of the selector-contact current by vibration set up by the step-by-step motion of adjacent selectors. This source is absent in crossbar switches. Figure 3 shows the typical variation of this noise voltage in time. The clearly evident periodicity is caused

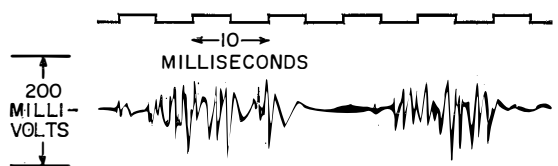


Figure 3—Typical selector noise on a switched telephone line.

by the horizontal homing motion of the selectors. Such disturbances may have amplitudes up to 50 or 100 millivolts and may last for several hundred milliseconds.

The statistical evaluation may be facilitated by thinking of blocks of information being transmitted in a sequence as sketched in Figure 4, each block having the same duration of, say, 100 milliseconds. Those blocks disturbed by one or more noise pulses are counted as erroneous blocks and are shown shaded in the figure. The number of noise pulses in an erroneous block is important. Figure 5 gives the probability distribution of the numbers of noise pulses in an erroneous block, with block duration as a parameter. As will be noted, the cases of only a few noise pulses appearing in a block are relatively rare. All curves are rather flat, that is, the probability of 10 noise pulses does not differ by orders of magnitude from the probabilities of 20 or 30 noise pulses appearing in a block. This shows the uselessness of an error-correcting code that operates only as long as a given number of erroneous elements is not exceeded. Large numbers of noise pulses per block have to be very rare for the successful use of an error-correcting code. Unfortunately, the measurements show that this condition does not exist with switched lines.

Another point of interest is the number or erroneous blocks referred to the total number of blocks. This ratio governs the loss of time in repeating erroneous blocks. The resulting time loss indicated by the shaded blocks in Figure 4 as a percentage of the total blocks was plotted as a function of block duration

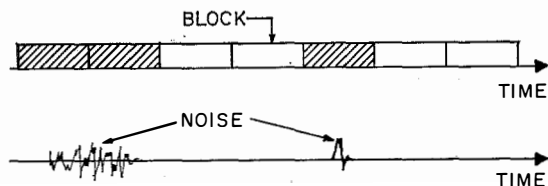


Figure 4—Blocks of information and noise bursts. Erroneous blocks are shaded.

in Figure 6. When the block duration is increased, the occurrence of a disturbance within the block becomes more probable, and the time lost will necessarily increase. Figure 6 also shows, however, that block duration may be increased to several hundred milliseconds without substantially increasing the loss of time; which will then not exceed a few percent and will be negligible in a system where erroneous blocks are repeated.

The result of the statistical evaluation of noise measurements is that considerable disturbances may occur. Fortunately, however, the intervals between such disturbances are large enough to permit transmission. From this it follows that the data-transmission system should provide block-by-block transmission of information with repetition of disturbed blocks.

Figure 7 indicates two possible modes of operation. In 7A, the transmitter is stopped after the emission of a block to await the decision signal q from the receiver. The waiting time equals at least twice the delay caused by the transmission path plus delay in transmitter and receiver. Depending on the decision signal

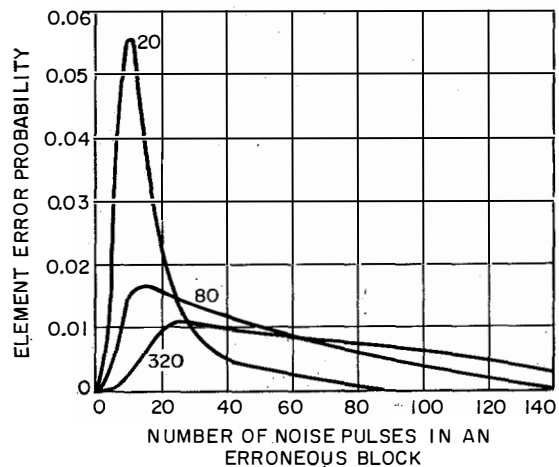
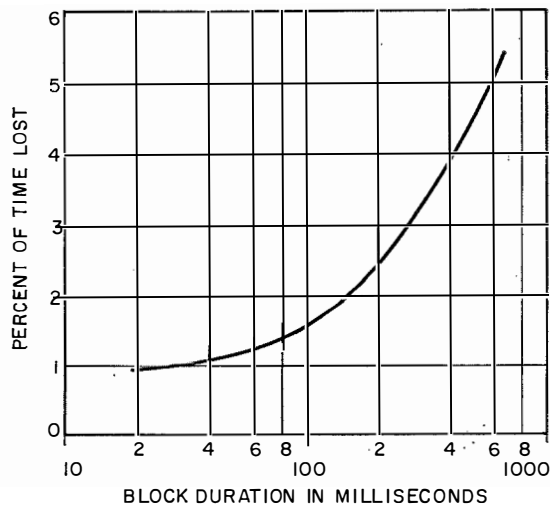


Figure 5—Element error probability plotted against the number of noise pulses in an erroneous block for the indicated block durations in milliseconds and a receiving level of -4 nepers (-35 decibels) referred to 1 milliwatt.

Data Transmission for Telephone Lines

Figure 6—Percent of time lost in repetitions as a function of block duration. Receiving level is -4 nepers (-35 decibels) referred to 1 milliwatt.

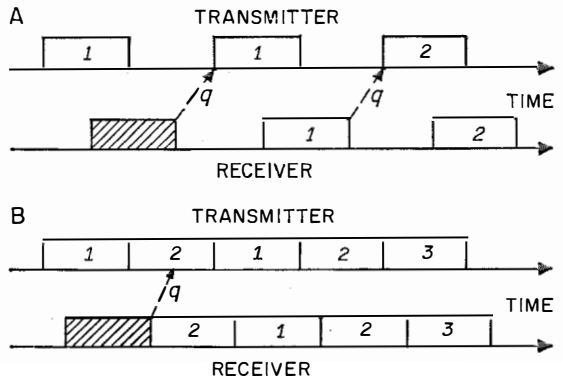


q , proceed to send or repeat, the transmitter either emits the next block of information or repeats the block just transmitted.

In the case of 7B, the second block is transmitted immediately after the first, the only requirement being that the decision signal related to the first block arrive at the transmitter before transmission of the second block is complete. When the decision signal is proceed to send, the third block is transmitted immediately after the second. In the case of a repeat signal, the first block takes the place of the third. In this system, the minimum block duration is determined by twice the line delay plus the equipment delay. Of course, 7B is more favorable than 7A as the waiting time is eliminated and the only time loss is in repeating erroneously received blocks, which does not exceed a few percent as shown in Figure 6.

Considering a maximum transmission delay of 20 milliseconds (say, 8 carrier-system sections in series) and a telegraph speed of 1000 bauds, the following reasonable limits are obtained.

Figure 7—In *A*, the transmitter waits for the q signal from the receiver before sending the next block or repeating the erroneously received shaded block. In *B*, the transmitter does not wait but if it receives a repeat request before the second block is completed, repetition of the erroneously received (shaded) and the following block is made.



Block duration: 50 milliseconds $< t_B < 200$ milliseconds.

Block capacity: 50 bits $< n_B < 200$ bits.

This data-transmission system is desired to have, it will be remembered, a character error rate not exceeding $p_{ch} = 10^{-7}$ to 10^{-8} . Since only a few percent of the blocks are disturbed, the erroneous blocks need to be detected with an undetected block error rate of $p_B' \leq 10^{-6}$ to fulfil this severe requirement.

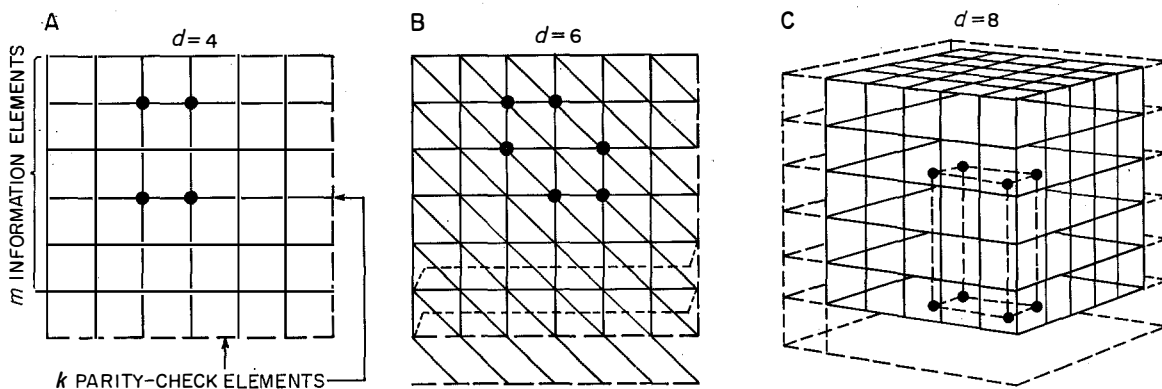
However, the noise amplitude may assume any value; hence, an element error rate covering the whole range $0 < p \leq 0.5$ has to be taken into account.

Compliance with this specification appears feasible when an error-detecting code is used in connection with a disturbance detector. On the other hand, it is possible and may be desirable to base the error detection on the code alone. Such a code should then meet the specification.

$$p_B' = 10^{-6} \text{ when } 0 < p \leq 0.5.$$

In general, computation of p_B' is difficult and calls for the use of an electronic computer.

Figure 8—Block code based on parity check elements k shown dashed for each row and for each column of information elements at *A*. *B* has added a diagonal-path parity check, and *C* is a three-dimensional system. The minimum number of incorrect elements, which must be in pairs in each parity check path, that will be undetected in the entire block equals d .



In the special case $p = 0.5$, however,

$$p_B' = 0.5^k - 0.5^n.$$

In this case, the probability is 0.5 that any one of the k parity checks proves right. Hence, the probability is 0.5^k that each of the k parity checks proves right, which would lead to an undetected block. The small probability 0.5^n that the block comprising n elements is transmitted correctly, should be subtracted from 0.5^k ; however, this may be neglected. For $p_B' = 10^{-6}$, it is thus required that $k = 20$. In other words, at least 20 parity checks and thus the transmission of 20 redundant check elements would be necessary. This is a high redundancy compared with the 6 information elements of a character code. Therefore, the character code should be replaced by a block code for each block contains a large number of information elements.

Examples of block codes are shown in Figure 8. Figure 8A is a two-dimensional matrix, for instance of ferrite cores, into which a block of information may be written row by row. Each row and column is completed with a parity-check element k . The check elements k are chosen to make the number of 1's in every row and every column either even or odd.

Incorrect blocks remain undetected only when 4 erroneous elements form a rectangle as indicated by the dots in Figure 8A. In this case, the so-called minimum Hamming distance is $d = 4$. This distance can be improved by adding diagonal checks to the above as in Figure 8B, where the matrix should be visualized as extended to the right and left to cover all diagonal elements. Here, at least 6 incorrect elements in a certain arrangement would be needed to result in an undetected incorrect block ($d = 6$). Figure 8C shows a three-dimensional arrangement or cube where the verticals are checked apart from the horizontal rows and columns. In this case, an incorrect block remains undetected only when 8 erroneous elements are located in the spatial arrangement indicated ($d = 8$).

The undetected block error rate p_B' as a function of the element error rate p , has been approximated by a calculation which showed p_B' to have a maximum that occurs at a somewhat lower error rate than $p = 0.5$. Because all values of p may occur, this maximum of p_B' alone is of interest; in Figure 9 it is plotted as a function of n/m the ratio of all block elements to the number of information elements.

Data Transmission for Telephone Lines

This ratio is a measure of the redundancy of the code. The figures noted along the curves in this diagram denote the block sizes n . The curves in Figure 9 are approximate as only the types of error patterns shown in Figure 8 have been taken into account.

The curves represent the three block codes of Figure 8. In addition, a plot designated "repetition" was computed for single repetition and element-by-element comparison of the original and repeated messages. It will be evident that this mode of operation is unsuitable inasmuch as the previously chosen block size $n < 200$ cannot be placed into the area of interest where $p_B' \leq 10^{-6}$ and $n/m \leq 2$. In this respect, the code of Figure 8A also would require too large blocks (1000 bits). The block codes for Figures 8B and 8C with three parity-check paths appear capable of meeting the requirements. The redundancy of the block code in Figure 8B is less than that of Figure 8C.

Thus the specification for high accuracy can apparently be realized even for blocks having the optimum size of about 100 bits as required for operation on noisy telephone lines, and the problem can be solved even by purely digital error detection.

5. Proposed System

Figure 10 is the block diagram of a data-transmission system based on the error-correcting method of Figure 8B. The input device is a tape transmitter and the output device is a reperforator. The transmitter has three stores cyclically connected to the tape transmitter and to the transmission channel by switches S1 and S2. After the read-in from the tape transmitter, the redundant check elements are added (not shown in Figure 10). In the switch positions indicated, information from store 2 is transmitted to the receiver while the input device works into store 3. In the preceding period, the information in store 1 had been transmitted and that store is now awaiting the decision signal from the receiver. If this signal

is to repeat, the information of store 1 is transmitted once more; if it is proceed to send, store 3 will be read out as the next in turn while new information will be read into store 1, at the same time erasing the previously stored information. In the solution shown, the appearance of a disturbance-alarm signal has the effect of calling for a repeat while its absence is evaluated as proceed to send. In accordance with Figure 7B, the disturbance-alarm signal has to reach the transmitter during the read-out time of store 2. The cyclic interrogation of the three stores 1, 2, 3 is retained because store θ is connected to the line in place of store 3 after which the sequence of 1, 2, and 3 is resumed. Store θ contains a permanently stored synchronizing signal having the duration of a block. It keeps the receiver in phase and signals the beginning of a repetition.

The receiver has two stores with alternating read-in and read-out. The coincidence gate for the θ signal as well as the code-checking unit always are connected to that store busy with read-in. When the code checker indicates an error, a disturbance-alarm signal is returned to the transmitter. This signal and the presence of a θ signal in the detector stops the read-out into the output device.

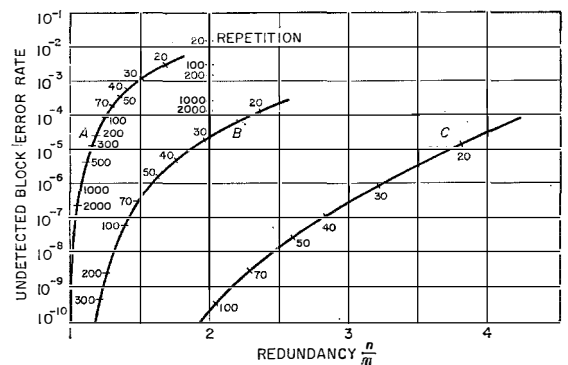


Figure 9—Undetected block error rate plotted against code redundancy. The numbers along the curves indicate the block sizes in elements. The letters identify the block codes with reference to Figure 8. Repetition is calculated for single repeats on an element-by-element comparison.

This arrangement causes the operation to stop when the transmission line in one or both directions is interrupted. As soon as the connection is reestablished, the operation is automatically resumed without introduction of an error.

The above discussion was primarily based on disturbances occurring on switched telephone lines; however, the results may also be applicable to other types of noise. Similar conditions might be encountered with radio communication systems where a heavily disturbed, but rare, fading period can be separated from the undisturbed transmission time permitting high-speed data transmission. The system conceived would seem appropriate for this case as well, and in general it may be summarized as follows.

Continuous transmission during the longer undisturbed periods of time at the highest possible telegraph speed and with the least

possible redundancy, detection of the shorter disturbed periods of time with high accuracy and repetition of the disturbed portion of the message.

6. Experimental System

On the basis of the proposal in the preceding section, an experimental system was built to verify the theory and gather operational experience. Figures 11 and 12 show the transmitter and receiver. The photograph of the transmitter includes a handset for voice communication and a remote control unit for signaling to the receiver the beginning of data transmission, evaluating the signals returned from the receiver, and indicating such signals. A line interruption lasting longer than 2 seconds releases an alarm at the transmitter. The receiver may be switched to unattended operation, in which the power supply is switched on and off by signals from the transmitter.

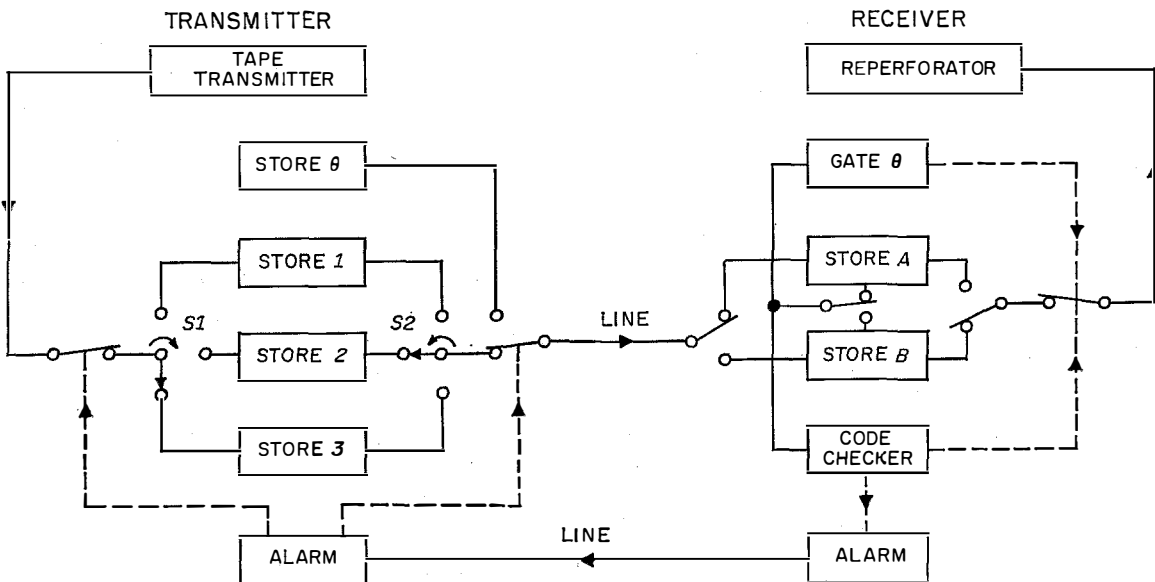


Figure 10—The tape transmitter through S1 progressively fills stores 1, 2, and 3, each of which through S2 transmits sequentially to the receiver while the following store is being filled. If the code checker in the receiver does not confirm the received elements, it will disconnect the reperforator and, through the alarm, stop the tape transmitter and send a synchronizing signal from store 0 until the store of the erroneously received material is again connected to repeat its message.

Data Transmission for Telephone Lines

The modulator of the equipment includes a frequency-modulation data channel for a telegraph speed of 800 bauds using frequencies of 1500 and 2100 cycles per second and a return channel for a telegraph speed of 150 bauds at frequencies of 540 and 660 cycles per second.

Error-correction is based on Figure 10. The stores utilize transistor flip-flop circuits. Interchangeable matching panels permit the accommodation of such commercial input and output devices as tape readers, perforators, et cetera.

A 63-element block has been chosen and is made up of 42 information elements and 21 redundant check elements. This block is not restricted with respect to the code used, that is, a block may consist of 6 characters of a 7-unit code or 8 characters of a 5-unit code. Excess elements, as in the last case, are filled up by zeros.

The coding scheme is given in Figure 13. It follows the principle of Figure 8B, some deviations being necessitated by the circuit technique. Thus, the column check elements and the diagonal check elements are not involved in an additional check. Figure 14 shows the calculated undetected block error rate p_B' versus element error rate p . Assuming an

equiprobable distribution of the errors within the erroneous blocks

$$p_B' = \sum_{v=1}^n Z_v p^v (1-p)^{n-v}$$

where n is the block size and Z_v , the number of undetected error patterns of v errors. The maximum of p_B' is about at $p = 0.1$ amounting to $p_B' = 2 \times 10^{-5}$. It is thus by one order of magnitude worse than should be expected according to Figure 9. This can be traced to the fact that the practical coding scheme will not detect a small number of specific patterns composed of 6 errors.

Error checking is employed in the return channel, too, where the repeat or proceed signals are sent back to the transmitter. Here the only critical case is conversion of the repeat signal into proceed. In the opposite case, no great harm is done since only an undesired repetition occurs.

Moreover, the three blocks of a storage cycle are numbered, for example, by using an odd-parity check for the rows in the first block, for the columns in the second block, and for the diagonals in the third block with even-

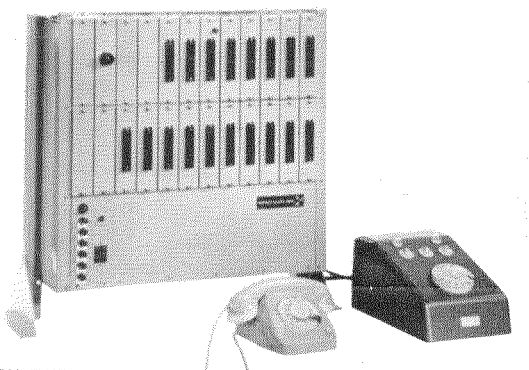


Figure 11—Transmitter for experimental system including telephone for voice communication and control unit for supervising data transmission.

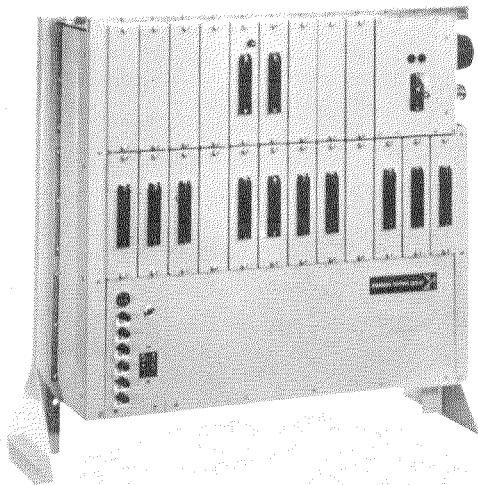


Figure 12—Experimental data-transmission receiver.

parity checks for the other elements. In this way the system can handle longer interruptions without trouble and then proceed with the correct block. To prevent undesired simulation of the proceed signal, the disturbance detector is employed in the return channel. The proceed signal is processed through a voltage gate of small tolerance at the demodulator output; if the output voltage is outside this range, the repeat operation results. With this error-detecting method, the return channel has no noticeable effect on the undetected block error rate.

For the experimental system, the relatively simple type of block coding described in Figure 13 has been used. Recent research⁶ on coding theory has shown that optimum performance can be achieved using the cyclic type of coding. Such coding can be performed relatively easily by a shift register with feedback connections having a number of stages equal to the number of redundant elements required. Using for instance a Bose-Chaudhuri code,⁷ a minimum Hamming distance of 8 can be achieved with 22

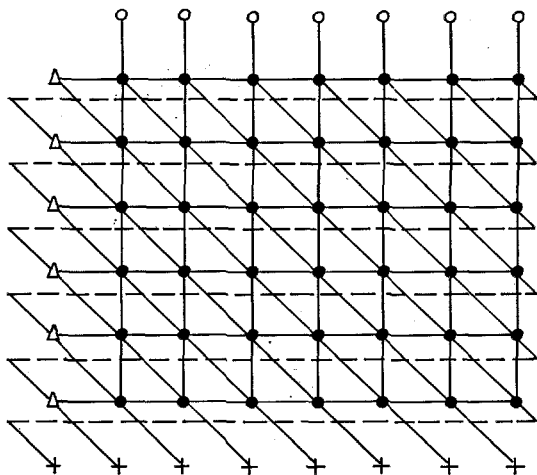


Figure 13—Block coding used in experimental system. The solid dots are information elements, the circles are column check elements, the triangles are row check elements, and the crosses are diagonal check elements, the paths of which may shift from one side to the other as indicated by the dashed lines.

redundant elements for a block of 105 information elements. With such coding, the maximum value for the undetected block error rate is in the order of 2^{-6} giving an improvement in comparison with Figure 14 by more than an order of magnitude.

For the experimental system, the small block size of 63 elements was chosen as a compromise with regard to the expense of storage capacity. This, however, limits the maximum permissible loop delay to a value that may be too small in some cases, especially when a modulation rate as high as 800 bauds is envisaged. For a practical system, therefore, a somewhat larger block size, in the order of 100 to 200 elements, may be advisable.

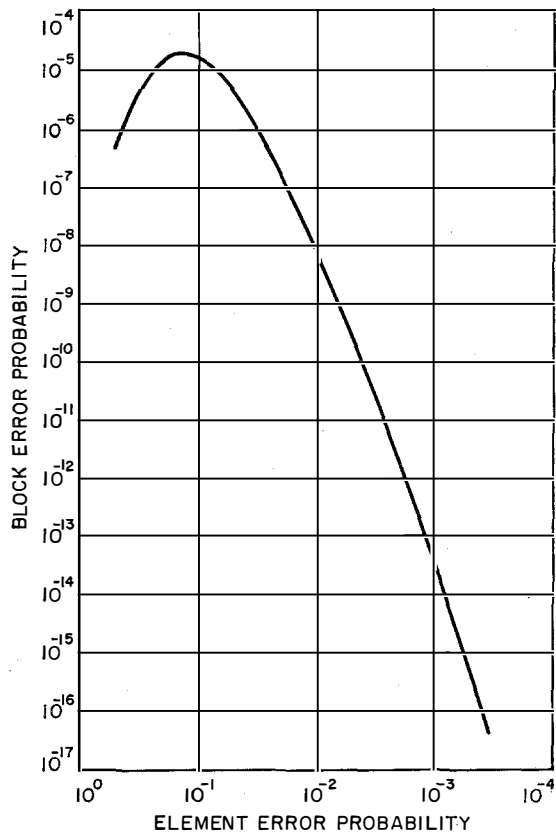
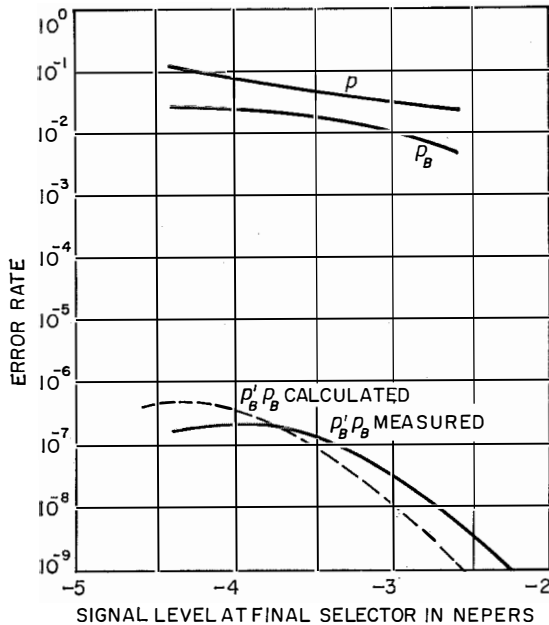


Figure 14—Block error rate as a function of element error rate.

Data Transmission for Telephone Lines

Figure 15—Performance of experimental system. p = element error rate for erroneous blocks. p_B = block error rate without error detection. $p_B' p_B$ = undetected block error rate with error detection.



7. Test Results

The experimental system described was tested for data transmission over switched lines of the Stuttgart telephone network.

First, the block error rate p_B was measured without employing error detection. As may be seen from Figure 15, p_B depends on the signal level at the final selector. This reference point was chosen because it may be assumed to contribute most of the noise shown in Figure 3.

Likewise, the element error rate p was measured, but only for erroneous blocks. It is higher by the factor $1/p_B$ than the element error rate referred to the whole time observed. The large values of p observed for erroneous blocks show that the errors appear mainly in bursts. This could be expected from Figure 3 and justifies the requirement in Section 4 that a coding method to handle all cases encountered must cover the whole range of values for the element error rate to be expected, that is $0 < p \leq 0.5$.

This is especially true because the transmission path will in many cases link two locations where the receiving levels are almost the same with each call and a p value unfavorable for the coding method may occur. In the case under discussion, the least favorable conditions were observed in the level range of -3.5 to -4.5 nepers (-31 to -39 decibels) referred to 1 milliwatt, where the unfavorable $p \approx 0.1$ was actually measured.

The curve designated $p_B' \times p_B$ in Figure 15 finally reaches the residual block error rate when the error detecting method is employed.

It was calculated with the aid of the curve in Figure 14 using p_B' values associated with the p values measured in Figure 15. It was measured by counting those blocks in which faults in transmission were not detected as such. Care was taken to have the same level and noise conditions for each measured point. The measurements obtained directly from the line were complemented by laboratory measurements where line noise recorded on magnetic tape was fed to the receiver input. This method has the advantage of shortening the test time: Noise-free tape sections are cut out, and the time becomes condensed (at a ratio 1:17 in this case). Another advantage of tape records is the uniformity of statistical conditions favoring the reproducibility of measurements and the adjustability of the signal-to-noise ratio.

The measured and calculated curves coincide well. Thus, the simplified assumptions used in planning (for instance, equiprobability of errors in erroneous blocks) have yielded useful results.

To compare the initially specified character-error rate with the results of Figure 15, it should be remembered that the most unfavorable case of an undetected erroneous block involves 4 to 6 elements or 2 to 3 characters that are in error. Since a block includes 7 or 8 characters, the residual character-error rate is about three times better than indicated by

the curve $p_B' \times p_B$ and therefore meets the initial specification. The block error rate p_B is at the same time a measure of the time lost in block repetition; this loss is on the average about twice the value of p_B , since during each repetition cycle 3 blocks are repeated, including the θ signal; two of the blocks, however, were frequently disturbed. As p_B amounts to only a few percent, the time loss for repetition is negligibly small. Even in particularly unfavorable single cases, a value reaching 10 percent seldom was observed.

The results have confirmed the planning considerations and show the feasibility of designing a data-transmission system with a warranted rate of errors between 0.01 and 0.1 characters in a million, regardless of the noise amplitude.

8. References

1. H. J. Held, "Fehlersicherheit binärer Übertragungen bei verschiedenen Modulationsarten," *Nachrichtentechnische Zeitschrift*, Band 11, pages 286-292; 1958.
2. R. W. Hamming, "Error Detecting and Error Correcting Codes," *Bell System Technical Journal*, volume 29, pages 147-160; April 1950.
3. D. Slepian, "A Class of Binary Signalling Alphabets," *Bell System Technical Journal*, volume 35, pages 203-234; January, 1956.
4. M. Jeppsson, "Frequency-Shift Modulation for Transmission of Binary-Coded Signals over Telephone Circuits," *Electrical Communication*, volume 37, number 2, pages 103-116; 1961.
5. W. T. Jones, "Transmission of Data over Telephone-Type Circuits," *Electrical Communication*, volume 37, number 2, pages 87-102; 1961.
6. W. W. Peterson, "Error Correcting Codes," John Wiley Sons, New York and London; 1961.
7. R. C. Bose and D. K. Ray-Chaudhuri, "On a Class Error Correcting Binary Group Codes," *Information and Control*, volume 3, pages 68-79; 1960.

9. Acknowledgment

The authors extend thanks to their co-workers for valuable discussions and for the completion and evaluation of the time-consuming measurements. They are particularly indebted to the Deutsche Bundespost for the interest displayed and the support given to the trial operation.

New Display for Frequency-Modulated Continuous-Wave Radars *

HERBERT H. NAIDICH

ITT Federal Laboratories, A Division of International Telephone and Telegraph Corporation; Nutley, New Jersey

1. Introduction

There has been a great deal of interest in recent years in improving the operating characteristics of radars by techniques more sophisticated than those of pulse echoing. To achieve maximum range, a radar system must have a high average transmitted power and a minimum noise figure in the receiver. Maximum target resolution and range accuracy are proportional to the bandwidth of the modulation of the carrier and the ability of the receiver to process the information contained within this modulation. Lastly, the longer the "time on target" of the radar energy, the more exactly the target velocity can be determined from the Doppler information contained in the received signal.

In pulsed radars, increasing accuracy and resolution by reducing pulse width (and increasing harmonic content of the modulation) causes problems in obtaining maximum average power on target and in the utilization of time on target to obtain the most-accurate velocity determination. The manipulation of pulse width, average power, and time on target for pulsed systems results in compromises that often degrade some of the operating characteristics of the radar. Frequency-modulated continuous-wave radars can often be designed with less compromise to performance specifications, but they encounter complex data-processing problems, especially if multiple targets are considered.

One advantage of pulsed radar systems is the range-echo-time relationship, which enables great simplification in the data processing of the returned signals. Many types of cathode-ray-tube displays have been used based on the deflection of an electron beam in synchronism with the transmitted energy. When the echo is

received, the electron beam is intensified forming a blip as in plan-position and range-height indicators or is deflected forming a pip as in A-scan and J-scan indicators. The echo time (12.2 microseconds per nautical mile) is thereby reduced to a displacement on the face of the cathode-ray tube and presented to an operator in a manner most applicable to the function of the particular radar. This simple echo-time relationship is one of the major reasons for the extensive utilization of pulsed radar systems. In frequency-modulated continuous-wave radars, where this echo-time relationship cannot be used, the processing of the information contained in the recovered modulation has been quite complex. Because of this difficulty, the use of frequency-modulated continuous-wave radars generally has been restricted to systems where multiple targets are not considered, thus simplifying the data-processing requirements. The radio altimeter is one type of single-target frequency-modulated continuous-wave equipment that has been in use for many years. The ground echo in this case is the only target under consideration.

It is the object of this paper to present a new recently developed display, which when used with a frequency-modulated continuous-wave radar system can process the information contained in the received echo in a simple manner and present it to an observer in the form of a range/velocity display.

2. Frequency-Modulated Continuous-Wave Radar Equations

Linear frequency modulation of the radiated energy will be considered although other types have been used in the past. Figure 1 illustrates various fundamental types of modulation that can be used. These types can be combined to obtain more-complex forms of modulation. Figure 1D is often used and is a combination of the modulations in Figures 1B and 1C. The basic equations from which it is possible to

* Reprinted from Institute of Radio Engineers, *Transactions on Military Electronics* (Special Edition on Advanced Radar Techniques), volume MIL-5, number 2, pages 172-179; April, 1961.

determine the target's velocity and position for the various types of modulation are

Type A (unmodulated carrier)

$$F_A = f_d = K_1 \dot{r} \quad (1)$$

Type B (negative frequency modulation)

$$F_B = f_d + f_r = K_1 \dot{r} + K_2 \dot{r} \quad (2)$$

Type C (positive frequency modulation)

$$F_C = f_d - f_r = K_1 \dot{r} - K_2 \dot{r} \quad (3)$$

where F_A is the frequency displacement of the returned echo from the carrier when the transmitted wave is unmodulated (Figure 1A). This displacement is, of course, due to the Doppler effect $f_d = K_1 \dot{r} = (2F_0/c)\dot{r}$. K_1 is the velocity-sensitivity factor and is established by the carrier frequency F_0 and the velocity of propagation c . \dot{r} is the radial velocity of the target and is considered positive for inbound targets.

F_B is the difference in frequency between the transmitted and received frequencies when the transmitted wave is linearly frequency modulated in a negative direction and the measurement is made at the time of reception (see Figure 1B). This frequency difference has two components, f_d and f_r . f_r is the amount of frequency shift that would be obtained if the target were stationary during B-type modulation and is due to the delay time t_r of the echo. In this type of modulation the echo would always be higher in frequency than the transmitted wave. f_r is proportional to the range by the range-sensitivity factor $K_2 = 2\dot{F}/c$, where \dot{F} is the rate of frequency change of the carrier, and c is the velocity of propagation. If the target is moving, the Doppler shift f_d would cause an additional shift in received frequency.

During type-C modulation, positive frequency deviation of the carrier, the received frequency for a fixed target would always be below the carrier, hence the negative sign in (3). The Doppler shift f_d would cause a higher-frequency return for inbound targets. Figure 1C illustrates this type of modulation. The range-sensitivity

factor is identical if the rate of frequency change were the same as in type-B modulation.

For a single target, only two of the three equations are required to obtain the necessary data to solve for the range and radial velocity of the target, and the triangular modulation of Figure 1D, combining Figures 1B and 1C would be suitable. This type of modulation is not adequate for multiple-target operation because of the resultant ambiguities due to the fact that the target returns during the B modulation— F_{B1} , F_{B2} , $F_{B3} \dots F_{Bn}$, and the returns during C modulation— F_{C1} , F_{C2} , $F_{C3} \dots F_{Cn}$ are not correlated. For n targets there will be n^2 possible solutions for the targets' range and velocity coordinates. If a third redundant mode is used, the $N^2 - N$ target ambiguities can be eliminated. For simplicity, the third mode will be considered to be type-A unmodulated operation. Type-B or C modulation with different range-sensitivity factors K_2 could also be used with possible advantage.

3. Frequency-Modulated Continuous-Wave Plane

If a plane is constructed where the ordinate is the range or f_r axis and the abscissa is the velocity or f_d axis, the resultant plane can be

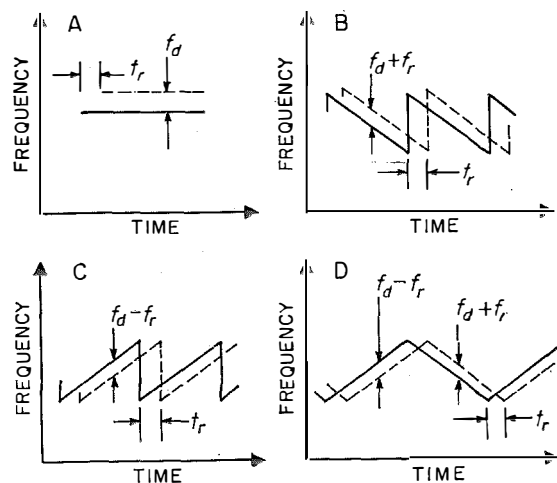


Figure 1—Various frequency-modulation methods.

New Display for Radars

considered to be the frequency-modulated continuous-wave plane (Figure 2). A target's coordinates f_d , f_r would be plotted in the first quadrant if inbound, and in the fourth quadrant if outbound. In Figures 2A–D, two targets are located in the frequency-modulated continuous-wave plane with the coordinates f_{d1} , f_{r1} and f_{d2} , f_{r2} .

Figure 2A represents the locus of (1). For unmodulated or *A*-type modulation, the target information F_{A1} , F_{A2} plots as two vertical lines with f_d axis intercepts at F_{A1} and F_{A2} . Figure 2B depicts the locus of the two targets when type-*B* modulation is used. The equation $F_b = f_d + f_r$ indicates that the locus of the two targets is on two lines with a slope of -1 with f_d and f_r axis intercepts of F_{B1} and F_{B2} , respectively.

Similarly, for *C*-type modulation, the locus of the targets must be on the two lines with a slope of $+1$ and f_d and f_r axis intercepts of F_{C1} and F_{C2} (see Figure 2C). Figure 2D illustrates the superposition of these lines. The points of triple intersection are the coordinates of the two targets f_{d1} , f_{r1} and f_{d2} , f_{r2} . Thus, it is seen that a graphical solution to the three basic frequency-modulated continuous-wave radar equations can be achieved. Plotting the three sets of returns as indicated using, F_{A1} , F_{A2} , $F_{A3} \dots F_{An}$; F_{B1} , F_{B2} , $F_{B3} \dots F_{Bn}$; and F_{C1} , F_{C2} , $F_{C3} \dots F_{Cn}$, results in N triple intersections at the proper target coordinates. From this graph, it is clear that removal of one of the modes—the *A* mode in this case—would result in four solutions, or $n^2 - n$ ambiguities. A solution by means of a cathode-ray-tube display seems to be indicated.

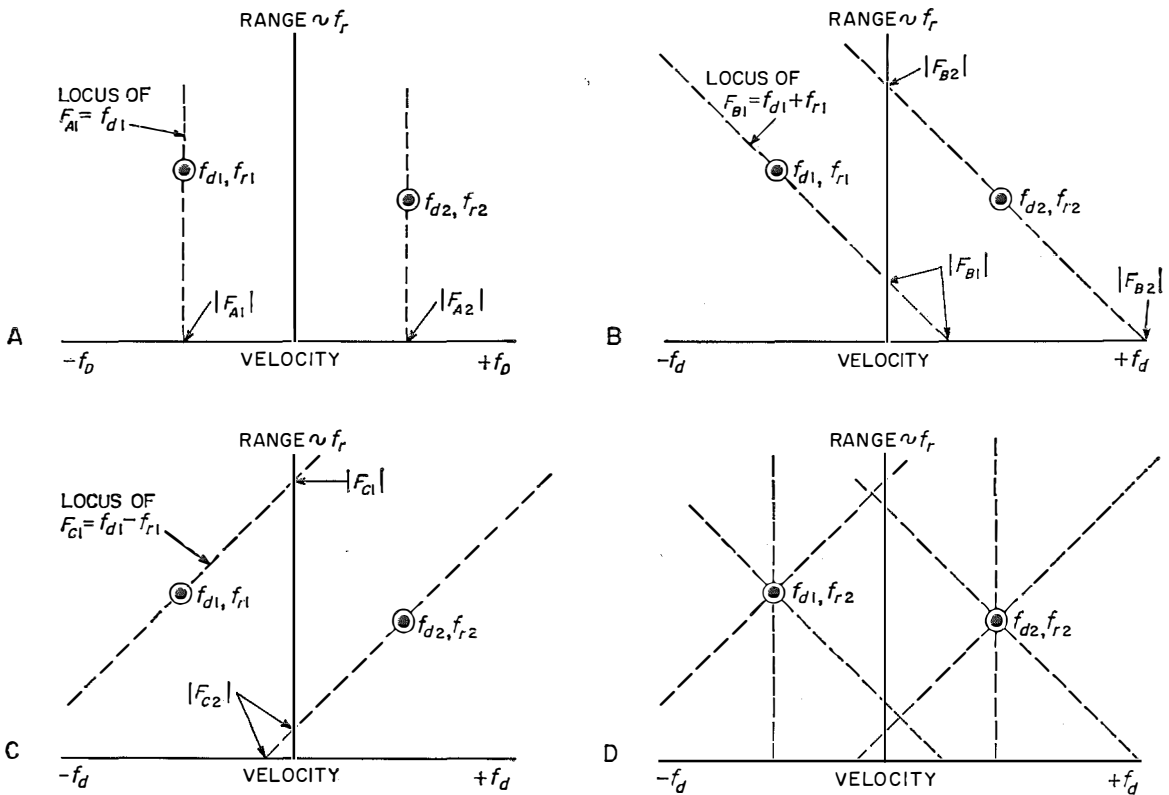


Figure 2—Graphical solution of the range-velocity coordinates of multiple targets.

4. Panoramic Display

While other types of spectrum analyzers are available, let us assume that three filter banks are used for frequency determination, one for each mode. The output of each filter is connected to a detector and storage element. The *A*, *B*, and *C* filter banks are sequentially scanned, and in synchronism with the filter scan, a spot is deflected from left to right on a cathode-ray tube. If the start of the *B* and *C* filter scans are successively displaced vertically, as indicated in Figure 3, and a vertical deflection is induced when a filter is reached whose storage element is energized, a single target will appear as indicated in Figure 3. More than one target could be present, but only one will be considered here. The resultant spectrum display is quite conventional and can be achieved by a number of other well-known methods.

5. Frequency-Modulated Continuous-Wave Display

The graphical solution of Figure 2 can be electronically implemented by means of the frequency-modulated continuous-wave plane display, using the same signals required for the panoramic display. The following is the sequence of events for operation of the frequency-modulated continuous-wave raster. During the *A* mode, the horizontal deflection is from left to right, in synchronism with the *A*-filter readout.

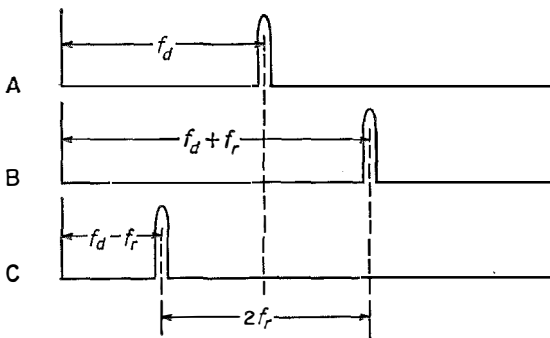


Figure 3—Frequency spectrum for single target.

Simultaneously, the vertical deflection plates of the cathode-ray tube are driven by a sawtooth whose period is equal to the sampling time per filter. By this means, a series of vertical lines is generated, one for each filter. During the *B* mode, an equal number of lines with a slope of -1 is generated. This is accomplished by using the identical wave shapes used for deflection during the *A* mode, but adding to the horizontal deflecting sawtooth wave shape a sawtooth that is identical to the one used for vertical deflection. Reversing the polarity of this added sawtooth during the *C*-mode scan causes an identical number of lines with a slope of $+1$ to be generated. With suitable persistence in the cathode-ray-tube phosphor, a frequency-modulated continuous-wave display raster is generated. Figure 4 is a photograph of such a raster generated on a 12-inch electric-field deflected cathode-ray tube. If the lines are intensified only when an energized filter is reached, the resultant display will contain triple intersections whose coordinates are proportional to range and velocity of the target. The signal used for vertical pip deflection in Figure 3 is used for intensification of the frequency-modulated continuous-wave plane display.

6. Frequency-Modulated Continuous-Wave Sector Display

It is quite often impracticable to supply enough filters to cover the entire range of anticipated target frequencies. This is especially true if the filter bandwidths are made extremely narrow to achieve high resolution. Filter banks covering only a limited spectrum can be used if variable-frequency oscillators are used to heterodyne the portion of the full spectrum that is of interest to the frequencies covered by the particular filter bank. Figure 5 illustrates the coverage on the frequency-modulated continuous-wave plane of the *A*, *B*, and *C* filter banks when a limited number of filters are used and the heterodyning frequencies f_{ha} , f_{hb} , and f_{hc} are properly inter-related. The diamond-shaped area of mutual coverage is the only place on the frequency-

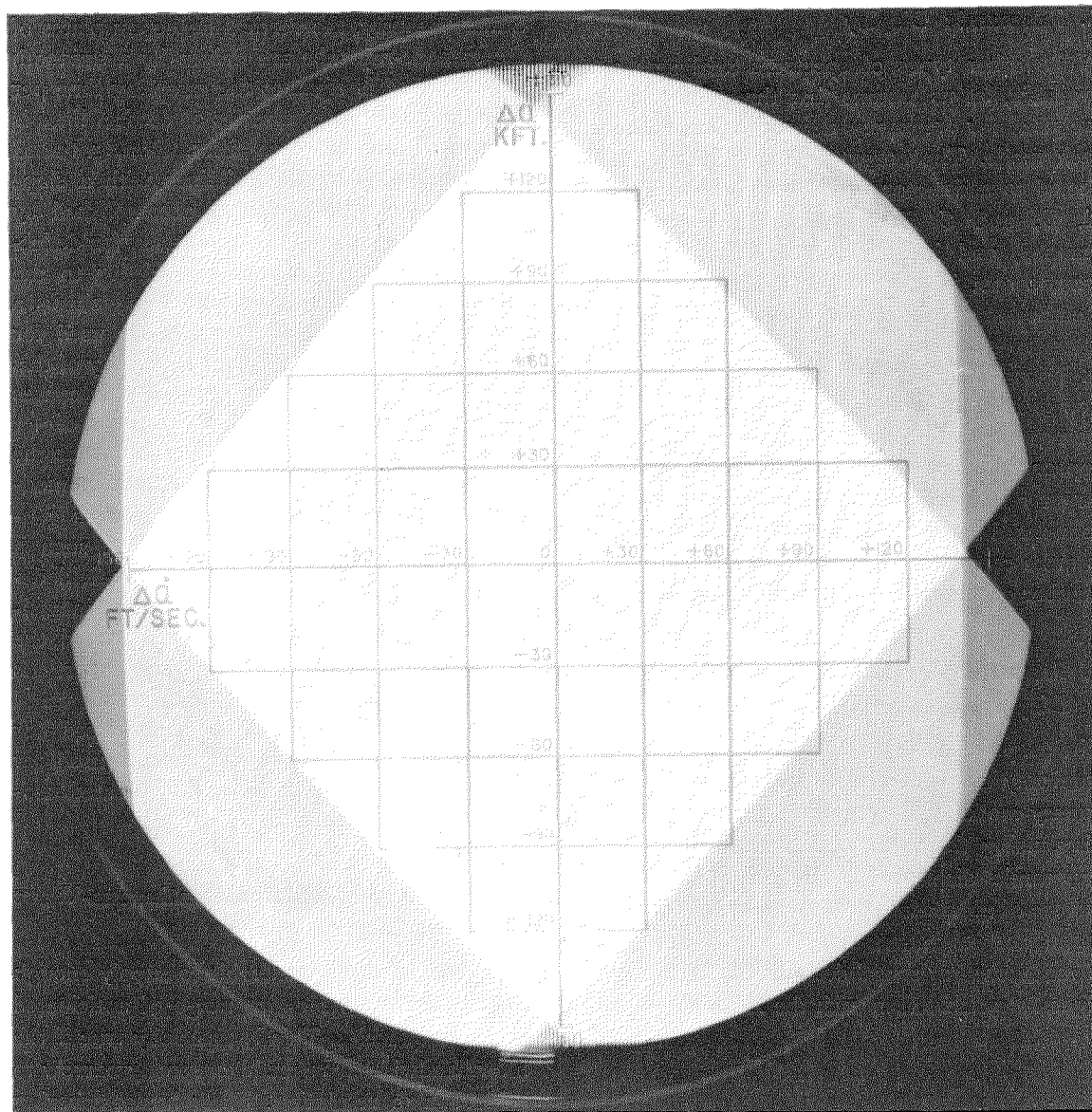


Figure 4—Frequency-modulated continuous-wave display raster.

modulated continuous-wave plane where it is possible to obtain a triple intersection. If the heterodyning frequencies are not properly interrelated, the coverage will be reduced. For instance, if only the heterodyning frequency used during the *A* mode f_{ha} is changed in frequency,

the vertical lines, which indicate *A*-bank coverage, will move horizontally reducing the mutual coverage. If this frequency change is sufficiently large there will be no mutual coverage. When properly interrelated the diamond-shaped area can be considered to be a “window” on the

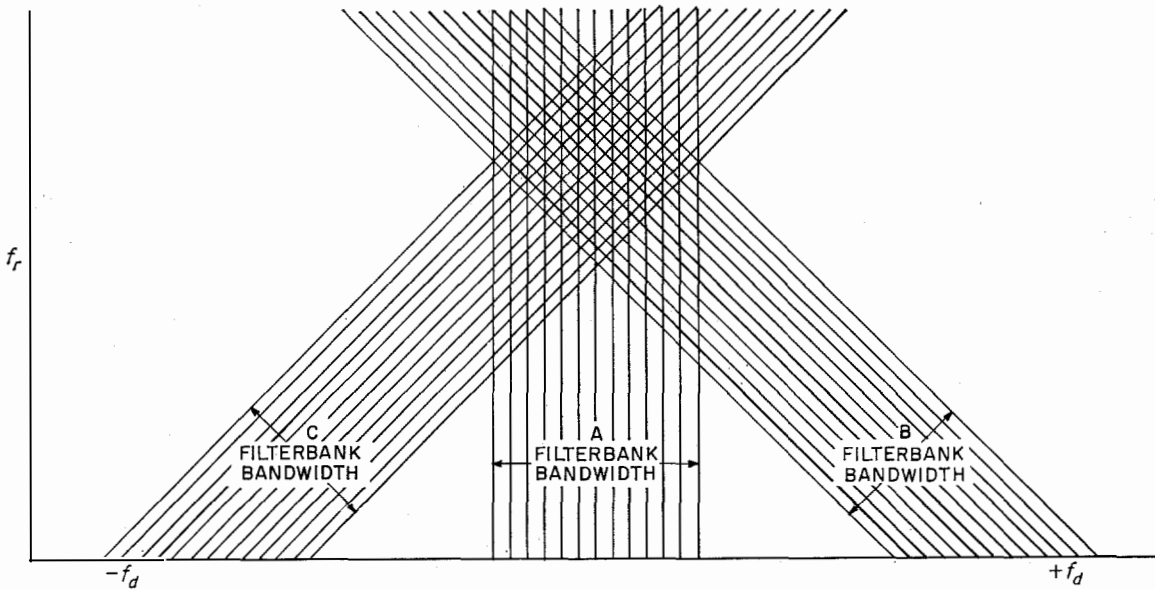


Figure 5—Sector coverage in frequency-modulated continuous-wave plane.

entire frequency-modulated continuous-wave space, and this window can be positioned to cover the coordinates of the area on the frequency-modulated continuous wave plane where the target is expected to appear. Several methods are available for achieving the correct relationship between the three heterodyning frequencies.

If it is desired to position the *A*, *B*, and *C* filter banks so that a particular target with the coordinates f_d, f_r appears in the center of the three filter banks, the three heterodyning frequencies required are

$$f_{ha} = f_{IF} + f_f + f_d \quad (4)$$

$$f_{hb} = f_{IF} + f_f + f_d + f_r \quad (5)$$

$$f_{hc} = f_{IF} + f_f + f_d - f_r \quad (6)$$

where f_{IF} is the carrier frequency of the intermediate frequency before the final mixer, and f_f is the center frequency of the filter banks.

Figure 6 is a block diagram of a system for obtaining these frequencies. By means of range

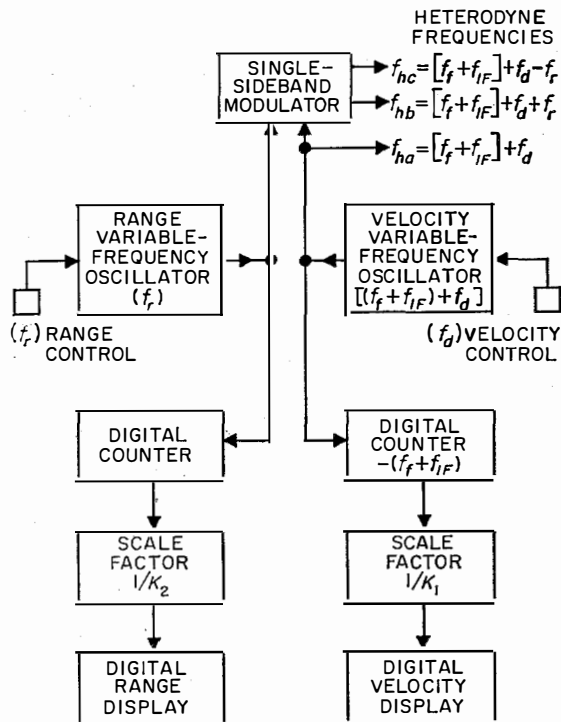


Figure 6—Variable-frequency-oscillator control for sector coverage.

and velocity controls, the center of the frequency-modulated continuous-wave sector coverage can be positioned to any place on the frequency-modulated continuous-wave plane. The range variable-frequency-oscillator moves the diamond-shaped area vertically and the velocity variable-frequency-oscillator positions this area horizontally. By measuring these two frequencies and using suitable scale factors, the center coordinates in range and velocity of the area of coverage can be displayed on a digital readout device. The frequency-modulated continuous-wave plane display is synchronized exactly as in the case of the full frequency-modulated continuous-wave display. When this sector display is used, a triple intersection, which represents a target, will move vertically on the display when the range variable-frequency-oscillator is tuned and horizontally when the velocity variable-frequency-oscillator is adjusted, indicating the movement of the window over the frequency-modulated continuous-wave plane.

Figure 7 is a block diagram of a possible receiver system that uses sector coverage.

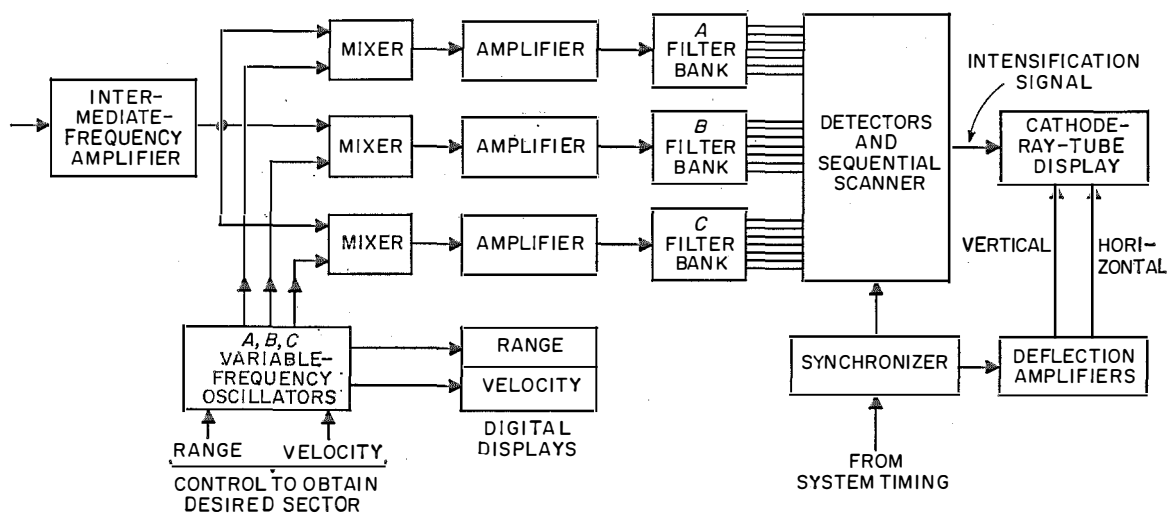


Figure 7—Block diagram of a frequency-modulated continuous-wave system with sector coverage.

7. Maximum Utilization of Available Filters

One interesting aspect of sector coverage is the determination of the maximum utilization of a given number of filters. Figure 5 illustrates the filter coverage when an equal number of filters are used in the *A*, *B*, and *C* filter banks. It is apparent that the filters at the high- and low-frequency ends of the *A* filter bank contribute little to the area in which it is possible to obtain a triple intersection. If these filters were removed and transferred to the *B* and *C* banks, this area is increased and the window shape becomes hexagonal.

With reference to Figure 8, the following derivation indicates that for a given number of filters, the maximum coverage is obtained when the *B* and *C* banks each contain 50 percent more filters than the *A* bank.

If *A* is the area of the hexagon, *2a* is the number of filters in the *A* bank, *2b* is the number of filters in the *B* or *C* bank and *N* is the total number of available filters.

$$N = 2a + 4b \quad \text{and} \quad b = \frac{N - 2a}{4}. \quad (7)$$

The area $A = 4 \left[\frac{a^2}{2} + a(b - a) \right]$. Simplifying and substituting for b

$$A = - (4a^2 + aN) \quad (8)$$

after differentiating and setting equal to zero

$$0 = \frac{dA}{da} = - 8a + N \quad \text{and} \quad \frac{b}{a} = 1.5. \quad (9)$$

8. Expanded Tracking Displays

A useful tracking or magnified display can be obtained by modifying the timing of the synchronizing triggers. With reference to Figure 3, a marker generator can be built that will allow superposition of the marker and the target returns. The marker generator has two delay controls. When the A mode is being scanned, the marker signal appears at a time t_a after the start of A -filter scan and the B marker appears at a time $(t_a + t_r)$ after the start of the B -filter scan. Similarly, the marker delay after the start of C scan is equal to $(t_a - t_r)$. The target can be tracked by means of the range and velocity delay controls. The delays t_a , t_r can be measured and, by suitable proportionality constants, the range and velocity of the tracked target can be displayed or recorded. These numbers can

be added to those obtained from the variable-frequency-oscillators for absolute determination of the target's velocity and range.

To increase the tracking accuracy and obtain a magnified $10\times$ display, a pretrigger is generated by the marker generator $\frac{1}{20}$ of the time it takes to scan a filter bank. If these A , B , and C pretriggers initiate a sweep on a panoramic display similar to Figure 3 with a duration $\frac{1}{10}$ of the filter scan time, the markers always will appear in the center of this expanded display; and when marker tracking is on target, the A , B , and C returns will be centered and positioned one above the other.

If this sweep voltage, which is synchronized to the pretriggers, is used in place of the horizontal deflection voltage used in the frequency-modulated continuous-wave display, an expanded display results covering $\frac{1}{100}$ the area of the frequency-modulated continuous-wave plane display. Adjustment of the marker controls t_a and t_r will position this smaller portion of the frequency-modulated continuous-wave plane within that portion covered by the filter banks in Figure 5. This positioning is similar to the orthogonal window positioning by variable-frequency-oscillator control and is illustrated in Figure 5. When the markers are positioned to coincide with the returns from a particular target, the triple intersection will appear at the exact center of this magnified tracking frequency-modulated continuous-wave display. Several of these tracking displays can be operated simultaneously with the addition of a marker generator and display for each tracking operator.

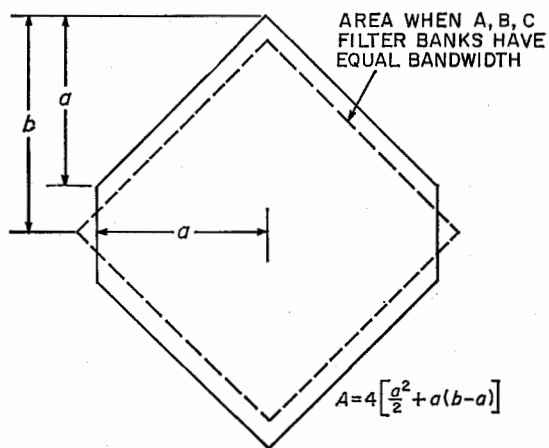


Figure 8—Maximum filter utilization in frequency-modulated continuous-wave system.

9. Results—Implementation

The frequency-modulated continuous-wave plane display was built using a 12-inch, electric-field-deflected cathode-ray tube, and is illustrated in Figures 4, 9, and 10. In Figure 9, a simulator is used to generate 11 signals in the A , B , and C filter banks, dividing each area into 10 equal spaces. The resultant test pattern illustrates the ability of the display to accurately

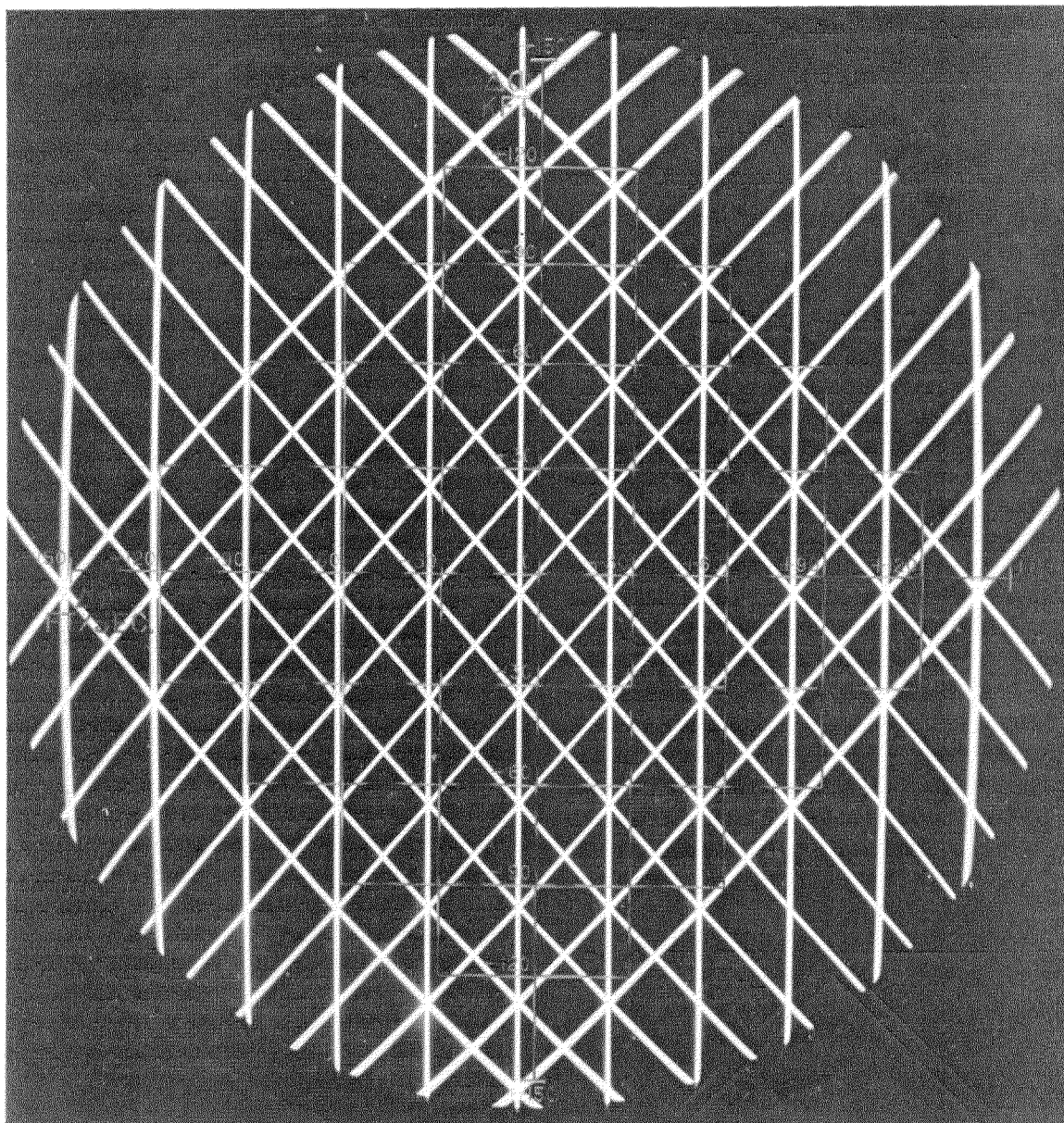


Figure 9—Triple-intersection test pattern.

resolve triple intersections over the face of the tube. In the design of such an indicator, there are two basic types of distortion to consider. One type is conveniently called "rubber" distortion, for it is equivalent to having the frequency-

modulated continuous-wave plane graph drawn on a sheet of rubber. Stretching this sheet can cause various types of inaccuracies but will not destroy a triple intersection. This type of distortion occurs when the nonlinearities are intro-

duced in stages that are commonly shared by the A , B , and C deflection signals. The geometric distortions in the cathode-ray tube, and nonlinearities in the deflection-driver amplifiers are examples of rubber distortion. An examination of Figure 9 indicates the presence of barrel-type distortion, which does not deteriorate the triple intersections. When distortions are introduced in deflection-signal paths that are not common to all three modes, it is possible that an exact point of triple intersection will not occur. Care was taken to reduce this form of distortion, and the results indicated in Figure 9 were obtained with comparatively simple circuits with good reliability and a minimum of adjustments.

Figure 10 is a photograph of the results obtained during a controlled 2-target flight test. The differences in range and velocity between these two targets are clearly evident. The panoramic display at the right was energized with the identical filter output signals used for intensification of the frequency-modulated continuous-wave display. Examination of the panoramic display illustrates the difficulty an operator would have in utilizing the spectrum information under multiple-target conditions. The sharp marker pips controlled by t_a and t_r are also evident on this display.

10. Future Developments

As the target's coordinate information is contained only in the point of triple intersection, it

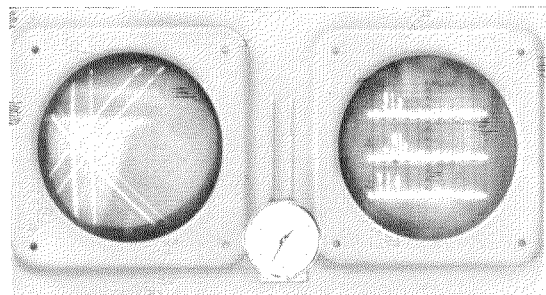


Figure 10—Multiple-target flight test.

would be desirable to eliminate all the excess lines from the display to reduce the confusion when there are a large number of targets. Several systems for accomplishing this end have been considered. One system in particular is being presently pursued. In addition to eliminating the excess lines, it has the capabilities of automatic readout of multiple target coordinates and adjustable persistence enabling the target coordinate point to be displayed as a track.

Other systems than those indicated in Figure 7 are applicable. A ramp with twice the frequency deviation of the B and C modes can be substituted for the continuous-wave mode. Returns would be plotted as a line with twice the slope of those in the B and C modes.

11. References

1. L. N. Ridenour, *Radio System Engineering*, Massachusetts Institute of Technology Radiation Laboratory Series; Cambridge, Massachusetts; 1948.
2. D. G. C. Luck, *Frequency Modulated Radar*, McGraw-Hill Book Company, New York, New York; 1949.
3. R. I. Bernstein, University of Michigan Fourth Annual Radar Symposium; Ann Arbor, Michigan; June 1958.
4. H. H. Naidich, Internal Memorandum 66872 of International Telephone and Telegraph Corporation; Nutley, New Jersey; 1958.

12. Acknowledgment

The author wishes to thank Colonel Nicholson and Captain George of Rome Air Development Center, under whose cognizance some of these developments were accomplished; L. Pugliese, S. Eisenmesser, J. Sur, and A. Plevy for their contributions to this program; and W. Heiser and R. Bailey for their advice and encouragement.

World's Telephones—1961 *

Recent years have seen a very rapid expansion in telephone systems throughout the world. The gain in 1960 amounted to 8 100 000 telephones, or more than 6 percent. With the exception of 1959, when the gain was 700 000 greater, the growth last year was the largest on record. A decade ago, some 57 percent of all telephones in the world were in the United States. During the past ten years, however, the rate of gain in the rest of the world has exceeded that in this country, with the result that today the United States proportion of the world total has receded to 52 percent. The gain outside the United States was at an annual average rate of 7.7 percent, compared with 5.6 percent for this country. The rate of growth abroad however has been relative to a much lower level of telephone development than in the United States. The ratio of telephones per 100 population in the rest of the world rose from 1.4 to 2.4 during the past decade while in the United States it rose from 28 to 41.

It is interesting to note that only seven coun-

tries accounted for over two-thirds of the entire decade's gain: The United States (made comparable by exclusion of Alaska and Hawaii) accounted for 47 percent, Japan 6 percent, West Germany 5 percent, the United Kingdom, Canada and Italy 4 percent each, and France 3 percent.

Not only were most of the new telephones automatic (dial), but there was rapid progress in replacing the nonautomatic (manual). In fact growth in automatic telephones was at an average rate throughout the decade of more than 9 percent a year, compared with a decline of 4.3 percent a year in nonautomatic. In line with rapid utilization of scientific advances is rapid gain in international telephone traffic. Since 1927, when the overseas radio link with Great Britain went into service, the growth of overseas messages to and from the United States has been at the extraordinary rate of 19 percent a year. At this rate, the volume of messages has doubled on the average every four years.

TABLE 1
TELEPHONES IN CONTINENTAL AREAS—1 JANUARY 1961

Area	Total			Privately Operated		Automatic	
	Number 1961	Percent of World	Per 100 Population	Number 1961	Percent of Total	Number 1961	Percent of Total
North America	79 830 600	56.3	40.0	78 884 200	98.8	76 057 100	95.3
Middle America	1 075 900	0.8	1.6	740 700	68.8	905 600	84.2
South America	3 337 600	2.3	2.4	1 626 400	48.7	2 886 400	86.5
Europe	43 172 700	30.5	7.4	7 357 200	17.0	36 430 600	84.4
Africa	2 005 300	1.4	0.8	31 800	1.6	1 493 800	74.5
Asia (1)	9 053 400	6.4	0.5	5 582 300	61.7	6 131 600	67.7
Oceania	3 224 500	2.3	19.5	240 300	7.5	2 533 900	78.6
World	141 700 000	100.0	4.7	94 462 900	66.7	126 439 000	89.2

(1) These data include allowances for the Asiatic parts of Turkey and the Union Soviet Socialist Republics.

* Abridgement from the 1961 issue of a booklet, "The World's Telephones," published yearly by the chief statistician's office of the American Telephone and Telegraph Company, New York, New York.

TABLE 2
YEARLY TOTAL NUMBER OF TELEPHONES IN SERVICE

Area	1960	1959	1958	1957	1956	1951
North America	76 036 400	71 799 300	68 484 000	64 720 700	60 422 900	45 939 000
Middle America	1 008 000	910 800	835 900	772 800	733 100	555 000
South America	3 145 900	2 999 600	2 845 000	2 695 300	2 568 300	1 815 000
Europe	40 340 900	37 598 100	35 218 700	32 510 000	29 990 000	21 574 000
Africa	1 904 500	1 768 600	1 663 200	1 546 100	1 411 200	895 200
Asia (1)	8 110 000	6 855 700	6 062 500	5 229 500	4 708 800	2 875 800
Oceania	3 054 300	2 867 900	2 690 700	2 525 600	2 365 700	1 646 000
World	133 600 000	124 800 000	117 800 000	110 000 000	102 200 000	75 300 000

(1) These data include allowances for the Asiatic parts of Turkey and the Union Soviet Socialist Republics.

TABLE 3
TELEPHONES BY COUNTRIES AS OF 1 JANUARY 1961

Country or Area	Number of Telephones	Per 100 Population	Percent Automatic	Telephones by Type of Operation	
				Private	Government
NORTH AMERICA					
Canada	5 728 167	31.82	87.6	4 837 191	890 976
Greenland	0	—	—	—	—
St. Pierre and Miquelon	397	7.94	0.0	0	397
United States (1) (2)	74 102 000	40.80	95.9	74 047 000	55 000
MIDDLE AMERICA					
Bahamas	11 398	10.65	98.7	0	11 398
Bermuda	13 800	30.67	100.0	13 800	0
British Honduras	1 018	1.09	2.9	0	1 018
Canal Zone (3) (4)	8 005	36.39	100.0	0	8 005
Costa Rica	15 933	1.33	78.9	15 275	658
Cuba	199 964	2.94	93.1	0	199 964
Dominican Republic	20 315	0.67	93.5	19 940	375
El Salvador	16 086	0.61	78.9	0	16 086
Guadeloupe and Dependencies	3 330	1.22	0.0	0	3 330
Guatemala	17 900	0.47	89.4	0	17 900
Haiti	4 400	0.13	86.0	0	4 400
Honduras	5 862	0.30	83.6	0	5 862
Martinique	5 960	2.13	71.4	0	5 960
Mexico	522 795	1.48	81.3	521 955	840
Netherlands Antilles*	13 300	6.86	99.0	3 990	9 310
Nicaragua	8 224	0.55	63.3	0	8 224
Panama	28 672	2.68	85.5	27 972	700
Puerto Rico	94 601	4.02	75.6	87 736	6 865
Virgin Islands (United Kingdom)	3	0.04	0.0	0	3
Virgin Islands (United States)	3 905	12.20	0.0	3 905	0

* Estimated.

- (1) Data for the State of Alaska are included. Data for the State of Hawaii are under Oceania, rather than here under North America. Data for Alaska in 1961 are as follows: number of telephones, 44 022; per 100 population, 22.93.
- (2) The number shown as governmentally operated is estimated. More than half of such telephones are in the State of Alaska.
- (3) Data are as of 30 June 1960.
- (4) Data exclude telephone systems of the armed forces.
- (5) Data for the following countries are necessarily stated as of the latest date for which statistics are at hand:

Bulgaria 1 January 1948
China, Mainland 1 January 1948
Rumania 1 January 1947

- Those parts of the telephone systems of China (Mainland) and Rumania that are shown in the table as privately operated continued under such operation until 1949, when they came under government operation. The Bulgarian system has been continuously under government operation in recent years. No later information is available concerning these three countries.
- (6) Data are as of 31 March 1961.

TABLE 3—Continued
TELEPHONES BY COUNTRIES AS OF 1 JANUARY 1961—Continued

Country or Area	Number of Telephones	Per 100 Population	Percent Automatic	Telephones by Type of Operation	
				Private	Government
West Indies Federation					
Antigua	807	1.47	0.0	0	807
Barbados	9 620	4.08	100.0	9 620	0
Cayman Islands	52	0.59	0.0	0	52
Dominica	657	1.10	0.0	0	657
Grenada	1 468	1.65	100.0	1 468	0
Jamaica	34 976	2.06	98.3	34 976	0
Montserrat	140	1.17	0.0	0	140
St. Kitts	400	0.70	0.0	0	400
St. Lucia	740	0.86	69.6	0	740
St. Vincent	450	0.56	0.0	0	450
Trinidad and Tobago	30 845	3.71	88.8	0	30 845
Turks and Caicos Islands	130	2.17	65.4	85	45
SOUTH AMERICA					
Argentina	1 295 856	6.13	87.3	94 531	1 201 325
Bolivia*	24 000	0.69	92.0	24 000	0
Brazil	1 022 793	1.54	83.0	983 927	38 866
British Guiana	8 158	1.42	91.3	0	8 158
Chile	193 175	2.63	75.8	192 126	1 049
Colombia	294 650	2.06	97.7	19 170	275 480
Ecuador	29 100	0.67	95.0	580	28 520
Falkland Islands and Dependencies	440	22.00	0.0	0	440
French Guiana	1 004	3.24	0.0	0	1 004
Paraguay	10 800	0.60	92.0	0	10 800
Peru	108 657	0.99	86.3	108 657	0
Surinam	5 450	1.89	96.2	0	5 450
Uruguay*	141 500	4.97	78.0	1 415	140 085
Venezuela	202 005	2.98	96.9	202 005	0
EUROPE					
Albania*	5 700	0.35	50.0	0	5 700
Andorra	200	2.50	0.0	0	200
Austria	701 465	9.88	94.1	0	701 465
Belgium	1 142 742	12.45	87.3	0	1 142 742
Bulgaria (5)	54 347	0.77	39.4	0	54 347
Channel Islands					
Guernsey and Dependencies	12 598	26.80	53.2	0	12 598
Jersey	17 796	28.25	63.9	0	17 796
Total	30 394	27.63	59.5	0	30 394
Czechoslovakia	1 015 993	7.42	80.6	0	1 015 993
Denmark	1 072 460	23.19	56.6	949 242	123 218
Finland	606 566	13.55	81.7	445 841	160 725
France	4 357 937	9.53	79.1	0	4 357 937
Germany, Democratic Republic	1 296 044	7.54	95.6	0	1 296 044
Germany, Federal Republic	5 994 051	10.71	99.4	0	5 994 051
Gibraltar (4)	2 757	10.60	100.0	0	2 757
Greece	222 359	2.66	93.2	0	222 359
Hungary*	475 000	4.74	80.0	0	475 000
Iceland	39 547	22.31	71.3	0	39 547
Ireland	151 196	5.34	75.9	0	151 196
Italy	3 860 849	7.80	96.7	3 860 849	0
Liechtenstein	4 286	25.21	100.0	0	4 286
Luxemburg	51 364	16.31	96.4	0	51 364
Malta and Gozo (6)	16 041	4.88	64.7	0	16 041
Monaco	8 580	39.00	100.0	0	8 580
Netherlands	1 612 915	13.96	99.6	0	1 612 915
Norway (3)	724 070	20.19	70.4	54 032	670 038
Poland	881 394	2.95	77.8	0	881 394
Portugal	394 827	4.31	75.1	274 194	120 633
Rumania (5)	127 153	0.77	75.8	126 131	1 022
San Marino	556	3.27	100.0	0	556
Spain	1 792 133	5.93	78.8	1 771 618	20 515
Sweden	2 760 572	36.81	88.7	0	2 760 572
Switzerland	1 658 715	30.65	100.0	0	1 658 715
Turkey*	304 500	1.10	85.0	0	304 500
U.S.S.R.*	4 276 000	1.99	50.0	0	4 276 000
United Kingdom (6)	8 270 000	15.69	83.6	0	8 270 000
Yugoslavia	259 560	1.38	77.5	0	259 560

TABLE 3—Continued
TELEPHONES BY COUNTRIES AS OF 1 JANUARY 1961—Continued

Country or Area	Number of Telephones	Per 100 Population	Percent Automatic	Telephones by Type of Operation	
				Private	Government
AFRICA					
Algeria, 13 Departments	195 123	1.86	83.4	0	195 123
Sahara, 2 Departments	2 594	0.45	0.0	0	2 594
Total	197 717	1.79	82.3	0	197 717
Angola	8 918	0.19	66.2	0	8 918
Ascension Island	58	13.36	82.8	58	0
Basutoland	868	0.12	1.8	0	868
Bechuanaland	785	0.23	0.0	0	785
Cameroon	6 805	0.17	76.2	0	6 805
Cape Verde Islands	188	0.09	77.1	0	188
Central African Republic	1 403	0.11	0.0	0	1 403
Chad	1 592	0.06	0.0	0	1 592
Comoro Islands	44	0.02	0.0	0	44
Congo Republic (Formerly Belgian)	28 278	0.20	85.3	0	28 278
Congo Republic	5 046	0.59	63.8	0	5 046
Dahomey	2 010	0.10	70.1	0	2 010
Egypt, United Arab Republic*	244 500	0.94	85.0	0	244 500
Ethiopia	12 012	0.06	81.4	0	12 012
Gabon	1 854	0.42	0.0	0	1 854
Gambia	700	0.22	99.0	0	700
Ghana	23 816	0.34	60.0	0	23 816
Guinea*	3 100	0.10	72.0	1 922	1 178
Ifni*	150	0.27	0.0	0	150
Ivory Coast	7 004	0.21	78.1	0	7 004
Kenya	40 954	0.62	81.5	0	40 954
Liberia*	2 100	0.16	100.0	600	1 500
Libya*	14 600	1.21	70.0	0	14 600
Malagasy	13 757	0.26	56.1	0	13 757
Mali, Republic of*	2 800	0.07	65.0	0	2 800
Mauritania*	300	0.04	0.0	0	300
Mauritius and Dependencies	8 989	1.39	8.4	0	8 989
Morocco	129 704	1.11	89.7	18 327	111 377
Mozambique	12 426	0.19	72.7	0	12 426
Niger	1 549	0.05	0.0	0	1 549
Nigeria	41 661	0.12	66.0	0	41 661
Portuguese Guinea	406	0.07	0.0	0	406
Reunion	6 106	1.80	0.0	0	6 106
Rhodesia and Nyasaland					
Northern Rhodesia	22 880	0.93	93.2	0	22 880
Nyasaland	5 177	0.18	87.9	0	5 177
Southern Rhodesia	80 378	2.58	87.5	0	80 378
Total	108 435	1.29	88.7	0	108 435
Ruanda-Urundi	2 395	0.05	82.0	0	2 395
Sahara, Spanish	241	0.96	0.0	0	241
Saint Helena	124	2.48	0.0	0	124
São Tomé and Príncipe	380	0.56	73.7	0	380
Sénégal*	17 000	0.53	73.0	0	17 000
Seychelles and Dependencies	206	0.50	100.0	206	0
Sierra Leone*	4 700	0.19	80.0	50	4 650
Somalia	2 015	0.10	0.0	0	2 015
Somaliland, French	865	1.20	100.0	0	865
South Africa, Republic of (6)	937 818	5.92	69.4	0	937 818
South West Africa	16 703	3.18	41.2	0	16 703
Spanish Equatorial Region	1 100	0.50	86.0	1 100	0
Spanish North Africa	7 696	4.97	100.0	7 696	0
Sudan	24 400	0.21	76.9	0	24 400
Swaziland	1 820	0.70	50.5	0	1 820
Tanganyika	14 858	0.16	73.1	0	14 858
Togo	1 776	0.12	63.7	0	1 776
Tunisia	26 218	0.62	54.4	0	26 218
Uganda	13 596	0.20	77.3	0	13 596
Upper Volta	1 228	0.03	0.0	0	1 228
Zanzibar and Pemba	1 798	0.58	64.0	0	1 798
ASIA					
Aden Colony	5 538	3.53	100.0	0	5 538
Aden Protectorate	0	—	—	—	—
Afghanistan*	7 700	0.06	30.0	0	7 700

TABLE 3—Continued
TELEPHONES BY COUNTRIES AS OF 1 JANUARY 1961—Continued

Country or Area	Number of Telephones	Per 100 Population	Percent Automatic	Telephones by Type of Operation	
				Private	Government
Bahrain	3 631	2.47	100.0	3 631	0
Bhutan	0	—	—	—	—
Brunei	694	0.83	96.7	0	694
Burma*	13 300	0.06	74.0	0	13 300
Cambodia	3 248	0.06	0.0	0	3 248
Ceylon	37 166	0.38	94.9	0	37 166
China, Mainland (5)	244 028	0.05	72.9	94 945	149 083
China, Taiwan	98 030	0.91	60.0	0	98 030
Cyprus	17 900	3.14	96.1	0	17 900
Hong Kong]	108 853	3.61	100.0	108 853	0
India (6)	470 559	0.11	64.8	3 553	467 006
Indonesia	122 000	0.13	12.0	0	122 000
Iran*	105 900	0.52	75.0	0	105 900
Iraq (6)	54 250	0.76	79.5	0	54 250
Israel	117 620	5.47	97.8	0	117 620
Japan (6)	5 526 461	5.88	69.2	5 526 461	0
Jordan*	24 400	1.41	70.0	0	24 400
Korea, Republic of	109 241	0.44	49.6	0	109 241
Kuwait	14 126	6.28	100.0	0	14 126
Laos	736	0.04	53.0	0	736
Lebanon	66 389	3.98	93.5	0	66 389
Macao	2 363	1.06	100.0	0	2 363
Malaya	76 164	1.09	71.0	0	76 164
Maldivo Islands	0	—	—	—	—
Mongolia, Outer	7 300	0.78	64.4	0	7 300
Muscat and Oman	244	0.04	100.0	244	0
Nepal	0	—	—	—	—
Netherlands New Guinea	2 232	0.32	13.1	0	2 232
North Borneo	3 319	0.72	98.7	0	3 319
Pakistan	79 586	0.08	68.2	0	79 586
Philippine Republic	113 440	0.41	79.2	102 069	11 371
Portuguese India	575	0.09	0.0	0	575
Portuguese Timor	496	0.10	0.0	0	496
Qatar	2 146	4.67	100.0	2 146	0
Ryukyu Islands (4)	10 967	1.24	74.6	0	10 967
Sarawak	4 513	0.59	75.6	0	4 513
Saudi Arabia*	26 500	0.40	40.0	0	26 500
Sikkim	0	—	—	—	—
Singapore	59 722	3.59	100.0	0	59 722
Syria	54 944	1.20	89.0	0	54 944
Thailand	42 638	0.17	83.9	0	42 638
Trucial Oman	500	0.58	100.0	500	0
Viet-Nam, Republic of	15 942	0.11	81.2	0	15 942
Yemen	0	—	—	—	—
OCEANIA					
Australia	2 216 500	21.32	78.5	0	2 216 500
British Solomon Islands	342	0.28	0.0	0	342
Caroline Islands	250	0.58	0.0	0	250
Christmas Islands	50	1.67	100.0	50	0
Cocos (Keeling) Islands	61	6.10	100.0	0	61
Cook Islands	286	1.59	0.0	0	286
Fiji Islands	7 206	1.80	59.0	0	7 206
Gilbert and Ellice Islands	0	—	—	—	—
Guam	14 200	21.52	100.0	0	14 200
Mariana Islands (less Guam)	350	4.38	71.4	0	350
Marshall Islands	678	4.84	100.0	0	678
Midway Island	1 135	37.83	100.0	0	1 135
Nauru	0	—	—	—	—
New Caledonia and Dependencies	3 317	4.31	74.1	0	3 317
New Hebrides Condominium ††	350	0.57	100.0	0	350
New Zealand (6)	744 797	30.85	72.0	0	744 797
Niue Island	88	1.76	0.0	0	88
Norfolk Island	34	3.40	0.0	0	34
Papua and New Guinea	5 866	0.31	80.4	0	5 866
Pitcairn Island	0	—	—	—	—
Polynesia, French	1 299	1.62	0.0	0	1 299
Samoa, American	370	1.85	100.0	0	370
Samoa, Western	899	0.83	0.0	0	899
Tokelau Islands	0	—	—	—	—
Tonga (Friendly) Islands	653	1.00	0.0	0	653
United States: Hawaii	240 294	36.97	100.0	240 294	0
Wake Island	140	12.00	100.0	0	140

TABLE 4
TELEPHONE CONVERSATIONS DURING 1960
Data were not available for all countries

Country or Area	Thousands of Conversations			Average Conversations Per Person
	Local	Long Distance	Total	
Aden	6 992	2	6 994	44.5
Algeria	123 604	20 143	143 747	13.0
Argentina	3 721 516	46 945	3 768 461	179.8
Australia	1 514 000	138 000	1 652 000	160.7
Bahamas, West Indies	24 630	162	24 792	236.1
Barbados, West Indies	20 000	8	20 008	85.1
Belgium	600 352	123 697	724 049	79.1
Bermuda	14 400	24	14 424	320.5
Brazil	5 341 200	89 706	5 430 906	82.6
Cameroon, Republic of	11 759	355	12 114	3.0
Canada	9 364 586	227 331	9 591 917	538.4
Ceylon	93 653	5 687	99 340	10.2
Channel Islands	16 236	757	16 993	154.5
Chile	481 064	19 359	500 423	68.6
China, Taiwan	307 520	12 351	319 871	30.1
Colombia	931 564	11 748	943 312	66.8
Congo Republic	3 452	241	3 693	4.3
Costa Rica	50 470	1 165	51 635	44.1
Cuba	607 420	8 595	616 015	91.0
Cyprus	15 242	1 828	17 070	30.3
Czechoslovakia	759 136	100 603	859 739	63.0
Denmark	1 146 136	249 195	1 395 331	302.3
Dominican Republic	74 340	353	74 693	24.9
El Salvador	50 980	8 276	59 256	22.7
Ethiopia	25 247	925	26 172	1.3
Fiji Islands	7 600	591	8 191	20.8
Germany, Democratic Republic	817 343	167 387	984 730	57.3
Germany, Federal Republic	3 471 616	1 075 191	4 546 807	81.8
Ghana	20 210	2 709	22 919	3.4
Greece	507 916	11 781	519 697	62.4
Guatemala	16 000	1 100	17 100	4.5
Ireland	132 037	13 057	145 094	51.2
Israel	247 588	5 752	253 340	119.8
Italy	5 518 764	451 753	5 970 517	121.0
Ivory Coast	5 500	246	5 746	1.8
Jamaica, West Indies	75 000	1 220	76 220	47.4
Japan	14 434 000	927 515	15 361 515	164.4
Korea, Republic of	855 269	7 556	862 825	35.2
Lebanon	98 000	12 000	110 000	66.8
Malagasy	8 842	981	9 823	1.8
Malaya	181 346	19 388	200 734	29.1
Mexico	1 035 499	17 323	1 052 822	30.4
Mozambique	15 952	595	16 547	2.6
Netherlands	1 048 610	456 036	1 504 646	131.1
Nigeria	32 723	2 896	35 619	1.0
Norway	540 954	52 640	593 594	166.2
Panama	114 183	868	115 051	109.3
Papua and New Guinea	4 808	72	4 880	2.6
Peru	541 884	6 117	548 001	50.5
Philippine Republic	763 915	1 377	765 292	27.8
Portugal	429 493	62 755	492 248	53.9
Puerto Rico	133 320	4 677	137 997	58.6
Singapore	177 403	1 307	178 710	109.4
South West Africa	15 015	2 000	17 015	32.7
Sudan	2 255	44	2 299	19.5
Surinam	8 510	610	9 120	31.6
Sweden	2 314 000	300 500	2 614 500	348.6
Switzerland	650 456	573 929	1 233 385	230.1
Syria	93 626	4 507	98 133	21.6
Thailand	65 005	125	65 130	2.6
Trinidad and Tobago, West Indies	63 380	5 548	68 928	83.4
Tunisia	29 450	5 290	34 740	8.3
United Kingdom	4 344 000	425 000	4 769 000	90.6
United States	90 560 000	3 427 000	93 987 000	520.0
Viet-Nam, Republic of	21 784	254	22 038	1.6
Yugoslavia	416 282	33 413	449 695	24.1

(1) Data are for year ended 31 March 1961.

(2) Data are for year ended 30 June 1960.

(3) Data are for the year ended 30 June 1961. This year the number of long-distance calls established

automatically is included under "long distance" rather than under "local," as in previous issues of this report.

United States Patents Issued to International Telephone and Telegraph System; February–April 1961

Between 1 February and 30 April 1961, the United States Patent Office issued 50 patents to the International System. The names of the inventors, company affiliations, subjects, and patent numbers are listed below.

R. T. Adams and J. B. Harvey, ITT Laboratories, Maximum Slope Pulse Detector, 2 975 367.

R. T. Adams and B. M. Mindes, ITT Federal Laboratories, Radio Diversity Receiving System, 2 979 613.

R. T. Adams, ITT Laboratories, Combining System for Diversity Communication Systems, 2 975 275.

B. Alexander, M. Rogoff, and M. C. Vosburgh, ITT Laboratories, Long Range Radio Navigation System, 2 975 417.

H. Avery, D. H. Kingsland, and E. G. Parker, ITT Federal Laboratories, Omnidirectional Beacon Antenna, 2 979 719.

A. H. W. Beck, D. C. Rogers, and P. F. C. Burke, Standard Telephones and Cables (London), Electron Gun for Electron Discharge Tube, 2 974 246.

J. I. Bellamy, Kellogg Switchboard and Supply Company, Telephone Paystation Circuit with Coin-Accept Control, 2 974 199.

A. D. Biagi, ITT Federal Laboratories, Transmitter Spectrum Monitor, 2 979 609.

H. Busignies, Federal Telephone and Radio Company, Position Finding System, 2 971 190.

S. A. Cottler, V. F. Glifford, and G. A. Deschamps, ITT Laboratories, Wideband Folded Monopole Antenna, 2 971 192.

D. W. Davis, ITT Laboratories, Image Converter and Method and Apparatus for Producing the Same, 2 975 015.

S. H. M. Dodington, ITT Laboratories, Radio Repeating Systems, 2 978 699.

S. H. M. Dodington, ITT Federal Laboratories, Variable Power Transmitter for Distance Measuring Interrogators, 2 981 943.

D. G. Fawcett and P. J. Carpenter, ITT Laboratories, Magnetic Core Switching Circuit, 2 975 298.

L. G. Fischer and L. L. Bibbins, ITT Federal Laboratories, Electro-Mechanical Correlator Multiplier, 2 981 472.

A. R. Gobat, ITT Federal Laboratories, Semiconductor Diode, 2 981 849.

F. P. Gohorel, Compagnie Générale de Constructions Téléphoniques (Paris), Priority in the Choice of Lines, 2 979 642.

L. Goldstein, ITT Laboratories, Radiant Energy Source, 2 975 375.

J. C. Groce and W. T. Rusch, ITT Laboratories, Data Translating System, 2 975 410.

H. Grottrup and W. Schiebeler, C. Lorenz (Stuttgart), Circuit Arrangement for Checking the Faultless Transmission of Teleprinting Characters, 2 971 055.

J. W. Halina, ITT Federal Laboratories, Synchronous Demodulation System, 2 979 611.

J. Handley, Creed & Company (Croyden), Printing Telegraph Selector Apparatus, 2 974 194.

- J. Heaton-Armstrong, Standard Telephones and Cables (London), Automatic Frequency Control Arrangements for Frequency Shift Telegraph Receivers, 2 971 059.
- L. Himmel, ITT Laboratories, Direction Finding System, 2 975 418.
- R. W. Hughes and W. Sichak, ITT Federal Laboratories, Diversity Communication System, 2 979 716.
- T. M. Jackson and E. A. Sell, Standard Telephones and Cables (London), Cold Cathode Tubes, 2 971 109.
- R. V. Judy, Kellogg Switchboard and Supply Company, Telephone Answering Service System, 2 971 061.
- J. Kaspar and A. J. Bielski, ITT Laboratories, Compressor System, 2 970 747.
- J. J. B. Lair, ITT Federal Laboratories, Automatic Echo Pulse Recapture Circuit, 2 979 712.
- A. N. Lawson, Standard Telephones and Cables (London), Communication Systems, 2 974 222.
- F. P. Mason and R. G. Stemp, Creed & Company (Croyden), Facsimile Apparatus, 2 977 179.
- E. M. S. McWhirter, International Standard Electric Corporation, Document Carrier for Mechanized Processing, 2 970 757.
- H. R. Meadows, Farnsworth Electronics Company, Interference Detecting Circuit, 2 972 677.
- F. Mittag and J. Lindner, Mix & Genest (Stuttgart), Arrangement to Produce Electrical Signals in Belt Conveyors Using Containers, 2 980 235.
- D. T. O'Connor and R. A. Fabish, ITT Laboratories (Fort Wayne), Automatic Digital Evaluator, 2 977 535.
- R. K. Orthuber and C. L. Day, ITT Laboratories, Method of Making Display Amplifier, 2 974 369.
- S. B. Pickles, ITT Laboratories, Air Navigation Radio System, 2 978 701.
- W. H. P. Pouliart and L. Jacobin, Bell Telephone Manufacturing Company (Antwerp), Record Tape Assembly and Magazine Therefor, 2 979 244.
- W. H. P. Pouliart and G. Van Mechelen, Bell Telephone Manufacturing Company (Antwerp), Electrical Comparator, 2 977 574.
- R. C. Renick and C. J. Pasquier, ITT Laboratories, Track Circuit, 2 975 272.
- D. S. Ridler, Standard Telecommunication Laboratories (London), Methods of Synchronizing Recorded Intelligence, 2 974 312.
- S. B. Silverschotz and E. Jorow, ITT Federal Laboratories, Density Sensing Device, 2 978 909.
- H. Steinback and R. Scheidig, Mix & Genest (Stuttgart), Electromagnetic Impulse Counter, 2 980 891.
- G. P. Thwaites and H. Downing, Standard Telephones and Cables (London), Method of Winding Grid Electrodes, 2 973 787.
- H. Wlodarczak, C. Lorenz (Stuttgart), Selective Blocking Device for Office Typewriter Keyboard, 2 980 228.
- H. H. Wolfish, ITT Laboratories, Multiar Circuit, 2 975 363.

E. P. G. Wright and V. J. Terry, Standard Telecommunication Laboratories (London), Synchronising Arrangement for a Regenerative Telegraphic Repeater Utilizing Signal Transitions, 2 974 197.

E. P. G. Wright, Standard Telephones and Cables (London), Accounting Systems, 2 973 900.

E. P. G. Wright, D. A. Weir, and J. Rice, Standard Telephones and Cables (London), Electric Signalling Systems, 2 981 789.

E. P. G. Wright, Standard Telecommunication Laboratories (London), Intelligence Storage Equipment, 2 977 577.

Record Tape Assembly and Magazine Therefor

2 979 244

W. H. P. Pouliart and L. Jacobin

A record tape magazine assembly in which a magnetic tape is drawn from the magazine in one direction and returned to the magazine in another direction after recording or reading a message. The invention provides a driven belt at the bottom of the magazine to move the returned tape continuously toward the exit end of the magazine.

Electron Gun for Electron Discharge Tube

2 974 246

A. H. W. Beck, D. C. Rogers, and P. F. C. Burke

An electron gun using combined electromagnetic and electrostatic focussing, having a non-

magnetic anode, for directing a beam along a path having a magnetic control such as used in traveling-wave tubes. The anode is fastened to the magnetic pole piece surrounding the cathode of the gun and spacing members are provided to position the entire assembly properly within a glass envelope.

Position Finding System

2 971 190

H. G. Busignies

A system by which the location of a receiver with respect to a rotatable beacon can be determined by using a direction finder at the receiver. It is essential that there also be a re-radiating object at a known distance from the beacon. By determining the directions from the receiver to the beacon and to the reradiating object and the difference in distance of the beacon and the object from the receiver, the position triangle may be calculated. This invention is the forerunner of the more complete navar system.

Document Carrier for Mechanized Processing

2 970 757

E. M. S. McWhirter

A carrier for transporting documents and a processing strip to provide for automatic machine processing of documents such as checks. The document is placed in the carrier and the processing strip, such as a coded magnetic tape, is placed in a second compartment of the carrier to control the processing steps.

In Memoriam



PAUL HARTMANN

Paul Hartmann was born in Niederurnen, Switzerland, on 4 May 1909. The Swiss Federal Institute of Technology in Zurich conferred its electrical engineering diploma on him in 1932. He then served at the Institute as an assistant for the following year.

His engineering career started in 1934 and three years later he joined Standard Telephone et Radio in Zurich. By 1957, he became general manager and shortly thereafter managing director of the company.

He was an active participant in the development and expansion of telephony in Switzerland, which now ranks very high in telephone utilization among European countries. His extensive knowledge, imagination, and sound judgment contributed substantially to the progress of elec-

trical communication. His devotion to his profession and talent for solving problems earned him the abounding respect of his associates.

His contributions were not limited to engineering but also embraced the economics of the industry and proved invaluable in his guidance of the company. The design of the new manufacturing plant opened in 1961 was greatly influenced by him and many will always associate it with his memory.

Paul Hartmann died at the age of 52 after a lingering illness. The passing of this friendly man of great and rare capacity will be mourned by all who were privileged to work with him, unfortunately for much too short a time, in the engineering and management fields.

Contributors to This Issue

HARRY ALTMAN

Harry Altman was born on 27 August 1928 in Philadelphia, Pennsylvania. He received a bachelor's degree in electrical engineering from the College of the City of New York in 1950 and a master's degree in electrical engineering from the Polytechnic Institute of Brooklyn in 1955.

During 1950 and 1951, he was engaged in research and development in commercial and military applications of television at Philco Corporation.

Mr. Altman joined ITT Federal Laboratories in 1952 and has been engaged in research and development in military electronics, including missile guidance and control systems, automatic test equipment, and range instrumentation systems for missile and space applications. He is an associate laboratory director in the Missile and Space Systems Center and is presently project manager of the Mobile Atlantic Range Stations program on the instrumentation of ships for space-vehicle evaluation.

He is a member of Sigma Xi, Eta Kappa Nu, Tau Beta Pi, and the Institute of Radio Engineers.

HERBERT AULHORN

Herbert Aulhorn was born in Dresden, Germany, on 2 October 1914. He studied in Dresden from 1933 to 1939. From 1939 to 1945, he served in the armed forces.

After 10 years as a radio mechanic, he joined Standard Elektrik Lorenz in 1949 as a development engineer. He has worked on voice-frequency telegraphy, inductive train control, planning and research on transmission systems, and data transmission.

JAMES P. BARBERA

James P. Barbera was born in New York City on 20 May 1929. He studied engineering at the College of the City of New York and at Fairleigh Dickinson University. He served from



HARRY ALTMAN



HERBERT AULHORN

1947 to 1950 in the United States Army Signal Corps, in charge of a communication and electronic repair shop. From 1951 to 1956, he worked for Bell Telephone Laboratories in research and development of telephone switching circuits, automatic testing equipment, stable platforms, and radar antennas.

In 1956, he joined Federal Electric Corporation and at present is a senior member of the engineering staff on early warning systems.

Mr. Barbera is a Member of the Institute of Radio Engineers.

LOUIS DE ROSA

Louis deRosa was born in Tenafly, New Jersey, on 11 September 1910. He received a BS degree in electrical engineering in 1932 from the Polytechnic Institute of Brooklyn.

Starting as an engineer for the deForest Tube Company in 1931 and going to Electrad in 1932, he became chief engineer of Electrotech-

nical Laboratories from 1934 to 1936 and of the Electrad Division of P. R. Mallory until 1938. After a year of private research, he served in the electronics laboratory of the National Cash Register Company until 1942.

He then joined ITT Federal Laboratories and in 1958 was advanced from a laboratory director to vice president in charge of electronic defense activities in the United States. In 1960, he became vice president of ITT Communication Systems and director of engineering for the 480L project on a communication system for the United States Air Force.

Mr. deRosa is a Member of Tau Beta Pi. He has received the Certificate of Achievement of the Polytechnic Institute of Brooklyn.

Mr. deRosa has been granted about 40 patents and has published numerous technical papers. He is a Fellow of the Institute of Radio Engineers and has served on several of its committees and professional groups. He also holds memberships in the American Physical Society and the Acoustical Society of America.



JAMES P. BARBERA



LOUIS DE ROSA

Contributors to This Issue

He serves on the Scientific Advisory Board of the National Science Administration and on the Advisory Board on Electronic Warfare of the United States Department of Defense, serving also as chairman of its working panel on reconnaissance.

WILLIAM G. DONALDSON

William G. Donaldson was born in Dubois, Pennsylvania, on 10 December 1921. He received a BS degree in 1945 from the United States Coast Guard Academy in New London, Connecticut. He took graduate courses at the University of Connecticut and at New York University.

While on active duty during the Korean conflict, he designed the Coast Guard port security communication systems for New York and Philadelphia. In 1955, he joined Western Electric Company and as a transmission engineering section chief was responsible for design and development phases of the Dewline communication and detection systems. He joined Fed-

eral Electric Corporation in 1957 and was recently appointed manager of the engineering department of the Early Warning Systems Division. He is now concerned with upgrading the Dewline systems.

Mr. Donaldson is a Senior Member of the Institute of Radio Engineers and a member of the American Institute of Electrical Engineers and of the Armed Forces Communications and Electronics Association. He is a registered professional engineer in the states of New York and New Jersey.

JACK HARVEY

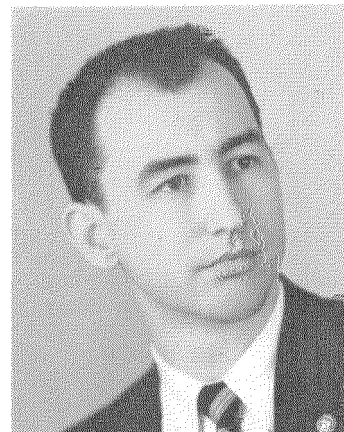
Jack Harvey was born in 1929. He received the BS degree in electrical engineering in 1951 from the University of Missouri.

He joined ITT Federal Laboratories in 1951 and then served in the United States Army Signal Corps from 1952 to 1954 on leave of absence.

He has worked on the development of numerous types of communication equipment and



WILLIAM G. DONALDSON



JACK HARVEY

antennas for both military and commercial use. He is now a project engineer in the system implementation group of the transmission laboratory.

Mr. Harvey is a registered professional engineer and a Senior Member of the Institute of Radio Engineers.

EARL W. KELLER

Earl W. Keller was born on 13 September 1922 in Milheim, Pennsylvania. He received a BE degree in electrical engineering from Johns Hopkins University in 1943 and an MS degree from the Massachusetts Institute of Technology in 1949.

From 1943 to 1955, he taught at Massachusetts Institute of Technology, becoming an assistant professor in 1953. From 1955 to 1957, he was assistant professor of electrical engineering at Columbia University.

In 1957, he joined the engineering staff of the Radio Corporation of America and in 1959 was assigned to ITT Communication Systems to work on the 480L project on a communica-

tion system for the United States Air Force. He is in charge of transmission system design.

He holds Memberships in the Institute of Radio Engineers, American Institute of Electrical Engineers, American Institute of Physics, American Physical Society, American Association for the Advancement of Science, and the Franklin Institute.

Mr. Keller received scholarships for scholastic excellence in all four years of undergraduate work at Johns Hopkins and a graduate teaching scholarship at Massachusetts Institute of Technology. He is a Member of Tau Beta Pi and of Sigma Xi.

HANS MARKO

Hans Marko was born on 24 February 1925 in Kronstadt, Siebenbürgen, Romania. He attended the Institute of Technology in Stuttgart, Germany, and received a Dr.Ing. degree in 1953.

In 1952, Dr. Marko joined Standard Elektrik Lorenz, where he has been active in planning



EARL W. KELLER



HANS MARKO

Contributors to This Issue

and research on transmission systems, radio links, and data transmission.

He has lectured at the Institutes of Technology in Stuttgart and Karlsruhe. In 1959, he became chairman of the Committee on Information and System Theory of the Telecommunication Association.

HERBERT H. NAIDICH

Herbert H. Naidich was born in New York, New York, on 6 May 1924. He received a bachelor's degree in electrical engineering in 1949 from the College of the City of New York and a master's degree in 1959 from Newark College of Engineering. His schooling was interrupted from 1942 to 1946 by service in the Army, where he worked in communication and fire-control systems.

From 1949 to 1955, he was concerned with radar developments, for the first year with the Civil Aeronautics Authority and then with Bendix Radio Division.

In 1955, he joined ITT Federal Laboratories, where he has been engaged in advanced countermeasures and radar systems.

Mr. Naidich has received four patents in the radar field.

S. M. POOLE

S. M. Poole was born in 1926. He attended Imperial College of London University and received the B.Sc., A.R.C.Sc. degree in 1948. He then served as a commissioned officer in the British Army for five years.

He joined the flight-simulator division of Redifon Limited in 1953, where by the time he immigrated to France in 1957 he was chief engineer.

Mr. Poole joined Le Matériel Téléphonique as chief engineer for flight simulators in 1958 and has been responsible for creating a rapidly expanding activity in the simulator field.

Mr. Poole is a member of the Société Française des Electroniciens et des Radioélectriciens and a member of the International Telephone and Telegraph Corporation Technical Committee 11 for Industrial Equipment, Instrumentation, and Control.



HERBERT H. NAIDICH



S. M. POOLE

International Telephone and Telegraph Corporation

Principal Divisions and Subsidiaries

North America

COMMERCIAL GROUP

ITT Canada Limited, Montreal, Canada
ITT Electronics Service Company of Canada, Ltd.,
Town of Mount Royal, P. Q.
Royal Electric Company (Quebec) Ltd., Pointe Claire,
P. Q.
ITT Components Division, Clifton, N. J.
Kuthe Laboratories, Inc., Newark, N. J.
ITT Distributor Products Division, Lodi, N. J.
ITT Industrial Laboratories Division, Fort Wayne, Ind.
ITT Industrial Products Division, San Fernando, Calif.
ITT Information Systems Division, New York
Airmatic Systems Corporation, Saddle Brook, N. J.
Intelx Systems Incorporated, New York
ISD Engineering Center, Paramus, N. J.
ITT Kellogg, Chicago
Jennings Radio Manufacturing Corporation, San Jose,
Calif.
Royal Electric Corporation, Pawtucket, R. I.
Electric Cords & Supply Corporation, Los Angeles
Surprenant Mfg. Co., Clinton, Mass.

DEFENSE GROUP

Federal Electric Corporation, Paramus, N. J.
International Electric Corporation, Paramus, N. J.
ITT Communication Systems, Inc., Paramus, N. J.
ITT Federal Laboratories, Nutley, N. J.

ADMINISTRATION AND FINANCE

International Standard Electric Corporation, New York
International Telephone and Telegraph Corporation, Sud
America, New York
International Telephone and Telegraph Credit Corpora-
tion, New York
Kellogg Credit Corporation, New York

Europe, Middle East, Africa

AUSTRIA

Standard Telephon und Telegraphen Aktiengesellschaft,
Czeija, Nissl & Co., Vienna

BELGIUM

Bell Telephone Manufacturing Company, Antwerp
ITT Europe, Inc., Brussels

DENMARK

Standard Electric Aktieselskab, Copenhagen

FINLAND

Oy Suomen Standard Electric AB, Helsinki

FRANCE

Compagnie Générale de Constructions Téléphoniques,
Paris
Les Téléimprimeurs, Paris
International Standard Engineering, Inc., Paris
Laboratoire Central de Télécommunications, Paris
Le Matériel Téléphonique, Paris

GERMANY

Standard Elektrik Lorenz Aktiengesellschaft, Stuttgart
Alpina Biromaschinen-Werk G.m.b.H., Kaufbeuren
Eduard Winkler Apparatebau G.m.b.H., Nuremberg
SEL Finanz G.m.b.H., Stuttgart

IRAN

Standard Electric Iran AG, Tehran

ITALY

Fabbrica Apparecchiature per Comunicazioni Elettriche
Standard S.p.A., Milan

NETHERLANDS

Nederlandsche Standard Electric Maatschappij N.V.
The Hague

NORWAY

Standard Telefon og Kabelfabrik A/S, Oslo

PORTUGAL

Standard Eléctrica, S.A.R.L., Lisbon

REPUBLIC OF SOUTH AFRICA

Standard Telephones and Cables (South Africa) (Pro-
prietary) Limited, Boksburg East, Transvaal

SPAIN

Compañía Internacional de Telecomunicación y Elec-
trónica, S.A., Madrid
Compañía Radio Aérea Marítima Española, S.A., Ma-
drid
Standard Eléctrica, S.A., Madrid

SWEDEN

Standard Radio & Telefon AB, Stockholm

SWITZERLAND

ITT Standard S.A., Basle
Standard Téléphone et Radio S.A., Zurich

TURKEY

Standard Elektrik ve Telekomünikasyon Limited Şirketi,
Ankara

UNITED KINGDOM

Creed & Company Limited, Croydon
International Marine Radio Company, Croydon
Standard Telephones and Cables Limited, London
Kolster-Brandes Limited, Sidcup
Standard Telecommunication Laboratories Limited,
London

Latin America

Manufacturing and sales

ARGENTINA

Compañía Standard Electric Argentina, S.A.I.C., Buenos
Aires

BRAZIL

Standard Eléctrica, S.A., Rio de Janeiro

CHILE

Compañía Standard Electric, S.A.C., Santiago

MEXICO

Industria de Telecomunicación, S.A. de C.V. (50% inter-
est), Mexico City
Standard Eléctrica de México, S.A., Mexico City

VENEZUELA

Standard Telecommunications C.A., Caracas

Telecommunication operations**ARGENTINA**

Compañía Internacional de Radio, S.A., Buenos Aires

BOLIVIA

Compañía Internacional de Radio Boliviana, La Paz

BRAZIL

Companhia Rádio Internacional do Brasil, Rio de Janeiro

Companhia Telefônica Nacional, Curitiba¹**CHILE**

Compañía de Teléfonos de Chile, Santiago

Compañía Internacional de Radio, S.A., Santiago

CUBA

Cuban American Telephone and Telegraph Company (50% interest), Havana

Radio Corporation of Cuba, Havana

PERU

Compañía Peruana de Teléfonos Limitada, Lima

PUERTO RICO

ISE Limited, San Juan

Puerto Rico Telephone Company, San Juan

Radio Corporation of Puerto Rico, San Juan

VIRGIN ISLANDS

Virgin Islands Telephone Corporation, Charlotte Amalie

Far East and Pacific**AUSTRALIA**

Standard Telephones and Cables Pty. Limited, Sydney

HONG KONG

ITT Far East Limited, Hong Kong, B.C.C.

JAPAN

ITT Far East and Pacific, Inc., Tokyo

NEW ZEALAND

New Zealand Electric Totalisators Limited, Wellington

PHILIPPINES

ITT Philippines, Incorporated, Manila

Worldwide Cable and Radio Telegraph Operations

American Cable & Radio Corporation, New York

All America Cables and Radio, Inc., New York

Commercial Cable Company, The, New York

Globe Wireless Ltd., New York

Globe Wireless Ltd. Philippines, Manila, Philippines

Mackay Radio and Telegraph Company, New York

Sociedad Anónima Radio Argentina, Buenos Aires

Associate Licensees for Manufacturing (Minority Interest)**AUSTRALIA**

Austral Standard Cables Pty. Limited, Melbourne

FRANCE

Lignes Télégraphiques et Téléphoniques, Paris

ITALY

Società Italiana Reti Telefoniche Interurbane, Milan

JAPAN

Nippon Electric Company, Limited, Tokyo

Sumitomo Electric Industries, Limited, Osaka

SPAIN

Marconi Española, S.A., Madrid

¹ Pôrto Alegre division seized by State of Rio Grande do Sul, February 16, 1962.**THE WORLD OF ITT****North America:**

22 500 employees

53 locations (factories, major laboratories, service units)

5 400 000 square feet of floor space

Europe, Middle East, Africa:

102 000 employees

68 locations (factories, major laboratories, marine radio companies)

15 500 000 square feet of floor space

Latin America (excluding Cuba):

21 000 employees

16 locations (factories, telephone and telegraph operating companies)

1 000 000 square feet of floor space

Far East and Pacific:

3 500 employees

5 locations

750 000 square feet of floor space

Total:

149 000 employees, including headquarters and service personnel in the United States

142 locations

22 650 000 square feet

Sales representatives in most countries

Principal ITT System Products

Telecommunication Equipment and Systems

Automatic telephone and telegraph central office switching systems
Private telephone and telegraph exchanges—PABX and PAX, electromechanical and electronic
Carrier systems: telephone, telegraph, power-line
Long-distance dialing and signaling equipment
Automatic message accounting and ticketing equipment
Switchboards: manual, central office, toll

Telephones: desk, wall, pay-station
Automatic answering and recording equipment
Microwave radio systems: line-of-sight, over-the-horizon
Radio multiplex equipment
Coaxial cable systems
Submarine cable systems, including repeaters
Data-transmission systems
Teleprinters and facsimile equipment

Military/Space Equipment and Systems

Aircraft weapon systems
Missile fuzing, launching, guidance, tracking, recording, and control systems
Missile-range control and instrumentation
Electronic countermeasures
Electronic navigation
Power systems: ground-support, aircraft, spacecraft, missile
Radar

Simulators: missile, aircraft, radar
Ground and environmental test equipment
Programmers, automatic
Infrared detection and guidance equipment
Global and space communication, control, and data systems
Nuclear instrumentation
Antisubmarine warfare systems
System management: worldwide, local

Industrial/Commercial Equipment and Systems

Distance-measuring and bearing systems:
Tacan, DMET, Vortac, Loran
Instrument Landing Systems (ILS)
Air-traffic control systems
Direction finders: aircraft and marine
Ground and airborne communication
Data-link systems
Inverters: static, high-power
Power-supply systems
Altimeters
Flight systems
Railway and power control and signaling systems
Information-processing and document-handling systems
Analog-digital converters
Mail-handling systems
Pneumatic tube systems

Broadcast transmitters: AM, FM, TV
Studio equipment
Point-to-point radio communication
Marine radio
Mobile communication: air, ground, marine, portable
Closed-circuit television: industrial, aircraft, and nuclear radiation
Slow-scan television
Instruments: test, measuring
Oscilloscopes: large-screen, bar-graph
Vibration test equipment
Magnetic amplifiers and systems
Alarm and signaling systems
Telemetry
Intercommunication, paging, and public-address systems

Consumer Products

Television and radio receivers
High-fidelity phonographs and equipment
Tape recorders
Microphones and loudspeakers
Refrigerators, freezers

Air conditioners
Hearing aids
Incandescent lamps
Home intercommunication equipment
Electrical housewares

Cable and Wire Products

Multiconductor telephone cable
Telephone wire: bridle, distribution, drop
Switchboard and terminating cable
Telephone cords
Submarine cable
Coaxial cable, air and solid dielectric

Wave guides
Aircraft cable
Power cable
Domestic cord sets
Fuses and wiring devices
Wire, general-purpose

Components and Materials

Power rectifiers: selenium, silicon
Parametric amplifiers
Transistors
Diodes: tunnel, zener, parametric
Semiconductor materials: selenium, germanium, silicon
Capacitors: wet, dry, ceramic
Ferrites
Tubes: power, transmitting, traveling-wave, rectifier, receiving, thyratron
Picture tubes
Relays and switches: telephone, industrial

Magnetic counters
Resistors
Varistors
Fluorescent starters
Transformers
Quartz crystals
Crystal filters
Printed circuits
Hermetic seals
Magnetic cores

Eglin Gulf Test Range

Flight Simulator for Mirage III

Potential Application of Recent Advances in Communication Technology

Dewdrop Communication System Performance

Parametric Converter Performance on a Beyond-the-Horizon Microwave Link

Experimental Data Transmission System for Switched Telephone Lines

New Display for Frequency-Modulated Continuous-Wave Radars

World's Telephones—1961

VOLUME 37 • NUMBER 3 • 1962

